



**ADDIS ABABA UNIVERSITY**  
**ETHIOPIAN INSTITUTE OF  
WATER RESOURCES**



---

**SCHOOL OF GRADUATE STUDIES**

**MSc. RESEARCH THESIS ON “ASSESSMENT OF VULNERABILITY OF  
ALLUVIAL AQUIFERS OF TRANSITION ZONE TO CONTAMINATION: THE  
CASE OF DANAKIL BASIN: NORTHEASTERN ETHIOPIA”**

**KUMNEGER MOLLALEGN ALELIGN and ID No: GSR/0442/12**

**MSc RESEARCH THESIS SUBMITTED**

**TO**

**ETHIOPIAN INSTITUTE OF WATER RESOURCES**

**WATER RESOURCES ENGINEERING AND MANAGEMENT  
SPECIALIZATION IN GROUNDWATER MANAGEMENT PROGRAM**

---

**JUNE, 2022**

**ADDIS ABABA**

**Addis Ababa University**  
**Ethiopian Institute of Water Resources**

This is to certify that the thesis prepared by Kumneger Mollalegn Aleign, entitled “ASSESSMENT OF VULNERABILITY OF ALLUVIAL AQUIFERS OF TRANSITION ZONE TO CONTAMINATION: THE CASE OF DANAKIL BASIN, NORTHEASTERN ETHIOPIA” and submitted in partial fulfillment of the requirements for the Degree of Master of Science in Water Resource Engineering and Management (Specialization: Groundwater Management) complies with the regulations of the University and meets the accepted stand concerning originality and quality.

Kumneger Mollalegn Aleign and ID No: GSR/0442/12

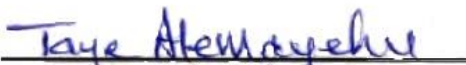

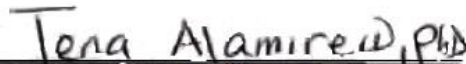
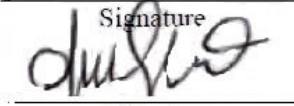
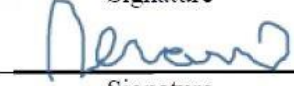
MSc. Research Thesis Submitted

To

Ethiopian Institute of Water Resources (EIWR)

Water Resources Engineering and Management (Groundwater Management Specialization)

**Approved by Board of Examiners:**

 Main Advisor	 Signature	09/05/2022 date
 Internal Examiner Behailu Birhanu(PhD)	 Signature	30.05.22 date
External Examiner	 Signature	8 May 2022 date
Chairperson	Signature	date
EIWR Education Coordinator	Signature	date
EIWR Director	Signature	date

## ACKNOWLEDGMENTS

I would like to appreciate EiWR (Ethiopian Institute of Water Resource) for enabling me to pursue my Master's program study by providing academic support and during the data collection period. I am grateful to all of my instructors and academic coordinators in the institute for granting my leave of absence to pursue my study.

Above all, I am indebted to my first supervisor Dr. Taye Alemayehu for his continuous support guidance, and encouragement throughout the course period (I will never forget his effort to continue the course by recording and providing for all of us, during a very challenging COVID-19 time) and thesis time. I benefited a lot from all assignments/projects and examinations, which I considered like mini-thesis, appreciate his constructive criticism and valuable advice which helped me to develop research and software skills. Without the impartation of those courses and his knowledge; this work would not have been achieved.

Finally, I owe special gratitude to the almighty GOD and my family members (Mr. Mollalegn Alelign, Mrs. Almaz Worku, Mr. Dagmawi Mollalegn, Mr. Mezgebu Mollalegn, Dr. Aynadis Tamene and his wife Eng. Bethlehem Sintayehu, Mr. Nigussie Seifu, Miss Asnaku Abebe and Miss Mimi Girma).

## ABSTRACT

*Groundwater is indispensable to humankind, but with the increasing load over this precious resource, it has become necessary to study it in detail with geological as well as hydro-geological aspects to understand the nature of the groundwater resource of a Danakil basin to manage it well and use it sustainably, vulnerability assessment of the resource is conducted to highlight the areas which are more susceptible to contamination. In the present study, an attempt has been made to account for the groundwater vulnerability using an overlay index method, DRASTIC, which is used to prepare a vulnerability map using GIS, of the study area, Danakil basin. The DRASTIC Vulnerability index (DVI) is calculated as the sum of the product of ratings and weights assigned to each of the parameters on a scale of 1 to 10 and 1 to 5 respectively. And a 2D finite element groundwater flow and solute transport model were developed to simulate the spatial and temporal variations of the salinity intrusion in the alluvial aquifer of the Danakil basin taking into account the transition zone between freshwater and saltwater. The available historical records of water table levels were used to calibrate the developed model. Emphasis was devoted to the response of the transition zone to different pumping scenarios in the study area. The vulnerability index ranges from 50-149 and is classified into three classes it reduced approximately 20%, 50% and 30% of the area lies in low, medium, and high vulnerability zones. Results from the solute transport model also indicated that the saltwater intrusion problem has evolved during over-abstraction (pumping). Unlike previous investigations, this study presents the most qualitative assessment of the available groundwater in the alluvial aquifer under different pumping scenarios. In conclusion, Danakil basin alluvial aquifer is vulnerable to geogenic sources of salt intrusion due to over abstraction. Results can be an important input for policymakers in the development of sustainable groundwater protection and abstraction strategies for the region.*

## Table of Contents

APPROVAL PAGE .....	i
ACKNOWLEDGMENTS .....	ii
ABSTRACT.....	iii
Table of Contents.....	iiiv
List of Figures.....	vii
List of Tables .....	viii
LIST OF ABBREVIATIONS.....	ix
CHAPTER 1: INTRODUCTION.....	1
1.1 Background.....	1
1.2 Statement of the Problem.....	2
1.3 Research Objectives.....	4
1.3.1 General Objective.....	4
1.3.2 Specific Objectives.....	4
1.4 Research Questions.....	4
1.6 Significance of the Study.....	5
1.7 Scopes and Limitations.....	5
CHAPTER 2: LITERATURE REVIEW .....	6
2.1 Tectonic Settings of Danakil Basin.....	6
2.2 Alluvial Aquifers .....	6
2.3 Groundwater Vulnerability.....	7
2.4 Groundwater Modeling.....	8
CHAPTER 3: GENERAL OVERVIEW OF THE STUDY AREA.....	10
3.1 Location and Accessibility.....	10
3.1.1 Topography and Geomorphology .....	11
3.1.2 Drainage .....	12
3.1.3 Physiography.....	12
3.2 Hydrometeorology .....	14
3.2.1 Hydrology.....	14
3.2.2 Climate .....	15

3.3 Geological and Hydrogeological Setting .....	16
3.3.1 Regional Stratigraphy.....	16
3.3.2 Regional Geological Setting.....	16
3.3.2.1 Precambrian Basement and Mesozoic Rocks .....	16
3.3.2.2 Neogene-Pliocene Sediments and Volcanics .....	18
3.3.2.3 Quaternary Sediments.....	18
3.3.3 Tectonic Setting.....	19
3.3.4 Local Geology and Structure of Study Area .....	23
3.3.4.1 Precambrian Rocks .....	23
3.3.4.2 Granitic Intrusion.....	23
3.3.4.3 Limestone Unit .....	24
3.3.4.4 Metasediments (Slates and Phyllites) .....	25
3.3.4.5 Meta-Conglomerate .....	25
3.3.4.6 Meta-Volcanic Rocks .....	26
3.3.4.7 Paleozoic Sediments .....	27
3.3.4.8 Mesozoic Sedimentary Rocks .....	27
3.3.4.9 Tertiary Rocks .....	28
3.3.4.10 Quaternary Deposits .....	29
3.3.4.11 Sedimentary Deposits .....	29
3.3.4.12 Evaporite Deposits.....	30
3.3.5 Geologic Structures .....	31
3.3.5.1 Fault Systems and Lineaments .....	31
3.3.5.2 Foliation and Lination.....	32
3.3.5.3 Joints and Fractures .....	33
3.3.6 Hydrogeology.....	36
3.3.6.1 Regional Hydrostratigraphy .....	36
3.3.6.2 Regional Groundwater Occurrence and Flow System .....	36
3.3.6.3 Local Groundwater Occurrence and Flow System.....	37
3.3.6.4 Aquifer Types of Different Geological Formations in Study Area.....	39
3.3.6.4.1 Alluvial Fan Aquifers of High Productivity .....	39
3.3.6.4.2 Sedimentary Rock Aquifers of Moderate Productivity .....	40
3.3.6.4.3 Basement Aquifers of Low Productivity .....	40
3.3.6.4.4 Aquicludes and Aquitard .....	40
CHAPTER 4: MATERIALS AND METHODOLOGY .....	43
4.1 Conceptual Model Development .....	43
4.1.1 Conceptual Framework of Developing Conceptual Model.....	44
4.1.2 Conceptual Model Approach .....	45
4.1.2.1 Defining Hydrostratigraphic Units .....	45
4.1.2.2 Preparing a Water Budget.....	48

4.1.2.3 Defining Flow System .....	48
4.1.2.4 Defining hydro-chemistry.....	49
4.1.2.5 Boundary conditions.....	50
4.1.3 Schematic Section of the Conceptual Model Groundwater Flow System .....	50
4.2 Numerical Model Development.....	53
4.2.1 SWAT Model Development.....	55
4.2.1.1 Checking Weather Data Quality .....	59
4.2.1.1.1 Daily Rainfall Data Used in Modeling .....	59
4.2.1.1.2 Available Meteorological Stations around the Study Area.....	61
4.2.1.1.3 Potential Evapotranspiration Estimation.....	62
4.2.2 MODFLOW Model Development .....	64
4.2.3 Integrated SWAT-MODFLOW .....	68
4.2.4 Vulnerability Assessment using DRASTIC Method .....	70
4.2.4.1 Depth to Water Table (D).....	73
4.2.4.2 Net Recharge .....	73
4.2.4.3 Aquifer Media.....	74
4.2.4.4 Soil Media.....	74
4.2.4.5 Topography.....	75
4.2.4.6 Impact of vadose Zone .....	75
4.2.4.7 Hydraulic Conductivity .....	76
4.2.4.8 Single Parameter Sensitivity Analysis (SPSA) .....	76
CHAPTER 5: RESULTS AND DISCUSSIONS .....	77
5.1 SWAT Model.....	77
5.2 MODFLOW Model .....	79
5.2.1 Steady-State Calibration.....	79
5.2.2 Density Dependent Transient Water Level Calibration .....	84
5.3 SWAT-MODFLOW .....	86
5.4 DRASTIC Method .....	90
CHAPTER 6: CONCLUSIONS AND RECOMMENDATION .....	92
6.1 Conclusions.....	92
6.2 Recommendations.....	93
References.....	95

**List of Figures**

Figure-1 Location map of the study area. .... 10

Figure-2. A physiographic map of the study area. .... 13

Figure-3 Drainage Pattern and existing gauging stations in the study area. .... 15

Figure-4. The temperature at Dallol, Ethiopia . .... 16

Figure-5. Geology of Danakil Depression, Ethiopia and Eritrea. .... 19

Figure-6. Regional map of Ethiopia, the western and eastern plateaus, Main Ethiopian Rift and the Danakil depression (Source: Umvoto, 2015 as cited in Towers, 2017). .... 22

Figure-7. Stylized geological section illustrating the nature of crustal attenuation across the western Afar margin. .... 23

Figure-8. Granitic Intrusion in the study area. .... 24

Figure-9. Limestone unit in the study area. .... 24

Figure-10. Contact between weathered limestone and low-grade metamorphic rocks. .... 25

Figure-11. Conglomerate interbedded with red series. .... 26

Figure-12. Meta-volcanic underlay by acidic materials. .... 26

Figure-13. Sandstone unit with conglomerate bed and intrusion of basalt in the study area. .... 27

Figure-14. Limestone unit near Gehartu River. .... 28

Figure-15. Sandstone unit. .... 28

Figure-16. Asabuye fan in the study area. .... 29

Figure-17. Carbonate precipitates in the study area. .... 30

Figure-18. Salt plane on the foot of Musley fan. .... 30

Figure-19. Sandstone unit and Conglomerate displaced by normal faults. .... 32

Figure-20. Foliation of Slate. .... 32

Figure-21. Fractured and Jointed in Limestone unit. .... 33

Figure-22. Geological map, cross-section and stratigraphic column of the study area. .... 35

Figure-23. Hydrogeological cross-section with the hydrogeological classification of the study area. .... 42

Figure-24. Conceptual framework of developing the conceptual model. .... 44

Figure-25. Schematic section of the conceptual model groundwater flow system of the study area. .... 52

Figure-26. Process flow diagram of the research study .... 54

Figure-27. Sub-watershed that contain alluvial aquifer of the transition zone. .... 56

Figure-28. Soil classes in the study area. .... 57

Figure-29. Land use classes in the study area. .... 58

Figure-30. Defined hydrological response units (HRUs) in the study area. .... 59

Figure-31. Potential evapotranspiration comparison, showing Penman-Monteith overestimation. .... 63

Figure-32. Stream cells in ModelMuse. .... 65

Figure-33. Existing boreholes in the area .... 66

Figure-34. Boundary condition in the study area. .... 67

Figure-35. Depth to water table. .... 73

Figure-36. Net recharge. .... 74

Figure-37. Topography (slope aspect). .... 75

Figure-38. Comparison of measured and predicted monthly stream flow during the calibration period (1999–2013). .... 78

Figure-39. The hydrologic cycle. .... 78

Figure-40. MODFLOW Head with existing boreholes before calibration in ModelMuse. .... 80

Figure-41. Groundwater level measurement on AY-MO1 (monitoring well)..... 80  
 Figure-42. Steady-state calibration water level results. .... 83  
 Figure-43. Groundwater head. .... 84  
 Figure-44. Transient Calibration in DTW-05 water level drawdown..... 85  
 Figure-45. Water balance monthly average (mm) in the study area. .... 87  
 Figure-46. Visualizing the exported recharge on the QGIS canvas, the recharge of the year 2011. .... 88  
 Figure-47. Sulfate concentration in MODFLOW-MT3DMS. .... 88  
 Figure-48. Drawdown map of the study area..... 89  
 Figure-49. DRASRIC vulnerability map.....91

**List of Tables**

Table 1. Lithostratigraphy and Hydrostratigraphy (Data source: MWH, 2015)..... 47  
 Table 2. The input data, source and type. .... 53  
 Table 3. The major software used for this study. .... 55  
 Table 4. Monthly averages of the CFSR dataset for the study area for the period 1998-2014. .... 60  
 Table 5. List of Meteorological Stations around the study area. .... 61  
 Table 6. Mean monthly rainfall (mm) with two months missing data around the study area..... 61  
 Table 7. Mean monthly evapotranspiration over the study area. .... 62  
 Table 8. Data used for the Hydro-Geological Parameters for DRASTIC Model. .... 70  
 Table 9. Drastic Rating and Weighting Values for the Various Hydrogeological Parameter Settings..... 72  
 Table 10. Water level data from the 21 wells, used in the steady-state calibration. .... 82  
 Table 11. Vulnerability group..... 90

## LIST OF ABBREVIATIONS

CFSR- climate forecast system reanalysis

DEM-Digital Elevation Model

DHRU-Disaggregated Hydrologic Response Unit

DTW - Dallol Test Well

E - East

EARS-East African Rift System

EC - Electrical conductivity (salinity)

EIGS-Ethiopian Institute of Geological Survey

ET-Evapotranspiration

et al. - and others

GIS-Geographic Information System

GPS-Global Positioning System

GSE-Geological survey of Ethiopia

GW-SW-Groundwater-Surface Water

HRUs- hydrologic response Inter-Tropicalalter Tropical Convergence Zone

K-Hydraulic Conductivity

Km - kilometer

km<sup>2</sup> - square kilometer

km<sup>3</sup> - cubic kilometer

m<sup>2</sup> - square meter

m<sup>3</sup> - cubic meter

Ma - million years

mams - meters above mean sea level

mbgl - meters below ground level

mbmsl - meters below mean sea level

MCM-Million Cubic Meters

MDRF - Main Danakil Rift-boundary Fault

MER-Main Ethiopian Rift

mg - milligram

mm – millimeter

MODFLOW-Modular Three Dimensional Finite Difference Groundwater Flow Model

MoWIE-Ministry of Water, Irrigation and Energy  $\mu\text{g}$  – microgram

N – North

NE/NW - northeast/northwest

NNE/NNW - north-northeast/north-northwest

PH-Potential of Hydrogen

Q – Discharge

RMSE-Root mean square error

S – Storativity

S– South

SCS-Soil Conservation Service

SRTM-Shuttle Radar Topographic Mission

Ss - Specific storage

SWAT-Soil Water Assessment Tool

SWL-Static Water Level

T – Transmissivity

TDS - Total Dissolved Salts

UNICEF-United Nations International Children’s Emergency Fund

USGS-United State Geological Survey

UTM - Universal Transverse Mercator

W – West

WHO - World Health Organisation

WNW/WSW - west-northwest/west-southwest

WWDSE - Water Works Design and Supervision Enterprise

## CHAPTER 1: INTRODUCTION

### 1.1 Background

Groundwater is among the peak valued natural resources, which sustain human welfare, facilitate development, and equilibrates the natural environment. In line with the number of indispensable qualities (e.g., steady temperature, wide and persistent accessibility, exceptional natural quality, low development cost, drought reliability), it turns out to be a significant and trustworthy source of water supplies all over the weather regions including both municipal and countryside areas of urbanized and unindustrialized countries (Todd, 2005).

The occurrence of groundwater is mainly influenced by the geology, geomorphology, and climate variability of the country. The variability of these factors in Ethiopia strongly influences the quantity and quality of groundwater in different parts of the country. The geology of the country provides usable groundwater and provides good transmission of rainfall to recharge aquifers, which produce springs and feed perennial rivers (Alemayehu, 2006). The groundwater potential of alluvial fans is considered high as they transmit groundwater from high elevation regions into lower-lying basins. This through flow recharges aquifers in adjacent basins or is discharged as surface water within the basin (Pelletier *et al.*, 2008).

Many kinds of literature state that water quality is influenced by a wide range of natural and human activities. The geological, hydrological, and climatic impacts are the most important natural influences because they affect the quantity and quality of water available. When available water quantities are minimal and maximal utilization of the restricted resource is required, they have the greatest impact; for example, high salinity is a common concern in dry and coastal environments. Seawater or saline groundwater can be desalinated if financial and technical resources are available, although this is not always possible. As a result, even if sufficient quantities of water are available, its poor quality restricts the applications that may be made of it.

Different studies stated that human activity and land use in places where rainfall or surface water may seep into the aquifer will play a role in the aquifer's pollution risk. Groundwater pollution is likely to occur in certain regions due to contamination of surface water or the unsaturated layer above an aquifer. Groundwater vulnerability refers to the variation in groundwater susceptibility over space. Contamination, regardless of pollutant loading, demonstrates how the natural

medium and terrain can influence or govern the groundwater system's vulnerability to contamination. The susceptibility of a groundwater resource to contamination is determined by its inherent susceptibility.

Many techniques exist for computing groundwater vulnerability, however, the most simple and widely used technique is a DRASTIC index which measures intrinsic vulnerability developed by Aller *et.al*, 1998. Intrinsic vulnerability is independent of the nature of the contaminant and the condition of the area where it is released but it takes into account the hydrological, geological, and, hydro-geological characteristics of the area under study (Zwahlen, 2004 as cited in Neha, 2014).

The research area is in the northern Danakil basin, Afar national regional state, northeastern Ethiopia, at the northern extremity of Africa's Great Rift Valley. The study will focus on estimating groundwater vulnerability to contamination of alluvial aquifers, which characterize much of the internal region, where population growth and livestock production have been extensively developed and groundwater demand is very high, as well as the risk of groundwater contamination. As a result, this research will look at how surface water activities, groundwater processes, and neotectonic movement affect a site's vulnerability and quality.

## **1.2 Statement of the Problem**

In Ethiopia's dry lowlands, which are characterized by complex geology, limited rainfall, and extremely changeable topography, groundwater is the primary source of rural and urban water supply. These are difficult conditions for groundwater supplies in these situations (Ketema *et al.*, 2016). In the Afar region, the quantity and distribution of water delivery schemes are insufficient to meet the demands of the population and cattle (UNICEF, 2019).

Regarding groundwater quality limited investigations have been carried out and possible interventions for community water supply in the lowland areas of Ethiopia. Quality data availability is very poor and little is known about hydrogeological investigations carried out so far to map the geological formations and/or structures that are potentially water-bearing. The drastic lack of water quality data is the major difficulty in understanding and managing groundwater resources. Even where the information is available, it is incomplete, uneven, and often of poor quality, which further complicates the problem. (Ketema *et al.*, 2016).

This study will be carried out in one of the lowland areas of Ethiopia in the Danakil basin. Danakil depression that hosts alluvial fans extending down to the Danakil rift in Northeastern Ethiopia. In such environments, the best available shallow groundwater resources are often associated with alluvial fans. The constraints posed by the hypersaline waters found in substantial quantities along the regional faults that transect the fans within the study area in the Danakil basin need to be considered (Kebede, 2013). Alluvial fans in the Danakil basin have a large amount of sub-surface water in terms of quantity, but not necessarily quality. The constraints to be considered in managing this water resource are therefore the water quality and the impact of abstraction on the naturally occurring freshwater lenses overlying the saline waters. As needed in terms of sustainable volume, and as possible in terms of water quality requirements, the rift fault system can also be targeted (Towers, 2017).

Further detailed investigation and analysis to evaluate the Alluvial fan aquifers with more test wells drilling and group testing to observe the interference and hydraulic connections between aquifer systems as well as groundwater modeling works are very important to fully understand the system and to find appropriate groundwater management system (WWDSE, 2013). Assessing alluvial aquifer vulnerability to contamination and mapping groundwater vulnerability in the Danakil basin has never been done. Hereafter, this study will contribute to filling the gap in vulnerability assessment to contamination of alluvial aquifers in the Danakil basin.

### **1.3 Research Objectives**

#### **1.3.1 General Objective**

The main objective of this study is to determine the vulnerability of the alluvial aquifers to contamination of both anthropogenic and geogenic sources.

#### **1.3.2 Specific Objectives**

The specific objectives of this research are:

- To assess the current state of the water quality of the alluvial aquifers; and
- To determine intrinsic susceptibility of the alluvial aquifers.

### **1.4 Research Questions**

By pursuing the above research objectives, the study will answer the following questions:

- Is the groundwater quality in the alluvial aquifers suitable for drinking and agricultural use?
- Is the alluvial aquifer vulnerable to contamination of intrinsic sources and salt intrusion?

## **1.6 Significance of the Study**

Assessment vulnerability is important in representing the spatial variability of the susceptibility of the alluvial fan aquifers to contamination. Alluvial fan aquifers are sources of shallow groundwater and are susceptible to both intrinsic types of vulnerability. Assessing the hydrological and hydrogeological conditions and impacts of surface processes, geological processes, and neotectonic processes on the water quality and vulnerability to contamination of alluvial aquifers will refine existing knowledge in the area. Understanding the interactions of surface water and groundwater is part of understanding the entire groundwater flow system and is vital in determining the intrinsic susceptibility of a groundwater resource.

Therefore, the result and findings of this study will be important for societies in the study area, where water shortages are due to a lack of quality. It will also be important as a tool and guideline for decision-making for policymakers in groundwater resources in arid and semi-arid regions, which are characterized by long dry seasons and short mild wet seasons. It has not been adequate studies in Ethiopia concerning the assessment of the vulnerability of the alluvial aquifers to contamination; therefore, this study will provide valuable mapping data and information for further studies in the study area and other similar areas.

## **1.7 Scopes and Limitations**

The research's major goal is to forecast and determine the vulnerability of alluvial aquifers in the northern Danakil basin to contamination. Because of the study area's isolated and complex geographical and geological environment, literature and data are scarce on surface water and groundwater quality in the area. As a result, the study's regional and temporal dispersion of results was narrowed.

Since there is no streamflow gauging station in the study area, physical similarity techniques from calibrated model to the uncalibrated catchment were used to calibrate the SWAT model. The method (DRASTIC vulnerability mapping) used is very good for regional-scale assessment due to the availability of certain parameters, however, it suffers from many flaws and due to this only cover a small size.

## CHAPTER 2: LITERATURE REVIEW

### 2.1 Tectonic Settings of Danakil Basin

A prominent feature of the East African Rift System (EARS) is the Afar Triangle, representing a triple junction where rifting of the Somali, Nubian and Arabian tectonic plates occurs (Chorowicz, 2005 and Eagles *et al.*, 2002). This triple junction is formed where the Red Sea rift (Arabia plate – Nubia plate) meets the Gulf of Aden rift (Arabia plate – Somalia plate) east of Djibouti and where the Main Ethiopian Rift (Somalia plate – Nubia plate), the northern Afar rift and the Gulf of Aden rift meet in the Afar depression. The northern Afar rift occurs along with the Danakil Depression and meets the Red Sea rift off the coast of Eritrea (Eagles *et al.*, 2002).

The formation relationships on the study area geological map show rift extension have occurred on an approximately east-west axis from the tertiary to the present. The extension has resulted in a deep rift filled with very thick sequences of Tertiary to Recent sediments in the east of the study area. The present rift floor is bounded on the west by the Dogua Range, a subsidiary horst block composed of Precambrian to Jurassic formations. A subsidiary rift (the Lelegehedi / Ayshet Graben) is present between the Dogua Range and the Ethiopian Highlands. This subsidiary rift is an important feature because it controls the drainage pattern and thus defines the edge of the groundwater model, and therefore the study area. Within the subsidiary rift, the tributary to the Regali River flows north to the Regali River, east to Badah, and then drains south into the main rift forming the western, north-west, northern and north-east model boundaries. The tributary to the Saba River flows southwards in the subsidiary rift, before joining the Saba River and flowing eastwards into Lake Assale. It forms the southwest and southern boundary of the model and study area (MWH, 2015).

### 2.2 Alluvial Aquifers

According to Terence and John (1994) alluvial fans are conical sedimentary features that form where a drainage element of a mountain catchment discharges into a basin. Alluvial fans in arid regions offer perfect deposits for investigation. Alluvial fan deposits are typically highly heterogeneous with coarse-grained and poorly sorted sediment, as is expected in debris flow and sheet flood deposits. The elevation difference or slope and large grain size further increase the groundwater flow potential. Abstraction of groundwater from alluvial fans could lower the water

table, which may result in destabilization of slopes and subsidence along with structural features such as faults and fracture zones. Faulting may intercept groundwater flow within an alluvial fan.

The groundwater potential of alluvial fans may be considered high as they transmit groundwater from high elevation regions into lower-lying basins. This through flow recharges aquifers in adjacent basins or is discharged as surface water within the basin. However, alluvial fan through flow is difficult to quantify for groundwater resource estimation. Identifying preferable infiltration locations and volumes is complicated by the heterogeneous nature of the sediment and complex flood behavior (Pelletier *et al.*, 2008).

According to Kebede (2013) Danakil depression hosts alluvial fans extending down to the Danakil rift in Northeastern Ethiopia. In such environments, the best available shallow groundwater resources are often associated with alluvial fans. Towers (2017) also stated that alluvial fans in the Danakil basin have a large amount of sub-surface water in terms of quantity, but not necessarily quality.

### **2.3 Groundwater Vulnerability**

Groundwater vulnerability studies are sources of essential information for the management of water resources, aiming at water quality preservation. The intrinsic vulnerability describes the water's vulnerability to different pollutants (independent of their nature) resulting from human activities and is related to the hydrological, geological, and hydrogeological aquifer's characteristics. Given that the aquifers have different reactions to the same contaminant due to their physicochemical characteristics, the specific vulnerability shows the groundwater vulnerability to a pollutant (or a group of pollutants), determined by the pollutant's properties, taking into account the time of impact, its intensity, and the interaction between the intrinsic vulnerability components and the contaminant (Barbulescu,2020).

Zwahlen (2004) as cited in Neha (2014) stated that many techniques exist for computing groundwater vulnerability, however, the most simple and widely used technique is the DRASTIC index that measures intrinsic vulnerability developed by Aller *et. al.*, 1998. Intrinsic vulnerability is independent of the nature of the contaminant and the condition of the area where it is released but it takes into account the hydrological, geological, and hydro-geological characteristics of the area under study.

## 2.4 Groundwater Modeling

Since the SWAT model has semi-distributed features, its groundwater component does not consider distributed parameters such as hydraulic conductivity and storage coefficient. In generating a detailed representation of groundwater recharge, it is equally difficult to calculate the head distribution and the distributed pumping rate. To solve this problem a method is proposed whereby the characteristics of the hydrologic response units (HRUs) in the SWAT model are exchanged with cells in the MODFLOW model. By using this HRU–cell conversion interface, the distributed groundwater recharge rate, and the groundwater evapotranspiration can be effectively simulated. By considering the interaction between the stream network and the aquifer to reflect boundary flow, the linkage is completed. For this purpose, the RIVER package in the MODFLOW model is used for the river–aquifer interaction. The application demonstrates that an integrated SWAT–MODFLOW is capable of simulating a Spatio-temporal distribution of groundwater recharge rates, aquifer evapotranspiration, and groundwater levels. It also enables an interaction between the saturated aquifer and channel reaches (Kim *et al.*, 2008).

Harbaugh and others (2000) as cited in Michael *et al.* (2013) describe that MODFLOW, a popular computer modeling code that solves the governing equations of groundwater flow, is often used for quantitative modeling of groundwater flow and assessment of salt intrusion. MODFLOW includes several process-based modules to simulate the interactions of key interacting components of the groundwater flow system. MT3DMS is a modular three-dimensional transport model for the simulation of seawater intrusion of advection, dispersion, and chemical reactions of dissolved constituents in groundwater systems (Zheng *et al.*, 2012).

SWAT–MODFLOW is a coupled hydro (geo) logical model that employs both the Soil and Water Assessment Tool—SWAT (Arnold *et al.*, 1998 as cited in David *et al.*, 2019) and MODFLOW (McDonald and Harbaugh, 1983 as cited in David *et al.*, 2019) (SW and GW models, respectively) to yield an integrated output. Coupling the component models covers the limitations inherent in each component model to yield a solution that is more faithful to real-world hydro(geo)logy. SWAT covers processes associated with SW hydrology, such as precipitation, temperature, river flow, surface runoff, soil water, actual evapotranspiration, and GW recharge, while MODFLOW is responsible for the GW processes, including saturated flow and GW discharge into rivers.

SWAT-MODFLOW integrates SWAT2012 and MODFLOW-NWT, and the linking code enables the two models to share their computations daily without the need for rewriting and importing the model inputs. Most importantly, the SWAT's groundwater function is replaced by the MODFLOW code in the integrated model. The coupling is based on geographically located HRUs (disaggregated HRU (DHRU)) and MODFLOW grid shapefile (Bailey *et al.*, 2016 as cited in Bisrat *et al.*, 2020).

## CHAPTER 3: GENERAL OVERVIEW OF THE STUDY AREA

### 3.1 Location and Accessibility

The study area is situated in the Danakil basin, the national regional state of Afar, the northeastern part of Ethiopia. The study area is located in zone two Dallol woreda of Afar National Regional State. Dallol has located 250 km northeast of Mekele town riding on an asphalt road of 50 km up to Agula town and driving eastwards from the main road for 200 km through Berehale woreda town up to the study area. The target study area for the alluvial fan aquifers is geographically located between UTM 560000 - 640000 East and UTM 1550000 - 1600000 North (See figure-1). The target study area is a part of the upper Dallol watershed areas to the west of Dallol Salt plain including two sub-catchment areas of Ayshet and Musley, which covers 1471.492 Km<sup>2</sup>.

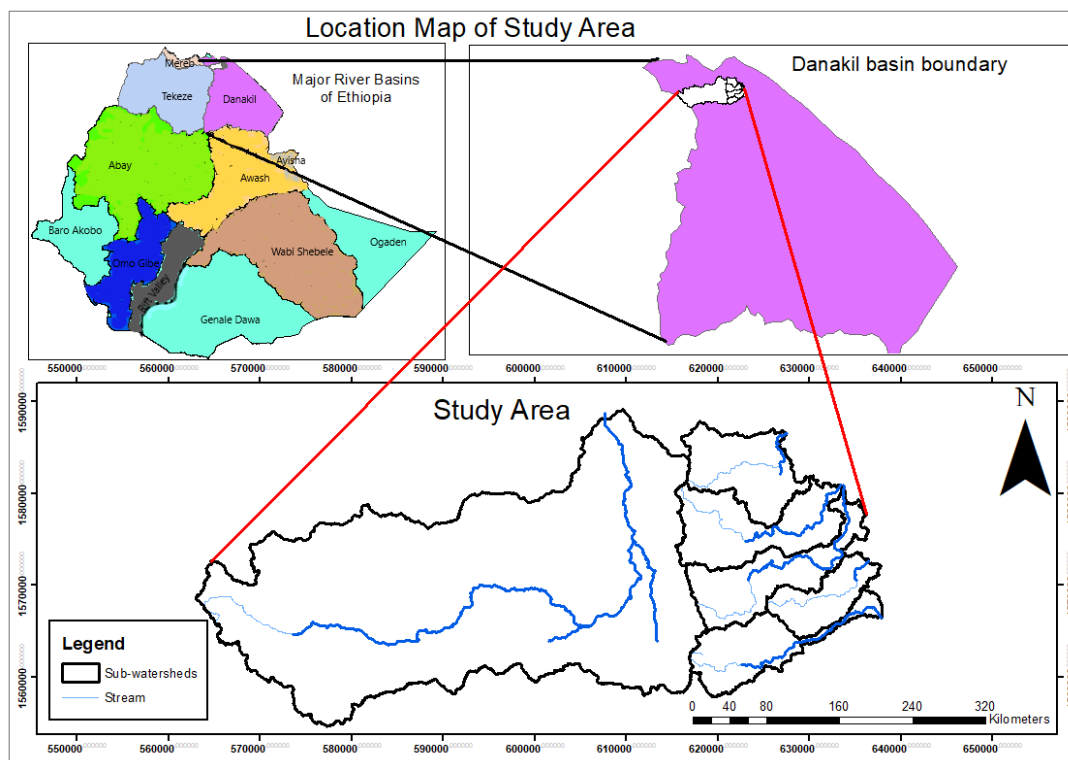


Figure 1. Location map of the study area.

### 3.1.1 Topography and Geomorphology

Many studies described that two major topographic zones, in general, describe the Dallol area. The first is the rugged dissected escarpment west of Danakil depression and the second topographic zone is the extensive low laying salt plain of the depression to the east with elevation more than 120-130m below sea level which is covered with evaporite or lake deposit (WWDSE, 2013).

The geomorphology of the present landscape of the study area is built up through uplift and volcanism, faulting, and denudation by erosion which produces sediment that is transported and deposited in low-energy areas within the landscape. To determine the types of landform in the study area geology and geologic structures, drainage, and geologic process were considered (Gebresilassie *et al.*, 2001).

The structural landform type covers the western and central parts of the study area. It is the result of subsequent faulting, rifting, and erosion and it has a high drainage density. It is characterized by highly dissected mountainous ranges and hills with steep slopes and rugged topography. This geomorphologic unit is comprised of the hilly terrain of faulted blocks, ridges, and rift escarpments. High relief Mountains having an altitude of more than 3000m (western rift escarpment) also comprise this landform. Generally, this landform evolves from tectonic activities of NW-SE, NE-SW, N-S, and rarely E-W trending normal faults and comprises rocks of metavolcanics and metasediments origin. Volcanic rocks of tertiary and Mesozoic-sedimentary rocks also comprise this landform (Eagles *et al.*, 2002).

Alluvial landform occupies low lying region and is formed by streams erosional, transport, and depositional action. The highly weathered and fractured material, creeps, toppled, eroded and transported by rivers and streams into the depositional areas. Sediments in this area are mainly composed of boulders, gravel, sand, silt and clay material derived from the escarpment area and have low drainage density. This geomorphologic unit occupies Musley and the adjacent fans area of the eastern part of the study area (WWDSE, 2013).

Evaporite landform is found in the eastern part of the study area. It is characterized by extremely flat and large evaporite salt beds devoid of topographic features except for some volcanoes and hot springs which are parallel to the depression trend. The depression gets lowest towards the east with an average altitude of 130 meters below sea level. Spectacular flowered red, yellow and

brown molds of salts, iron oxides and sulfur deposits are a prominent feature of the area of Dallol Mountain (Warren, 2016).

### **3.1.2 Drainage**

The Danakil basins catchment area extends from the Ethiopian plateau in the west to the Danakil Alps in the east with all runoff, rivers and streams flowing towards and ending in the endorheic Danakil depression (Umvoto, 2014a as cited in Towers, 2017). The rivers and streams are non-perennial or sub-surface flows that occur as steeply carved ravines within the plateau and as braided and meandering flows within the alluvial fan and lower-lying areas of the depression (Holwerda and Hutchinson, 1968). The depression is bordered by the tributaries of the Ragali River in the west, one such tributary is the Lelegheddi River. The Lelegheddi River alluvium and the underlying limestone are a potential source of freshwater but have not yet been explored.

The Ragali River flows in a northerly then easterly direction towards the village of Badah, where it flows out onto the salt flats (Holwerda and Hutchinson, 1968 and Kebede, 2013). The Ragali River flows at the subsurface as baseflow or as a sheet wash within the depression (Umvoto, 2015 as cited in Towers, 2017). To the south, the Seba River flows east into Lake Assale.

The Ragali river is the only perennial river close to the study area. The other largest nearby river, the river Awash, occurs far to the south and drains to the northeast through the rift floor, to Lake Abhe (Ayenew *et al.*, 2008).

### **3.1.3 Physiography**

WWDSE (2013) stated that the physiographic landscape of the area is the result of magmatism, volcanism, tectonic activities, erosion and depositional events. From field observation and DEM analysis, four major physiographic regions were identified in the project area and namely: Western highlands and rift escarpment, Graben area, Alluvial fans and Salt plain (see figure-2).

The western highlands and rift escarpment physiographic region is part of the northwestern Ethiopian plateau and separated from the Dallol depression by the western rift escarpment which extends from the Belakiya mountain range area towards the west in the mapped area. It is characterized by elevated ridges dissected by deep gorges, rift escarpments and rugged terrain having the highest peak at an altitude of 2964m (WWDSE, 2013).

The Graben area region occupies the central part of the study area. It is characterized by low-lying areas within the mountain ranges and is characterized by boulders of different rocks from the surrounding highland area filling the Graben floor (WWDSE, 2013).

The alluvial fans region occupies the eastern portion of the study area. The region is characterized by low-lying and undulating plains composed of boulders of different rocks and gravel terraces transported by rivers from the nearest highlands and forms these depositional features. These include major and small rivers which emanate from the western highlands and flow towards the rift salt plains with an average elevation of 110 m below sea level (Towers, 2017).

The salt plain landscape is found at the eastern tip of the mapped area. It is characterized by a large salt plain. The rift floor gets thin towards the east with an average altitude of 120 meters below sea level. Dallol depression is a prominent feature in the area (WWDSE, 2013).

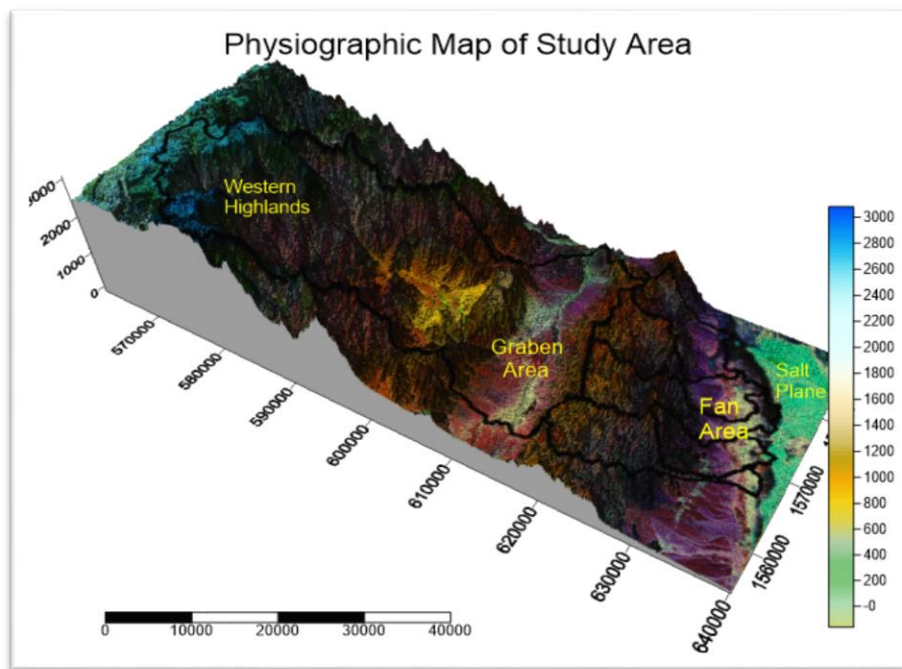


Figure 2. A physiographic map of the study area.

## 3.2 Hydrometeorology

### 3.2.1 Hydrology

The study area is located in the northeastern part of Ethiopia in the Danakil depression, an extensive interior basin with below sea level elevation as low as 120m. WWDSE (2013) stated that the basin constitutes the northern part of a much larger topographic region of the Afar depression. The Danakil basin is bordered to the west by the Tekeze River basin, to the north-west by the Mereb River basin, and the south by Awash River basin, and the east by a Dallol Red sea.

The study area is a part of upper Dallol watershed areas to the west of Dallol Salt plain including six sub-basins areas of the upper watershed and lower watershed (Musley and adjacent fans) covering 1471.492 Km<sup>2</sup>, both of which drain from west to east. Blake *et al.* (2017) stated that these catchments are typified by steep slopes in the upper reaches with high energy flows and steep flow paths. The lower reaches are typified by lower energy flows with wider flatter flow paths over deep alluvium. There is a significant range in slope characterization within the considered catchments.

According to MWH (2015) it is assumed that there would be a fairly rapid runoff response, particularly in the upper reaches of the catchments following significant rainfall events. Runoff is expected to be highest during the rainy season (June to August). Runoff at the lower reaches will be more lagged than the runoff in the upper reaches due to the nature of the topography (flatter) and riverbed material (alluvium).

In considering the comment by the local community near the Regali, it is the expectation that the average monthly streamflow for July and August is not a sustained flow, but rather several more sporadic events where flows are likely to significantly exceed the average values.

From an observed wall section of stream channel that has cut down through alluvial fan deposit in Musley, the interbedded layers of fine sand gravel and clay materials that confined the groundwater system in the upper reaches of the fan probably represent major storm events where flood flows contributed a new layer of sediment to the surface of the fan (WWDSE, 2013).

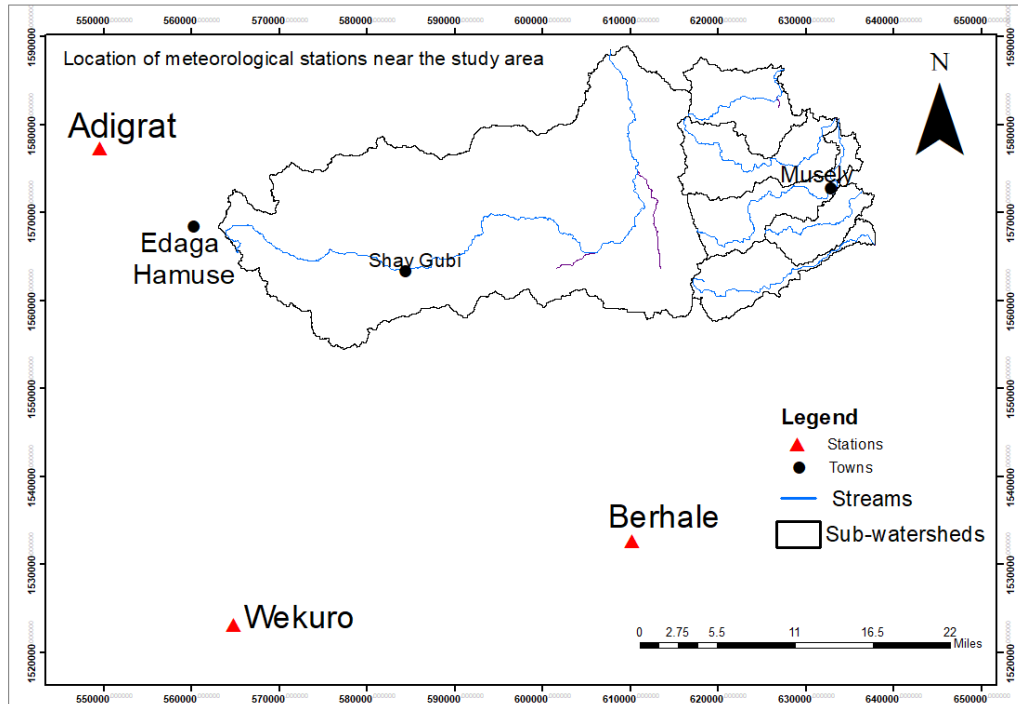


Figure 3. Drainage Pattern and existing gauging stations in the study area.

### 3.2.2 Climate

It is seen that the Danakil basin is characterized by monomodal type rainfall patterns with an arid to semi-arid climate. The northeastern part of the Danakil basin (around Dallol) receives most of its rainfall during July, August and September associated with the northward passage of the Inter-Tropical Convergence Zone (ITCZ). The main influences on weather circulation in Ethiopia are the Inter-Tropical Convergence Zone (ITCZ), the northeastern trade winds and the southwestern monsoons. In particular, the watersheds under the study area have characteristics of getting rain from the movement of ITCZ towards the northern part of the country, during the wet season (Blake *et al.*, 2017).

The climate of the Danakil region is hot and dry with desert to semi-desert conditions. Average daily temperatures vary between 20-28 °C in winter and reach up to 50 °C in summer (Darrah *et al.*, 2012)

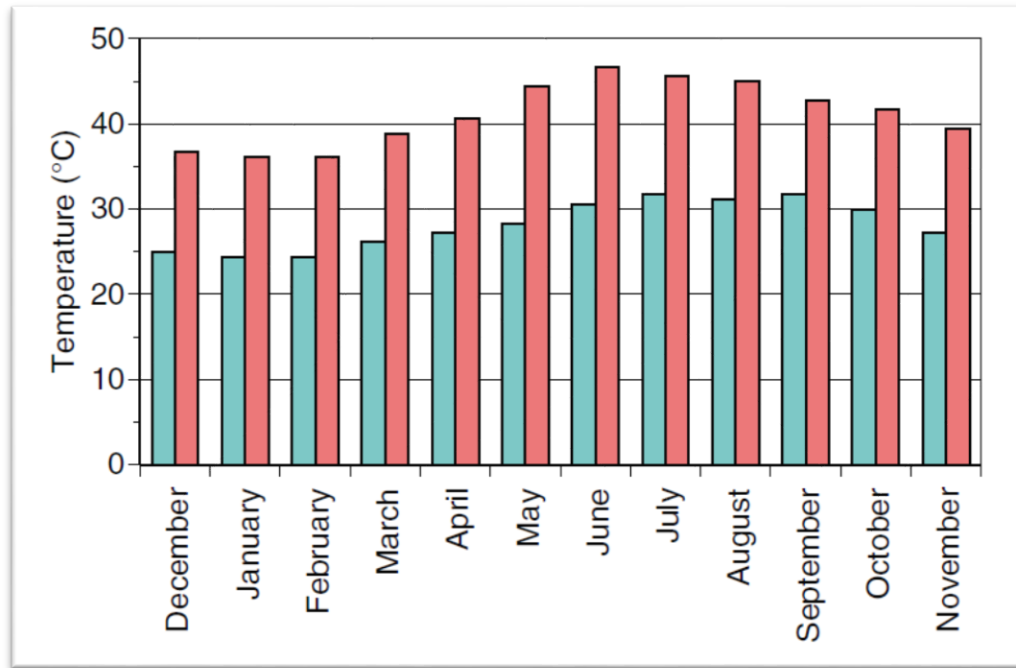


Figure 4. The temperature at Dallol, Ethiopia.

### 3.3 Geological and Hydrogeological Setting

#### 3.3.1 Regional Stratigraphy

The regional stratigraphy of the Danakil depression can be classified into three main divisions, from youngest to oldest (Holwerda and Hutchinson, 1968). Quaternary (2.6-0 Million years old) rocks are poorly cemented and weakly compacted playa-lake sediments, evaporites and alluvium continuously being deposited in the Danakil depression. Paleogene and Neogene (66-2.6 Ma) clastic sedimentary rocks and volcanic, deposited in the Danakil depression in the early stages of rift and basin development; and Pre-Paleogene bedrock with clastic and carbonate sediments from the Jurassic era and early Palaeozoic (Permian) to Precambrian (Proterozoic) crystalline basement rocks (Blake *et al.*, 2017).

#### 3.3.2 Regional Geological Setting

##### 3.3.2.1 Precambrian Basement and Mesozoic Rocks

Neoproterozoic 1000-540 million years old (Ma) crystalline basement rocks of the Arabian-Nubian Craton outcrop within the Ethiopian Plateau and the Danakil block, consisting of metamorphosed volcanic and sedimentary rocks of the Tsaliet Group (Gebresilassie *et al.*, 2011). The highly deformed, fractured and faulted basement rocks were intruded by dykes and sills of diorite, granodiorite and granite, which then also underwent extensive metamorphism and

deformation with the basement rocks (GSE, 2009). The metavolcanic show a high degree of heterogeneity in original composition as well as metamorphic grade and consist of meta-andesite, meta-dacites, meta-rhyolites, chlorite-sericite-graphite phyllites, marbles, slate and quartzite (Umvoto, 2015 as cited in Towers, 2017). As Per Holwerda and Hutchinson (1968), the phyllites of the Tsaliet Group likely exceed a thickness of 1500m and rest on top of an undefined thickness of Precambrian gneiss and migmatites.

The Tsaliet Group underlies Cretaceous to Late Jurassic (230-145 Ma) sedimentary rocks, which were deposited in continental to the shallow marine environment. The marine sequences were deposited during the Jurassic transgression of the Indian Ocean, from intra-continental rifting during the Gondwanan break-up (Gebresilassie *et al.*, 2011).

The Adigrat Formation reaches thicknesses of between 300-1600 m and is described as an unfossiliferous, coarse-grained, red arkosic sandstone. The formation fines upward from conglomerate at the base to grey shale at the top. Ferruginous sandstone beds common to the Adigrat Formation give it a distinct red color (Holwerda and Hutchinson, 1968).

The conformable Antalo Group, which is 1080m thick and composed of intercalated fossiliferous limestone and marl, is overlain by the Agula formation shale and Amba Aradom formation sandstone. The lower Antalo Group is described as “a dense, grey, locally fossiliferous marine limestone...” locally intruded by mafic dykes and sills. These intrusions are more extensive and frequent in the underlying Adigrat Formation. The upper Antalo Group is described as an impure, thin-bedded, grey-blue, fossiliferous limestone with lenticular gypsum beds of up to 5m thick occurring near the top of the group (Holwerda and Hutchinson, 1968 and Gebresilassie *et al.*, 2011). After the deposition of these Cretaceous to Late Jurassic sediments, the region was affected by tectonic uplift and erosion, which resulted in the formation of a pen plain (Gebresilassie *et al.*, 2011).

The Adigrat Formation and Antalo Group are potential fractured rock and karstic aquifers respectively. The outcrop geometry and thickness of the units are, however, difficult to determine due to the extensive faulting of both units and their juxtaposition against each other and the basement rocks of the Tsaliet Group (Umvoto, 2015 as cited in Towers, 2017).

### 3.3.2.2 Neogene-Pliocene Sediments and Volcanics

Profuse eruption of volcanic rock, up to 3km thick, occurred from approximately 30 Ma, resulting in the rifting that formed the Danakil Depression. These volcanic sequences, which overlie the Danakil block, form the base of the Danakil depression. There is a transition in composition from basaltic at the base of the pile to andesitic and rhyolitic at the top (Gebresilassie *et al.*, 2011).

Pleistocene to Recent (2.5-0 Ma) volcanic rocks of the Afar, Samoti, Alid, Oss and Abaeded Formations have erupted in and around the Danakil Depression and are comprised of hawaiiite, mugearite, trachyte, andesine basalt, Ferro basalt, rhyolite, spatter cones and hyaloclastites ranging in composition from alkaline to tholeiitic. The Afar volcanic are usually intercalated with the Danakil Group sediments described below. The Abandoned Formation volcanic surface around Badah village. The Samoti, Alid and Oss Formation volcanics are mainly localized to Eritrea (Umvoto, 2016a as cited in Towers, 2017).

According to Mesfin and Yohannes (2014) the Danakil group or red series was deposited during the of 23-2.6Ma and consists of Lower, Middle and Upper subgroups. Limestone and mudstone units were likely deposited during Miocene-Pliocene marine incursion into the Danakil Depression, whereas conglomerates are likely debris-flow or alluvial fan erosional deposits sourced from the plateau.

The Lower Danakil Subgroup consists of blueish-grey marl overlain by marly limestone. The Middle Danakil Subgroup consists of chocolate brown sandstones and chocolate brown to violet conglomerates. The sandstones and conglomerates are overlain by partially cemented gravels, sands and silts. The Upper Danakil Subgroup consists of red to yellow-grey, clayey, gravelly, sandy silts, which are underlain by intercalated creamy to grey marls and limestones with localized grey coral reefs limestone (Kebede,2013).

### 3.3.2.3 Quaternary Sediments

The Zariga Formation (Brinckmann and Kursten, 1970), also called the Enkafala Formation (Abbate *et al.*, 2004) uncomfortably overlies the Danakil Group along the western side of the rift basin. At certain locations, the oldest Pleistocene alluvial fans are also overlain by the Zariga Formation. The Zariga formation represents marine ingression into the northern Danakil

depression. It is predominantly comprised of “laminated gypsum and marls with oolitic and reef limestone (Holwerda and Hutchinson, 1968).

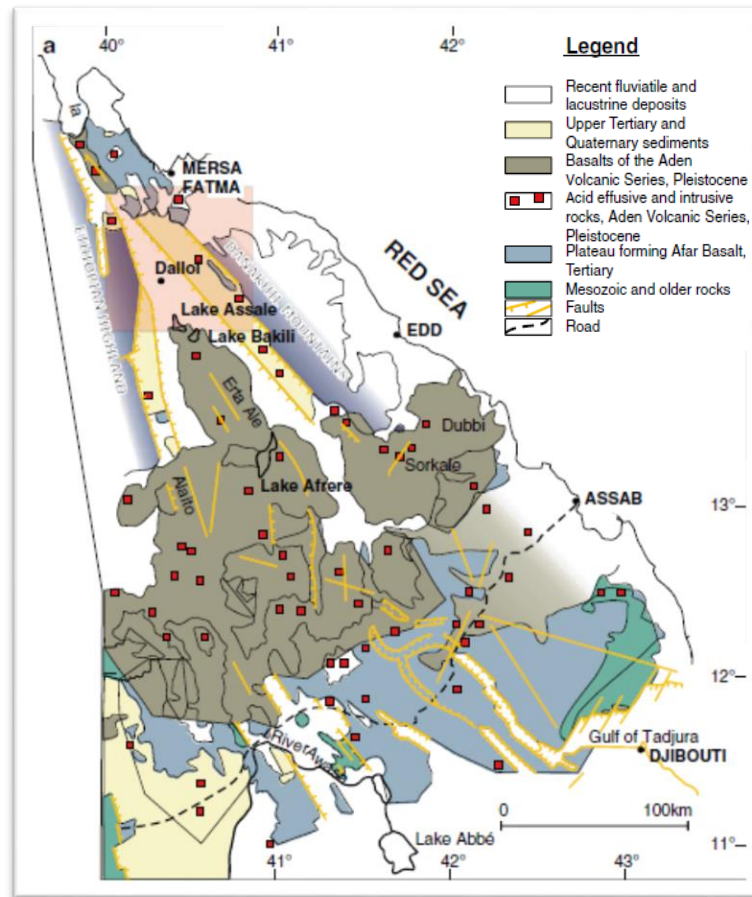


Figure 5. Geology of Danakil Depression, Ethiopia and Eritrea, (After Ercosplan 2011 as cited in Warren, 2016).

### 3.3.3 Tectonic Setting

The Danakil depression lies within the Afro-Arabian Rift System (AARS). This rift system extends from Syria in the north and passes through the Afar depression and East African Rift System (WWDSE, 2013).

The Afar depression has a triangular shape, bounded by marginal rift escarpments. It is flanked by the Ethiopian plateau in the west, the Somalian plateau in the southeast, Ali-Sabieh blocks in the east and Danakil blocks in the northeast side. The central part of the Afar depression is dominated by lowland plains with horst and graben and rare high relief shield volcanoes (WWDSE, 2013).

The Danakil depression is an adown faulted block within the Afar triple junction bounded by the escarpment of the Ethiopian plateau (Balakai mountain range) in the west and the uplifted block of the Danakil horst in the east (WWDSE, 2013).

A prominent feature of the East African Rift System (EARS) is the Afar Triangle, representing a triple junction where rifting of the Somali, Nubian and Arabian tectonic plates occurs (Chorowicz, 2005; Eagles *et al.*, 2002). This triple junction is formed where the Red Sea rift (Arabia plate – Nubia plate) meets the Gulf of Aden rift (Arabia plate – Somalia plate) east of Djibouti and where the Main Ethiopian Rift (Somalia plate – Nubia plate), the northern Afar rift and the Gulf of Aden rift meet in the Afar depression. The northern Afar rift occurs along with the Danakil Depression and meets the Red Sea rift off the coast of Eritrea (Eagles *et al.*, 2002).

The Nubian, Arabian and Somalian Plate motions have induced major tectonic elements in the Afar Depression. These include the Danakil, Ali-Sabieh and East-Central Blocks. Understanding how regional tectonics may control the general geomorphology and geology of an area is crucial in understanding the groundwater flow system of rift zones. This requires the definition of the overall rift structure and the related geological features of particular emphasis are given to the understanding of the geometry and segmentation of the main fault patterns (Beyene *et al.*, 2005).

In a regional context, Cenozoic (Quaternary, Palaeogene and Neogene) rocks occur within the boundaries of the rift system as they were deposited after rifting had begun. Pre-Paleogene rocks are more extensive geographically and have been subject to older block faulting and folding that predate rifting (Umvoto, 2015 as cited in Towers, 2017). The pre-rift faulting is predominantly normal faulting, which influenced rift formation and propagation in the early stages of continental extension (Mesfin and Yohannes, 2014). These fractures and faults are of hydrogeological significance as they juxtapose Jurassic and Proterozoic rocks (Mesfin and Yohannes, 2014) and create groundwater flow paths between the two units through the shared fractures and faults (Umvoto, 2015 as cited in Towers, 2017).

These basement rocks are overlain by Permian to Palaeogene sedimentary rocks, which were deposited in the continental and shallow marine environment. Marine successions were produced during the Jurassic transgression of the sea by the Indian Ocean after the intra-continental rifting

caused by the breakup of the Gondwana Supercontinent (Davidson *et al.*, 1994; Drury *et al.*, 1994 as cited in Gebresilassie *et al.*, 2011).

After completion of the deposition of the sedimentary successions, the region was affected by tectonic uplift and subsequent erosion, which resulted in the formation of a peneplain (Davidson *et al.*, 1994; Drury *et al.*, 1994 as cited in Gebresilassie *et al.*, 2011). This was followed by a rifting that formed the Afar depression and deposition of Quaternary fluvial-lacustrine deposits in the graben (Holwerda and Hutchinson 1968 as cited in Gebresilassie *et al.*, 2011).

ERCOSPLAN (2015) Stated that the regional geological, as well as the tectonic chronology of the Danakil Depression, is closely attendant to mid-Miocene rifting processes. Tectonic controls on the morphological characteristics of the deposit are related to structural rifting events. Three main structural units can be described, which characterize the Southern Red Sea area:

- Red Sea Graben (striking NW-SE),
- Ethiopian Graben (striking NE-SW merging into the East-African Rift System),
- The main structure of the Gulf of Aden (striking ENE-WSW).

The Danakil Depression strikes NW-SE with an extension of more than 300 km from Lake Bada in the north to Lake Acori in the south. The structure of the Danakil Depression extends to the south, widening from 10 km in the north to about 70 km in the south. The northern part of the Depression is the deepest and has elevations as low as 128 m below sea level. The Danakil Depression is bordered by the Danakil Alps to NE with elevations of up to 1,300 m. The Danakil Alps can be described as an NNW-SSE striking horst structure of 40 km-70 km width, separating the Depression from the Red Sea. The SW border of the Danakil Depression is the transition area to the Ethiopian Highlands, which rise to elevations of about 2,500 m.

The Depression is limited to the Ethiopian Highland by NNW-SSE trending fault scarps. These fault scarps are dislocated against each other in the ENE-WSW direction. High subsidence rates favored the formation of a thick (1,000 m) evaporite series in proximity to the Red Sea, which is assumed to be the provenance area for the shallow marine basin infill (ERCOSPLAN, 2015).



Figure 6. Regional map of Ethiopia, the western and eastern plateaus, Main Ethiopian Rift and the Danakil depression (Source: Umvoto Aferica, 2015 as cited in Towers, 2017).

The stylized geological cross-section illustrating the nature of crustal attenuation across the western Afar margin consisted of the Ethiopian plateau, Ethiopian escarpment, Marginal basin and Marginal area of the Afar depressions (Alebachew *et al.*, 2005 as cited in WWDSE, 2013).

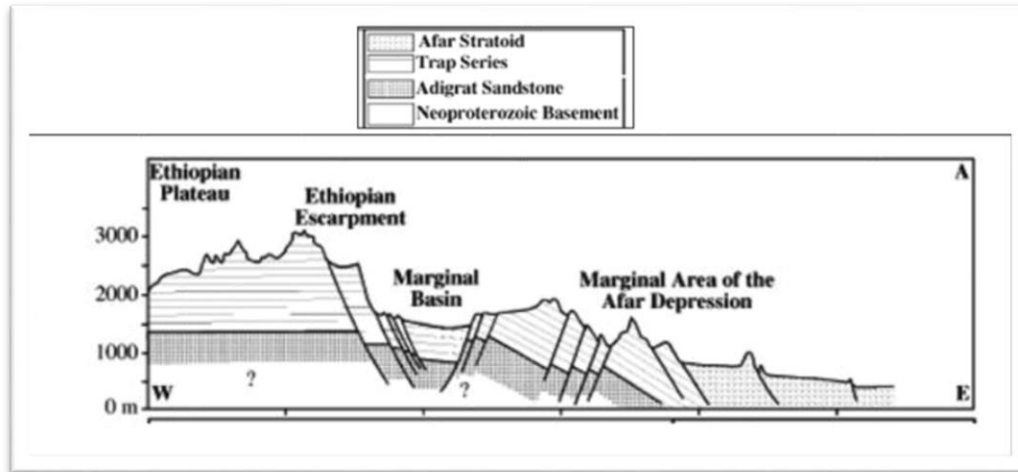


Figure 7. Stylized geological section illustrating the nature of crustal attenuation across the western Afar margin (source Alebachew *et al.*, 2005 as cited in WWDSE, 2013).

### 3.3.4 Local Geology and Structure of Study Area

The lithological description in this study is mainly based on field observation and studies of relevant previous works to map the main geologic features and tectonic structures of the area. An inventory of lithological units and fault patterns has been made from the geological and hydrogeological map to investigate the relationship between the nature of different outcropping lithological units and tectonic patterns with the hydrogeologic system.

#### 3.3.4.1 Precambrian Rocks

The northern Ethiopian Precambrian rocks to which the study area belongs are characterized by the occurrence of low-grade volcanic, sedimentary, and plutonic rocks of typical Arabian-Nubian Shield assemblage (WWDSE, 2013).

#### 3.3.4.2 Granitic Intrusion

This unit is outcrops in the western part of the mapped area along the western rift escarpment. It is the oldest unit underlying the sedimentary rock in the area. The unit is exposed as a circular outcrop unit on a river bed and it is slightly weathered, pinkish to dark color, and medium to the coarse-grained intrusion of quartz diorite, granodiorite and granite veined with quartz. There is lateral and vertical displacement after the intrusion.



Figure 8. Granitic Intrusion in the study area.

#### **3.3.4.3 Limestone Unit**

A sequence of thick massive limestone crops out in the western part of the mapped area. It is dark gray, highly fractured, fine-grained, closely folded, sheared, foliated and related with underlain slates and Phyllites by an angular unconformity. It is brown to black color, well-bedded, and veined with calcite. In some places, it is highly re-crystallized.



Figure 9. Limestone unit in the study area.

#### 3.3.4.4 Metasediments (Slates and Phyllites)

Metasediments represent the major and oldest rock formations in the area. These rocks are slates, but in some places a significant amount of phyllites and interbedded limestone are present and the area belongs to Tambien group of northern Ethiopia. They are intruded by granite, diorite, and by sills and irregular masses of basalt and andesite. These rocks are exposed in the western rift margin at the foot of a major fault escarpment in the mapped area. In fresh samples, it is greenish dark, but dark brown in weathered ones, and has hard and compact in appearance. They are highly foliated, sheared, foliated and tilted.



Figure 10. Contact between weathered limestone and low-grade metamorphic rocks (Phyllites and Slate).

#### 3.3.4.5 Meta-Conglomerate

The study area is dominated and characterized by low-grade Meta-sedimentary rocks. The meta-conglomerate unit in the mapped area exposed in and along river beds indicates evidence of shallow-water origin. The western part of the mapped area is dominated by several conglomerates which are composed of not well-rounded or irregular shape clasts. The clast's sizes are variable, ranging from millimeters up to a few centimeters. In the study area, these rocks are associated with Meta-volcanic rocks and interbedded with red series. It is coarse-grained, greenish-gray, densely welded rock containing lithic fragments, marine clasts, and associated tuffs and lava flow.



Figure 11. Conglomerate interbedded with red series.

#### **3.3.4.6 Meta-Volcanic Rocks**

This unit is exposed in the western and central part of the mapped area occupying. Its composition ranges from basalts to rhyolites and associated meta-sediments. The major components of these sediments are of volcanic origins, agglomerates, breccias, bedded tuffs and lavas. These extensive low-grade metamorphic rocks belong to Tsalit group of northern Ethiopia. The meta-volcanic rocks are rich in acidic minerals, dark grey to brownish color and are fine-medium grained. The same change probably occurred further north in the study area.



Figure 12. Meta-volcanic underlay by acidic materials.

### 3.3.4.7 Paleozoic Sediments

These sediments are exposed at the very west and top part of the study area, particularly in Senkata, Edaga-Hamus, and on the Astbi plateau. They are characterized by white, coarse-grained, cross-bedded calcareous sandstone with silty beds with some pebbles, cobble and boulders overlain by tillite.

### 3.3.4.8 Mesozoic Sedimentary Rocks

The sandstone unit is the oldest of the Mesozoic sediments exposed to the area. It is a thick sequence of sandstone that is equivalent to the Adigrat sandstone which is also believed to be of Triassic -Jurassic in age. It rests unconformably on the Precambrian basement rocks of the area.

The maximum thickness of this unit reaches more than 800m in the region. It is exposed only at the northern periphery of the study area. The unit is pink to red, coarse-grained, well-sorted arkosic sandstone with a conglomerate bed. It has also whitish gray, friable, cross-bedded and well-sorted structure containing rounded quartz pebbles and local shale beds. Dykes and Intrusion of basalt and gabbro occur in the lower unit of this formation.



Figure 13. Sandstone unit with conglomerate bed and intrusion of basalt in the study area.

The limestone unit is composed of thinly laminated limestone, marls and calcareous Shales and gypsum intercalation. It is the major sedimentary succession in the region. It is also a major stratigraphic unit covering a large part of the mapped area. This limestone is characterized by thinly bedded intercalated marl and shale. It is yellowish, fossiliferous and well-bedded limestone.



Figure 14. Limestone unit near Gehartu River.

### 3.3.4.9 Tertiary Rocks

The tertiary rocks in the study area include pebble to boulder size conglomerate, fine to coarse-grained sandstone, sand, shales and variegated color clay beds, with interbedded basaltic lavas and acidic intrusion. These sediments are exposed along the margins of the Denakil depression underlain by basement and Mesozoic rocks.



Figure 15. Sandstone unit.

#### 3.3.4.10 Quaternary Deposits

Quaternary deposits in the study area include volcanic and sedimentary rock origins. Despite their limited areal coverage, these geological units play a significant role in understanding the surface and subsurface water movement and occurrence in the past and at present in the project area. Hence, a brief account is given below for these rocks.

#### 3.3.4.11 Sedimentary Deposits

The sedimentary rocks in the mapped area include the salt, gypsum and clay deposits of the evaporite beds, calcium precipitates, and alluvial deposits of unconsolidated gravels, sands, and silts which form the alluvial fans. Alluvium, these sediments have a limited areal extent and are found mainly in some depressions and flat basins in the study area.

Alluvial fans are extending from the foot of the escarpment in the west and spread eastwards over the flat floor of the depression. These sediments occupy flood plains, grabens, rift floors, and the bases of escarpments and cover the salt plains. Mosley fans, Gehartu and Asabuye fans are the major alluvial fans in the sub-basin.

These fans are composed of fluvial sediments of different sizes ranging from poorly sorted and sub-rounded pebbles and boulders to poorly sorted mixtures of gravel, sand, silt and clay. Exposure of these sediments is found along with river courses and flood plains and graben regions of the study area.



Figure 16. Asabuye fan in the study area.

Carbonate precipitates like travertine are formed from the precipitation of dissolved calcium carbonates. These precipitates are found on feet of western escarpment and they have a light color and are fine-grained. An exposure of Carbonate precipitates deposits with some corrals. They are very limited in size and spatial distribution.



Figure 17. Carbonate precipitates in the study area.

#### **3.3.4.12 Evaporite Deposits**

The evaporite beds in the mapped area cover the easternmost extension of the sub-basin. The evaporites include potash, sulfur, gypsum, halite and other minerals present in these deposits. Recent lava flows and unconsolidated alluvial exposed over part of the salt plain and alluvial fans occur at higher levels in the mapped area.



Figure 18. Salt plane on the foot of Musley fan.

### 3.3.5 Geologic Structures

The study area is bounded by the western rift escarpment in the west and the Danakil horst in the east. Hydrogeological map, Satellite images and DEM of the study area have been used to define the location and pattern of the major lineaments, which are inferred to be faulted. The field analysis has been focused on the most significant lineaments, to verify that they are faults and to identify the fault geometry. A hydrogeological map of Axum-Adigrat with a scale of 1:250000 (GSE, 2014) was used to digitize the local geological structures.

The geological structures observed in the study area are faults, lineaments, foliations, lineation, joints, and fractures. These structures are associated with tectonic and geomorphologic features of the Danakil depression that control the groundwater flow and occurrence.

#### 3.3.5.1 Fault Systems and Lineaments

The study area structural pattern is characterized by two main fault systems roughly NNW-SSE and NNE-SSW trending border faults and an NW-SE trending fault system mainly affecting the rift floor. The western section of the mapped area is characterized by an NNW-SSE trending border fault system separating the Ethiopian plateau from the rift floor. These structures are all normal faults developed at different stages of the evolution of the rift and forming major fault blocks (ERCOSPLAN, 2015).

Faults and lineaments are developed in the study area, particularly in the sedimentary succession of the area. These are pre-rift structures aligned obliquely with the NNW-SSE-directed marginal faults of the rift. They are characterized by major rift escarpments, exceeding 3000m in height. Cross-rift structures trending E-W to ENE-WSW are also common in the area. They affect the western rift escarpment and the marginal horst blocks. In addition to normal faults, reverse faults have also been observed along the escarpment region (ERCOSPLAN, 2015).

Lineaments are either linear or curvilinear features observed in the map area. They are traced following ridge crests and river channels and are from a few centimeters to tens of centimeters long on the map. They have variable trends; NW-SE, NE-SW, N-S and E-W. The NW-SE trending lineaments appear to be more dominant than the others (ERCOSPLAN, 2015).



Figure 19. Sandstone units and Conglomerate rock units are displaced by normal faults.

### 3.3.5.2 Foliation and Lination

Other prominent small-scale structures observed in the basement complexes of the area are foliations and lineation. These are penetrative planer fabrics that mainly occur in meta-sediments and meta-volcanic, the latter is susceptible to deformation, so that good alignment of foliation is more present in meta-sediments. Very closely spaced cleavage planes consisting of parallel orientation of clays and micas represent the foliation in slates in the study area.



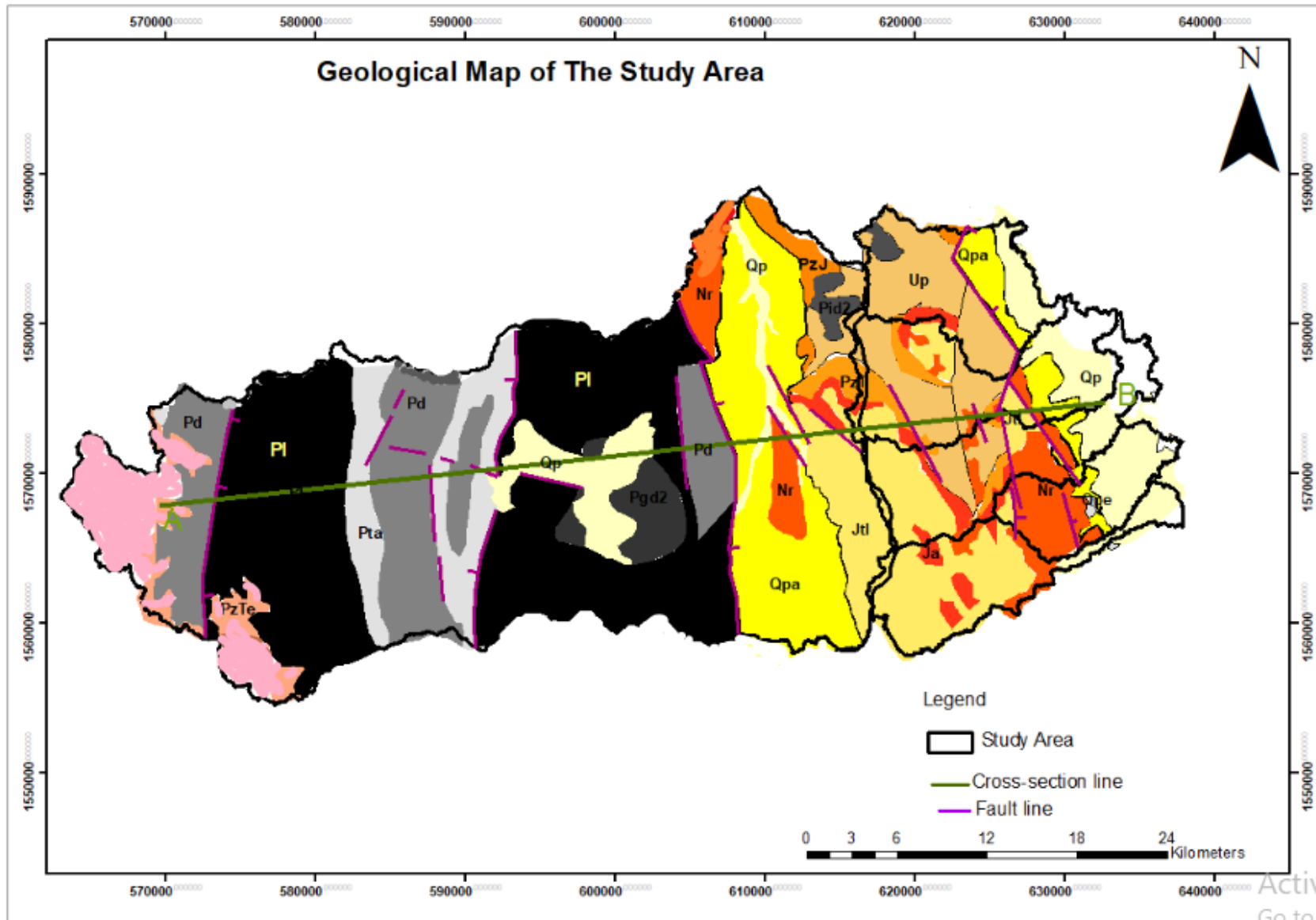
Figure 20. Foliation of Slate.

### 3.3.5.3 Joints and Fractures

Joints and Fractures are the common structures present in almost all kinds of rocks in the study area. Types of joints in the mapped area are columnar joints, concentric joints, and tiny normal joints of which columnar and tiny normal joints are the most commonly observed. Quartz veins are observed in granitic and granodiorite intrusions of the study area.



Figure 21. Fractured and Jointed in Limestone unit.



Activate  
Go to Set

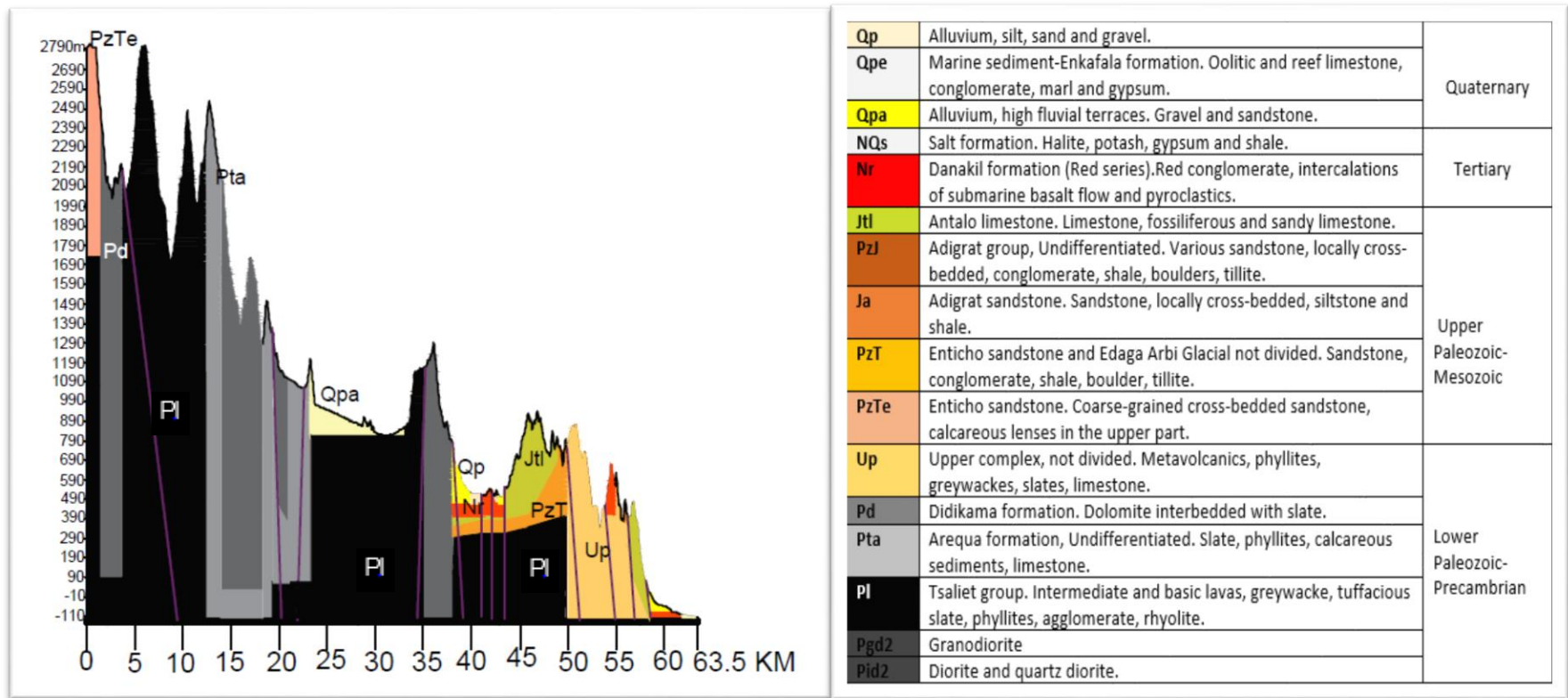


Figure 22. Geological map, cross-section and stratigraphic column of the study area.

### 3.3.6 Hydrogeology

#### 3.3.6.1 Regional Hydrostratigraphy

The Lithostratigraphy of the Danakil Depression is grouped into four broad hydrostratigraphic units (Blake *et al.*, 2017).

- The Precambrian metavolcanic and metasedimentary basement rocks of the Tsaliyet Group constitute a relatively impermeable, low-yielding, poor-quality aquitard.
- Adigrat Formation and Antalo Group fractured sandstones and limestones, respectively representing more permeable fractured rock or karstic aquifer units with good quality water.
- Danakil Group and Zariga Formation fine-grained sediments are unlikely to constitute a significant regional source of fresh groundwater, although local primary or fractured-rock aquifers are potentially present in conglomerates and sandstones of the Middle Danakil Subgroup, while local karstic aquifers may be present in the limestones of both the Danakil Group and Zariga Formation.
- Dogua Formation alluvial fans on the west side of the rift basin, form a major, regional primary aquifer.

#### 3.3.6.2 Regional Groundwater Occurrence and Flow System

The Precambrian metamorphic basement with intrusive rocks and tertiary lava flows dominates the geology of the aquifer on the escarpment to the west of the Danakil depression. This aquifer occurs west of the study area on the plateau and north of the study area in Eritrea. The basement rocks have undergone greenschist metamorphism and contain joints, fracture zones and weathered layers which produce secondary aquifers within this broader aquifer. Quartz veins, 10-50 m weathering zones and intrusive dolerite and other mafic dykes represent groundwater targets in the basement. Most of the basement lithologies are, however, aquicludes and hydraulic conductivities in metavolcanic rocks are recorded as being low. Springs are rare but occur along with regional fractures. Groundwater exploitation within basement rocks occurs on a small scale in the form of dug wells and occasional boreholes (Towers, 2017).

Jurassic limestone and cretaceous sandstone deposited on this highly-fractured crust imply high groundwater potential aquifers in the Danakil Depression. The northern part of the depression contains Triassic quartz-rich sandstones that extend into Eritrea which also represent high

groundwater potential aquifers. The productivity of these aquifers will be dependent on the thickness and lateral extent of the formations (Towers, 2017).

Ayeneu *et al.* (2008) confirm that the fractured volcanic covered with thick quaternary sediments of alluvial fans at the shoulder of the rift are the most productive aquifers because of faulting and the occurrence of relatively permeable unconsolidated sediments. Towers (2017) stated that lateral continuity of aquifers and groundwater flow might be locally disrupted by major faults. In this case, groundwater is forced to flow parallel and sub-parallel to the axis of the rift, but to a large degree, the groundwater contours are a subdued imitation of the topographic contours.

The regional groundwater flow system in the Dallol basin is in general controlled by the topographic setting, structures and hydraulic gradients. Much part of the deep groundwater which is recharged from Dallol water shade areas of the western plateau is supposed to drain towards the salt plain in the east.

Groundwater elevation contours were generated from the water level data of existing boreholes. The groundwater flow in the upper and lower subbasin is towards the east and northeast recharging the alluvial fan areas in Musley and Gehertu fans. Here it is supposed from the map that the fan areas in Musley and Gehertu area in addition to percolation from surface recharge, get deep recharge from regional groundwater flow from western highland or water shades through deep structures beneath the ridge which serves as a surface water divide in the area. The elevated ridge or fault escarpment groundwater flow across these elongated structures is along fault lines that form deep river canyons and drainage channels across the ridge towards the salt plain (WWDSE,2013).

### **3.3.6.3 Local Groundwater Occurrence and Flow System**

Locally groundwater is channeled along the dominant faults within the plateau north towards the Ragali River. Adjacent to the Danakil block similar largescale faults occur which possibly channel deep-seated groundwater towards the south. Groundwater flow directions are based on fault orientation, topography and slope (Blake *et al.*, 2017). The weathered regolith and fractured rock aquifer of the basement material is therefore a poor aquifer to target concerning groundwater, east of these faults. The various compartments of the basement material have also

been divided into numerous faulted blocks resulting in smaller recharge areas for each block (Towers, 2017).

Groundwater movement along the larger north-south oriented faults is expected to be large as numerous smaller faults show interconnectivity with the large regional faults (Towers, 2017). The large faults represent secondary aquifers of possibly high groundwater potential and likely good water quality. These faults occur 5-10 km west of the study area.

The Adigrat and Antalo aquifers are of unknown thickness in the lowlands and at the edge of the plateau. These units could represent extensive aquifers at depth, but the lack of lateral extension due to erosion and faulting limits groundwater potential. Faults along the edge of these blocks may represent better groundwater targets west of the study area (WWDSE.2013).

The Danakil Group or Red Sea series represents a large primary aquifer of unknown thickness to the southwest, west and underlying alluvial fan deposits of the study area. This aquifer though extensive, may however be of brackish to saline water quality (Towers, 2017).

The alluvial fan aquifer including alluvium and excluding the clays and saline material at the base of the Danakil depression is of moderate to possibly high groundwater potential. The water quality in these alluvial fans will be fresh to brackish water quality as is seen through the testing of some of the DTW boreholes. Numerous faults underlie and occur along the eastern edge of these alluvial fan deposits and discharge may occur from these faults into the overlying fans (WWDSE, 2013).

Musley Fan, where rocks of the Antalo Group are down-faulted against the alluvial fans structures, separates the horst into northern and southern sections. This separation is a crucial factor in evaluating the potential for fracture through flow from the plateau to the alluvial fans. The difference in lithologies in the study area has implications for the likelihood and quality of water that is transferred through the faults to the alluvial fan aquifers. Limestones and sandstones of the Jurassic-Cretaceous sediments store and consequently transmit fresher quality water into the southern fans, while the Precambrian basement predominantly acts as an aquitard and seemingly allows limited amounts of potentially poorer quality water to recharge the northern fans (MWH, 2015).

Faulting within the rift is complex and extensive with numerous faults playing off the MDRF creating a step-like pattern. Some such faults associated with the MDRF were mapped to be present below and in some cases, transect the alluvial fans. This was confirmed in the geophysical survey carried. The presence of such faults within the alluvial fans implies a possible source of vertical recharge where the water of numerous possible origins flows vertically into the fans via faults and may be considered a possible source of vertical recharge to the aquifer. This may have implications for pump test data analysis as numerous assumptions coupled with analytical analysis techniques are rendered invalid if such a recharge source is present (Driscoll, 1986 as cited in Towers, 2017).

Groundwater Contour map from Water table elevation of test wells drilled on the fan areas shows that in general the groundwater table slopes downwards from the escarpment towards the salt flats and this indicates that groundwater is moving from areas of recharge in the upper reaches of the fan to areas of discharge in the salt flat (WWDSE, 2013).

### **3.3.6.4 Aquifer Types of Different Geological Formations in Study Area**

#### **3.3.6.4.1 Alluvial Fan Aquifers of High Productivity**

The shallow aquifers system in Dallol fan areas consists of inter-fingering layers and lenses of fine to coarse sand, gravel and pebbles which are porous and highly permeable beds that can store and transmit large quantities of groundwater. These aquifers exist commonly in the unconfined system. However, in some parts of the fan, there are thin impermeable clay beds interbedded with these coarse materials forming a confining system for the groundwater in this aquifer. Groundwater trapped between impermeable layers within the fan exhibits artesian flow as the groundwater builds up pressure within the fan. The rise of the water table to a shallow depth that is 44m in test well DTW-5 near to escarpment in Musley fan is an implication of this condition (WWDSE, 2013).

The fresh groundwater aquifer on the fan area has irregular thickness depending on the geomorphologic setting of the fan where the depth to the top of the aquifer is as deep as 90-100m for Gehartu fan test boreholes ( DTW-1 with a well depth of 189m) and shallower 30-70m for Musley fan area ( DTW-10 well depth 130m). The thickness decrease as one goes from the escarpment towards the salt flat. The lateral extension of this aquifer is estimated to be around 12kms towards north and South Musley including Bekerti fan.

#### **3.3.6.4.2 Sedimentary Rock Aquifers of Moderate Productivity**

These are escarpment rocks of sedimentary origin mainly limestone and sandstone and the Danakil red series. Deep test well drilling on the fan area very close to the escarpments shows the existence of these aquifers at different depths beneath the fan sediments. In DTW-2 test drilling (depth 220m) highly fractured limestone aquifer appeared below 160m depth yielding more than 10 l/s with brackish groundwater (TDS 11,000 mg/l). The water table is deep 144m below the ground surface. Similarly in deep test well drilling DTW-4 (250m depth) in the north Musley fan near the escarpments was observed (WWDSE, 2013).

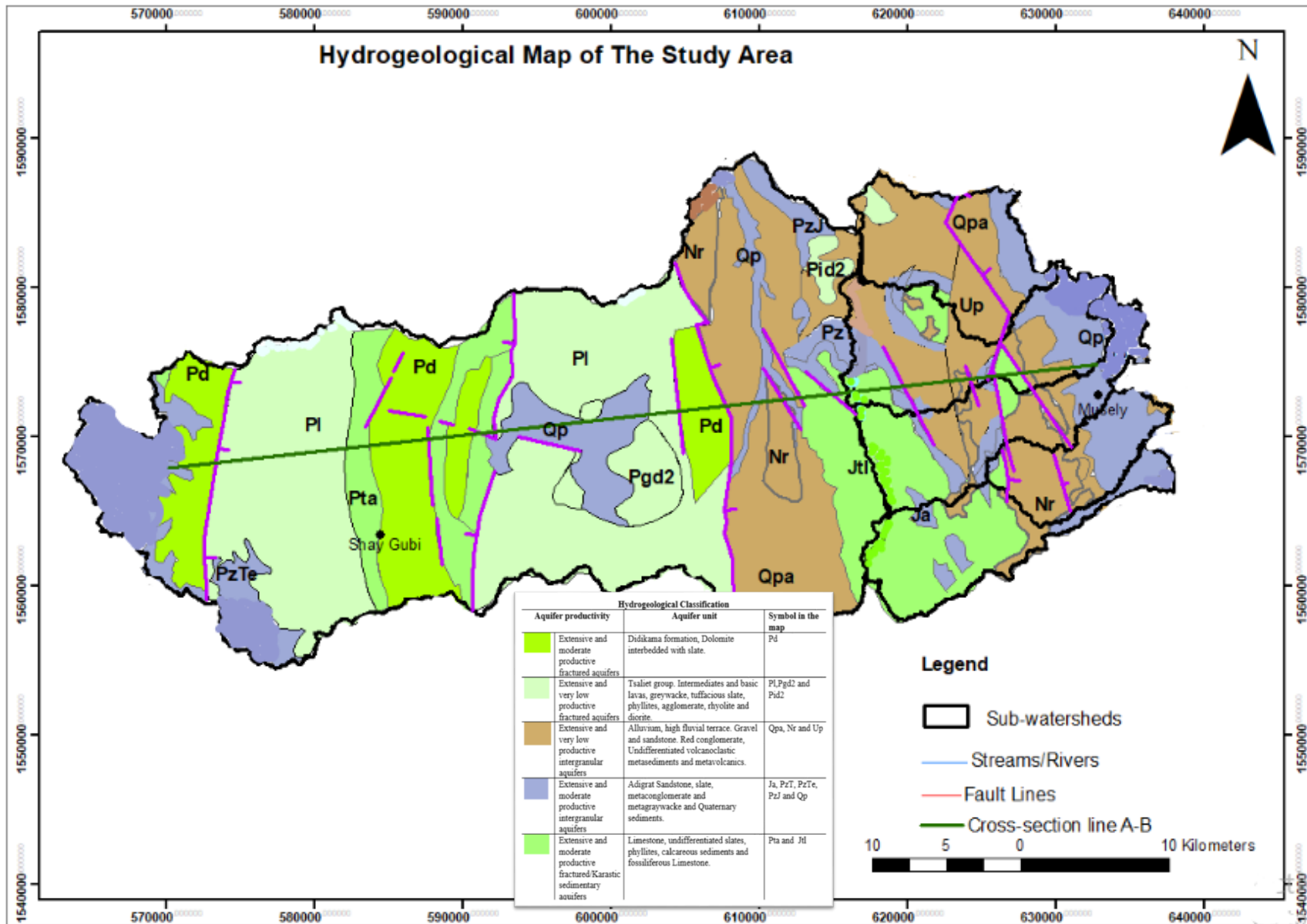
According to WWDSE (2013) the meta-sandstone aquifer appears at a shallow depth 40m below the ground surface. Groundwater in this aquifer exists in secondary openings along fracture zones with a water table 132.8m below the ground surface. The test well drilled in this aquifer yields 12 l/s with minimum drawdown and the water quality is brackish (TDS around 13,600 mg/l). The transmissivity value in these aquifers calculated from pump testing, in general, is around 700 m<sup>2</sup> /day. The aquifer is supposed to be recharged from groundwater flow of water shade areas as subsurface flow along fracture and fault lines.

#### **3.3.6.4.3 Basement Aquifers of Low Productivity**

These are consolidated rock aquifers of low productivity that form wide areas of the western water shade parts of the Danakil basin. Hydrogeological data from Existing boreholes which are drilled for community water supply in the area shows that the aquifers yield 2-3 l/s in the basement rocks with moderately fresh groundwater ( TDS < 1500mg/l ). This aquifer gets recharged from direct rainfall and surface percolation from runoff through fracture zones in the upper water shade areas. The water table is shallow depth and the groundwater quality is fresh (TDS < 1000mg/l).

#### **3.3.6.4.4 Aquicludes and Aquitard**

These include localized Aquicludes of Carbonate precipitates of travertine type and intrusions to extensive mudflats on the salt plain and evaporite beds to the east. The permeability of these formations is very low due to the occurrence of clay beds which retards the groundwater movement. The carbonate precipitates and granitic intrusion serve as local groundwater divides for the shallow groundwater movement in the area.



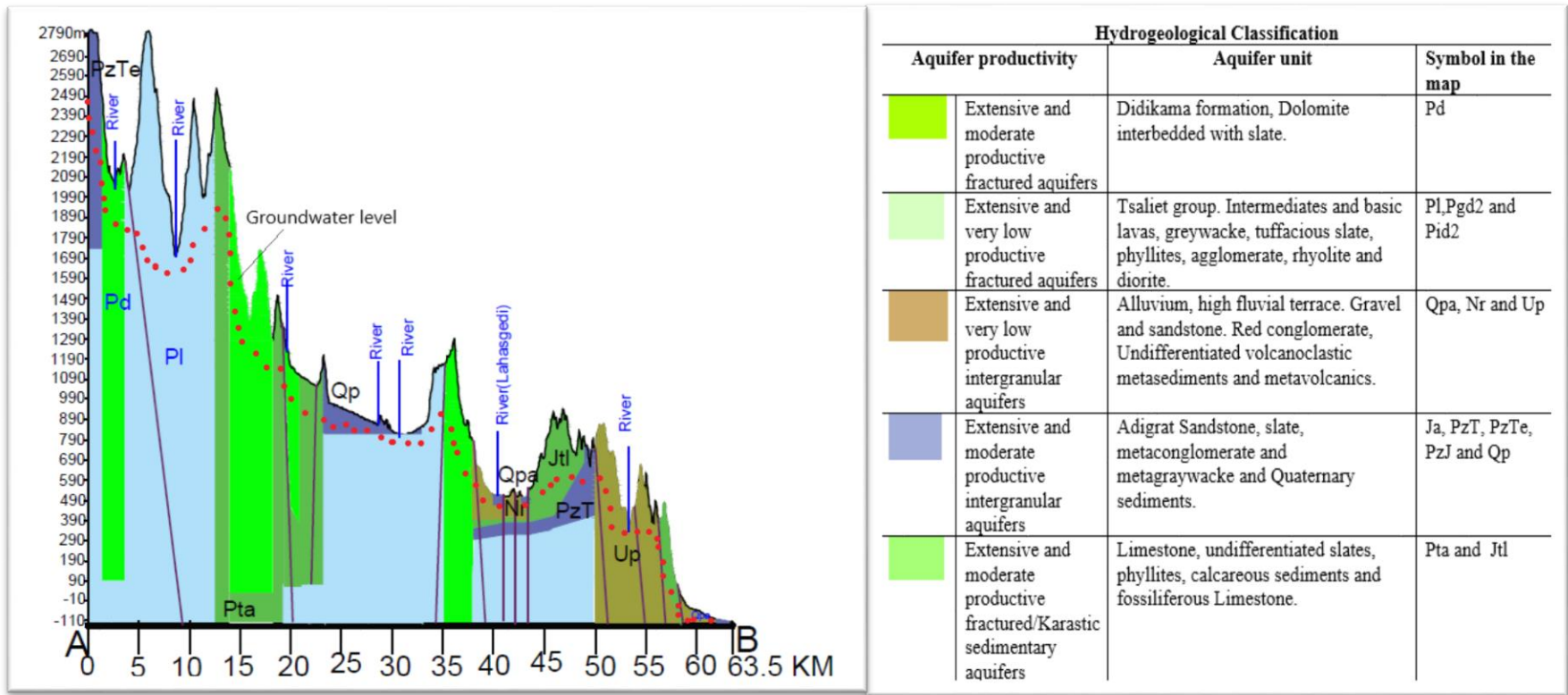


Figure-23. Hydrogeological cross-section with the hydrogeological classification of the study area.

## CHAPTER 4: MATERIALS AND METHODOLOGY

### 4.1 Conceptual Model Development

A conceptual model is a diagram that depicts the groundwater flow system, usually in the form of a block diagram or a cross-section (Anderson and Woessner, 1992). A conceptual model is a simplified representation of the site to be modeled, including the model domain, boundary conditions, sources, sinks, and material zones, in the broadest sense. Building a conceptual model has the goal of simplifying the field problem and organizing the accompanying data so that the system may be more easily studied (Anderson and Woessner, 1992). The simplifying assumptions are necessary partially because a comprehensive reconstruction of the field system is not possible, and partly because sufficient data is rarely available.

All numerical groundwater models are based on a conceptual model, (whether defined or undefined), that at best provides a good approximation of the groundwater conditions. This is because aquifers exhibit increasing complexity as the scale is reduced (even in simple groundwater flow systems) and because natural systems always have significant spatial variability. Consequently, the purpose of the conceptual model is to identify all the relevant groundwater processes that have a significant effect on the groundwater flow system, so that these processes are adequately captured in the numerical model (MWH, 2015).

The first step in the preparation of the conceptual model for this study was identifying the purpose than the identification of the study area, deciding appropriate boundary conditions, creating two-dimensional models of the hydrogeological system and estimating sources and sinks. The primary purpose of this study, therefore, is to understand the boundary conditions, groundwater flow dynamics and the functioning of faults in the study area, to see the hydrochemical evolution, the impacts of the tectonic setting of the rift, and finally to develop a conceptual model with a purpose of running a groundwater flow model along the study area.

#### 4.1.1 Conceptual Framework of Developing Conceptual Model

The conceptual model of the study area is developed based on previous studies and current field investigations to understand the groundwater flow.

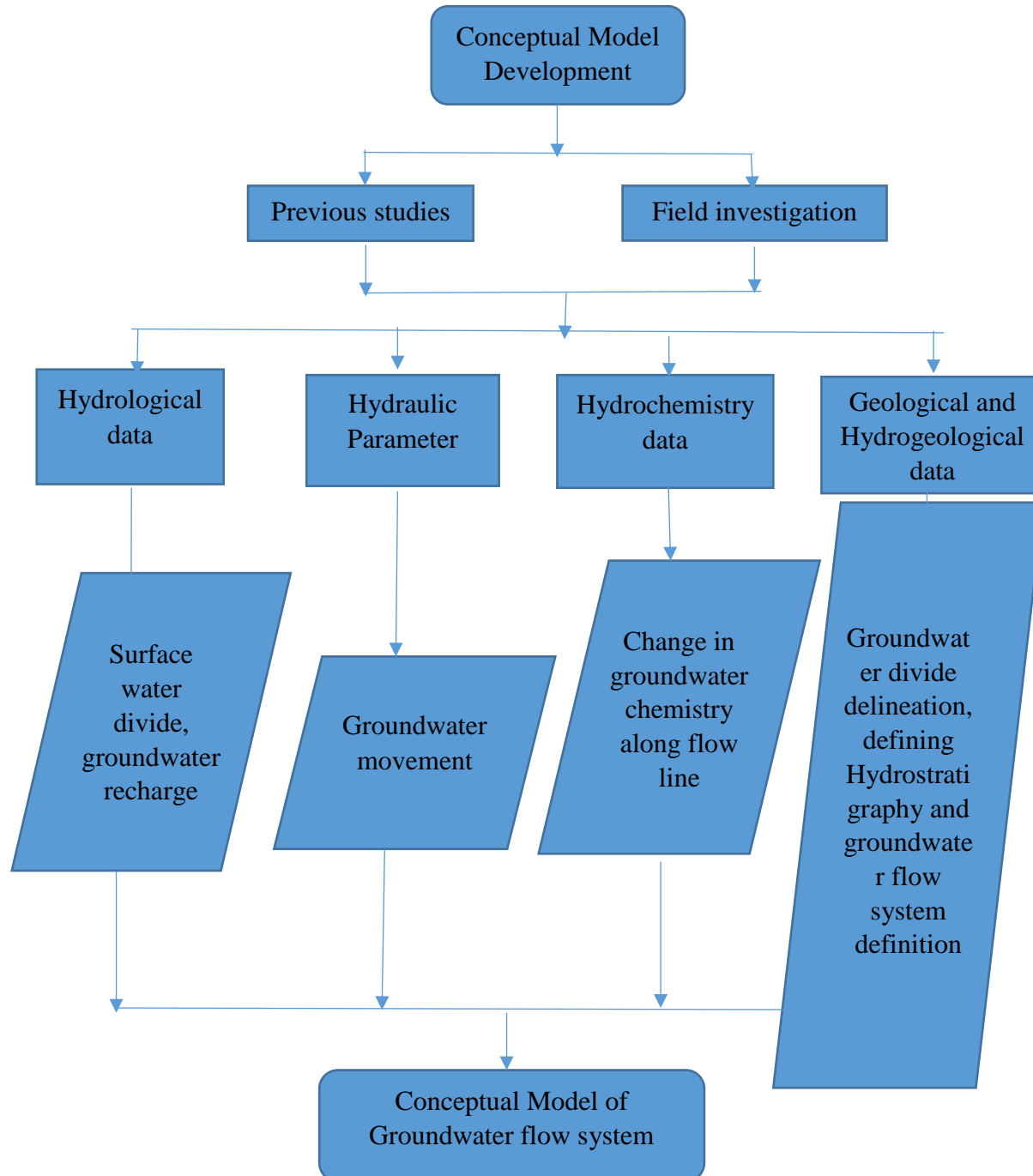


Figure-24. Conceptual framework of developing the conceptual model.

### 4.1.2 Conceptual Model Approach

Geological and hydrogeological mapping, structural mapping, hydrochemical analysis, drilling and pumping data analysis and interpretation, static water level measurement (to estimate flow direction) and analysis also contributed to developing the conceptual model.

Significant steps in building a conceptual model include:

- defining hydrostratigraphic units
- preparing a water budget
- defining a flow system
- defining hydro-chemistry
- boundary conditions

#### 4.1.2.1 Defining Hydrostratigraphic Units

To define hydrostratigraphic units it is good to rely on hydrogeologic information. Site-specific information on stratigraphy and hydraulic conductivity data is required to synthesize hydrogeologic information that is used to identify different hydrostratigraphic units. The regional geological setting of the study area consists of three main geological formations: Precambrian basement and Mesozoic rocks, Neogene-Pliocene sediments and volcanic and quaternary sediments. The Danakil depression lies within the Afro-Arabian Rift System (WWDSE, 2013).

According to Blake (2017), the lithostratigraphy of the Danakil Depression is grouped into four broad hydrostratigraphic units

- ✓ The Precambrian metavolcanic and metasedimentary basement rocks of the Tsaliet Group constitute a relatively impermeable, low-yielding, poor-quality aquitard.
- ✓ Adigrat Formation and Antalo Group fractured sandstones and limestones, respectively representing more permeable fractured rock or karstic aquifer units with good quality water.
- ✓ Danakil Group and Zariga Formation (Coralline reef, limestone, marl and gypsum, (alluvial, lacustrine marine sediments)) fine-grained sediments, which are unlikely to constitute a significant regional source of fresh groundwater. Although local primary or fractured-rock aquifers are potentially present in

conglomerates and sandstones of the Middle Danakil Subgroup, local karstic aquifers may be present in the limestones of both the Danakil Group and Zariga Formation.

- ✓ Dogua Formation (Undifferentiated alluvial fan and debris flow, intercalated with lacustrine and beach sediments) alluvial fans on the west side of the rift basin, which form a major, regional primary aquifer.

The local hydrogeologic units and their aquifer characteristics are:

- Alluvial fan aquifers of high productivity (Shallow Aquifer System);
- Alluvium Aquifers of Graben Areas and Intermountain plains of Moderate productivity;
- Sedimentary Rock Aquifers of moderate productivity (Deep Fractured Aquifer System near the Escarpments) ;
- Basement Aquifers of low productivity ( Metasedimentary and Metavolcanics rocks) and
- Aquicludes and Aquitard

Table 1. Lithostratigraphy and Hydrostratigraphy (Data source: MWH, 2015)

Geological Age	Formation name	Symbol on Map	Proven- indicated Thickness	Lithostratigraphy	Hydrostratigraphy
Quaternary(Holocene –Pleistocene)		Qp	0-192m	Alluvium, silt, sand and gravel	Thin primary aquifers at the surface, but predominantly (aquicludes)
	Enkafala formation	Qpe		Marine sediments. Oolitic and reef limestone, conglomerate, marl and gypsum	Local karstic aquifers
		Qpa		Alluvium, high fluvial terraces. Gravel and sandstone	Primary aquifers
Tertiary(Neogene)	Salt formation	NQs	500-2500M?	Halite, potash, gypsum and shale	Thin primary aquifers at the surface, but predominantly evaporites (aquicludes)
	Danakil formation(Red series)	Nr	150-350M	Red conglomerate, intercalated basalt flow and pyroclastics	Local primary and/or secondary (fractured-rock) aquifers in conglomerates and sandstones
Upper Paleozoic-Mesozoic	Antalo group	Jtl	600-1080M	Limestone, fossiliferous and sandy limestone	Possible karstic and fractured aquifers
	Adigrat group	PzJ	250-820M	Undifferentiated (various sandstone, conglomerate, shale, erratic boulders, tillite)	Possible secondary (fractured-rock) aquifers
		Ja		Sandstone, siltstone and shale	
		PzT		sandstone, conglomerate, shale, erratic boulders, tillite	
	PzTe	Coarse-grained cross-bedded sandstone			
Precambrian (lower Paleozoic)	Upper complex	Up	>1520M	Not divided (Metavolcanics, phyllites, greywacke, slate)	Aquicludes
	Didikama formation	Pd		Dolomite interbedded with slate	
	Arequa formation	Pta		Undifferentiated (Slate, phyllites, calcareous sediment, limestone)	
	Post tectonic intrusion	Pgd2, Pid2		Granodiorite, Diorite and quartz diorite	
	Tsaliel group	Pl		Intermediate and basic lavas, greywacke, tuffaceous slate, phyllites, agglomerate, rhyolite	

#### 4.1.2.2 Preparing a Water Budget

Moreover, a conceptual model should consist of the source of water as well as the expected flow directions and outflows. From the total inflows (recharge) and outflows (sub-surface outflow, well withdrawal, spring discharge and baseflow) in the system, a water budget should be prepared to summarize the magnitudes of different flows and changes in storage (UNVOTO, 2017).

The inflows, through flows and outflows of the pertinent part of the groundwater system, were based on direct or indirect measurements, where available, or otherwise calculated values. The water balance defines the upper limit (Safe Yield) of the alluvial fan groundwater systems. However, it is important to note that other factors such as water quality deterioration may reduce the Deployable Output (the water supply yield that can be obtained) from a wellfield in an alluvial fan. As a result wellfield pumping rates are likely to be less than the Safe Yield defined by the water balance (MWH, 2015).

#### 4.1.2.3 Defining Flow System

The study area is a part of the upper Dallol watershed including six sub-basin covering 1471.492 Km<sup>2</sup>, all drained from west to east. These catchments are typified by steep slopes in the upper reaches with high energy flows and steep flow paths. The lower reaches are typified by lower energy flows with wider flatter flow paths over deep alluvium.

Understanding how regional tectonics may control the general geomorphology and geology of an area is crucial in understanding the groundwater flow system of rift zones. This requires the definition of the overall rift structure and the related geological features of particular emphasis given to the understanding of the geometry and segmentation of the main fault patterns (Beyene *et al.*, 2005).

The Danakil basin's catchment area extends from the Ethiopian Plateau in the west to the Danakil Alps in the east with all runoff, rivers and streams flowing towards and ending in the endorheic Danakil depression (Umvoto Africa, 2017). The rivers and streams are non-perennial or sub-surface flows that occur as steeply carved ravines within the plateau and as braided and meandering flows within the alluvial fan and lower-lying areas of the depression (Holwerda and Hutchinson, 1968).

According to Umvoto Africa (2017) it is assumed that there would be a fairly rapid rainfall-runoff response, particularly in the upper reaches of the catchments following significant rainfall events. Runoff is expected to be highest during the rainy season (June to August). Runoff at the lower reaches will be more lagged than the runoff in the upper reaches due to the nature of the topography (flatter) and riverbed material (alluvium).

Fault structures extend into the escarpment which increases the likelihood of them being significant conduits of groundwater flow from the plateau to the alluvial fans. This is particularly the case in the southern region near the Musley Fan, where rocks of the Antalo Group are downfaulted against the alluvial fans (Umvoto Africa, 2017).

#### **4.1.2.4 Defining hydro-chemistry**

The groundwater chemistry of Dallol watershed areas is generally characterized as moderately freshwater with a mean TDS value of 957.7 mg/l. The topographic control on the variation of TDS is observed with increased values towards the lower elevation. Regarding the pH of the groundwater, almost all samples show basic water with a measured pH value greater than 7 only very few 17 % of the total samples show Acid water with pH less than 7 value and only very few samples show values close to neutral (6.95).

Water quality analysis results from test boreholes on the fan areas show all ranges of water quality fresh, brackish and highly saline groundwater depending on the depth of boreholes and the nature or thickness of the fan sediment. The groundwater quality analysis result of the two major fan areas of Musley and Gehertu clearly shows the availability of fresh groundwater with TDS values less than 1000 mg/l with a higher quantity of groundwater (DTW-1, DTW-5 and DTW-10).

The depth of drilling, the lithology of the fan sediment (fine to coarse material) and the thickness of the fan are the major controlling factors for the variation of groundwater quality at depth and laterally.

From the above summary of the water quality analysis results, it is observed that excessive mean concentration values of TDS ( total dissolved solids) are resulted due to excessive concentration values of Sodium, Calcium and Chloride ions which resulted from gypsum and evaporites beds at depth below the fan sediment.

Test boreholes where the bottom depth of drilling crossed the fresh and saltwater interface have yielded highly saline groundwater in the fan area. The depth of fresh and saltwater interface on the fan areas varies depending on the fan thickness and hydro lithology of the fan material.

#### **4.1.2.5 Boundary conditions**

Boundary conditions assigned to the conceptual model were chosen to approximate the regional groundwater flow patterns. The boundary system for the study area was considering both surface water boundaries and hydrogeological boundaries. For hydrological boundaries, the main western boundary is located along the Lelegheddi River (a major tributary of the Ragali River). And the western escarpment is also a major divide for surface water flow. For the groundwater divide, hydrogeological boundaries, complex fault systems in the study area and the special continuity of rocks are considered. The groundwater divide study area west to east coincided with the surface water divide.

#### **4.1.3 Schematic Section of the Conceptual Model Groundwater Flow System**

A schematic section of the conceptual model groundwater flow system is presented in Figure-27 below. This shows a section from the western highlands at the Danakil rift catchment boundary down to the Danakil rift floor along a transect through the Gehertu fan. Formation thicknesses in this schematic figure are merely indicative of previous studies.

The schematic figure also shows groundwater flow through the bedrock from the highlands to the graben where some of the flow is discharged into the tributaries to the Regali River. Some of the bedrock flows pass under the river alluvium and continue down to the Danakil rift. This system contributes fresh and brackish water. The brackish water flows up from depth along the margin of the rift and at least some of the flow is transferred upwards in the rift boundary fault. However, it is likely that flow occurs in a zone and not exclusively up the rift boundary fault.

The groundwater at the top of the Precambrian bedrock is fresh but the percentage and depth of the freshwater are not known. Wadi sands and gravels appear to act as a drain capturing a significant percentage of the shallow bedrock freshwater flows and transferring these flows into their respective alluvial fans.

Jurassic Adigrat Formation and Antalo Group as well as the Danakil Group hydrostratigraphic units are also expected to transmit fresh and brackish groundwater from the Precambrian bedrock as throughflows via the alluvial fans to the density-interface zone.

Groundwater levels in the playa salt flats indicate that groundwater is almost entirely lost as soil evaporation, and the rate of evaporation is controlled by the groundwater depth. The groundwater evaporation and bedded halite rock within the rift generate saturated brine conditions. The brines form a density interface with the fresh and brackish water flowing out of the escarpment bedrock. The brine has a density that is 10% higher than fresh water and forms an impenetrable barrier to the escarpment bedrock flows. It thus forces the groundwater up towards the ground surface.

The alluvial fans transmit fresh, and also brackish, water from the bedrock to the salt flats. The clay layers within the alluvial fans are important because the low hydraulic conductivity of these units limits the groundwater flows through the fans and requires the west to east directed flows to leak across each clay layer, it potentially protects the fresh water in the fans by preventing backflow of brine from the brine density interface mixing zone and it protects the fresh water in the fans by preventing saltwater upcoming during pumping of the brine present in the bedrock below the fans. This shows that over-abstraction can be a cause of salt water intrusion.

The spatial patterning of hydrochemistry and isotope results from individual boreholes, including available hydrochemistry data from earlier studies was combined with an analysis of probable flow paths using the hydrostratigraphy, structural geology, climatic data, and observed patterns and processes in the field to summarise components of the modeled recharge scenarios.

The recharge is from high rainfall along the escarpment and direct infiltration since the aquifer in the study area comprises unconfined. The regional and local groundwater from the fractured basement in the highlands and intergranular and karstic rocks in the gentler slopes discharges in an easterly direction. It can be into rivers, streams, gulleys, in the foothill of the escarpment or flow along faults, also discharged into fans, groundwater flow in silty and sandy sediments discharged through evapotranspiration, groundwater discharged into wadis, evaporites. Some of the discharge ends up as streamflow, whereas the main discharge path is evapotranspiration.

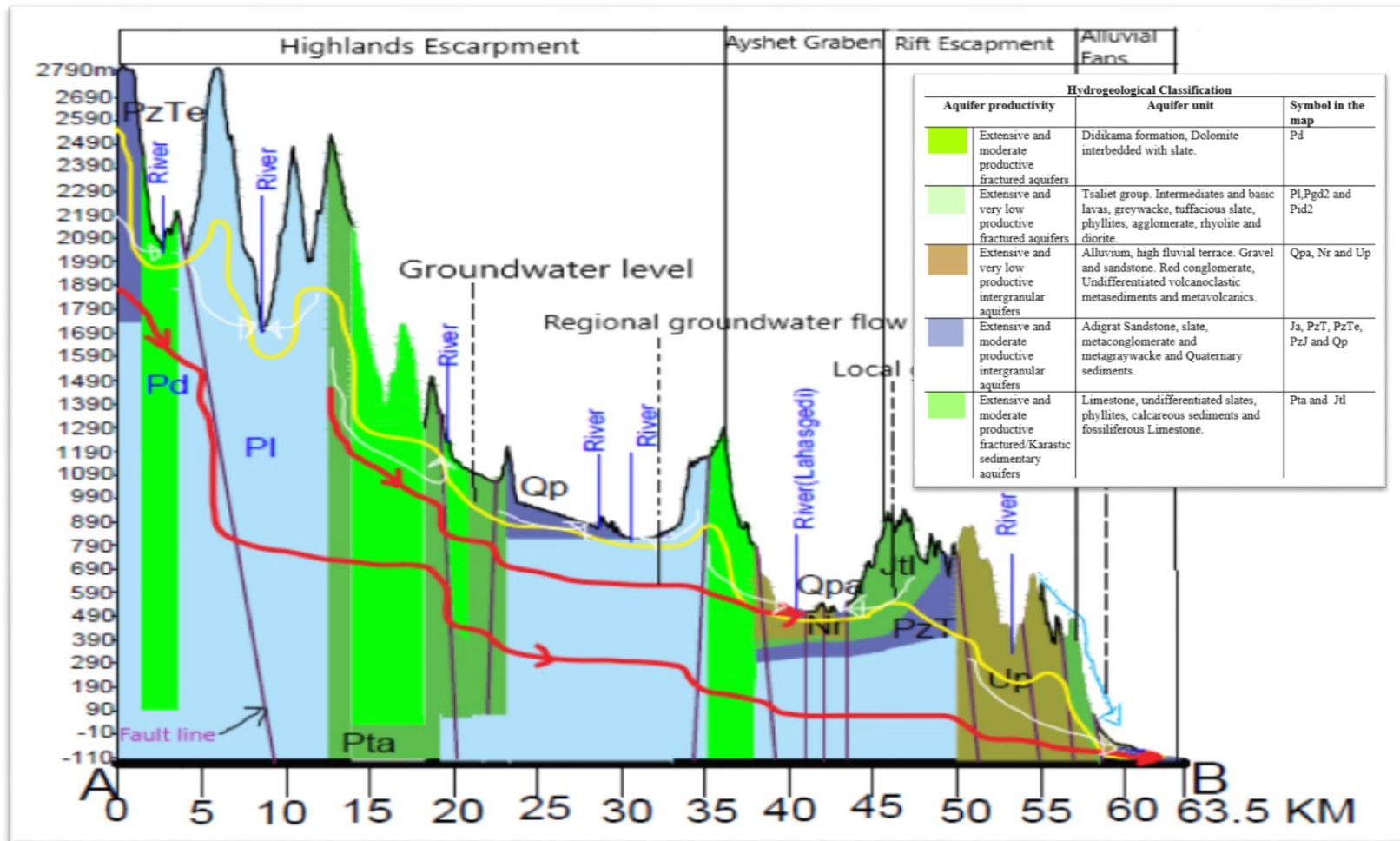


Figure-25. Schematic section of the conceptual model groundwater flow system of the study area.

## 4.2 Numerical Model Development

Because of its ability to efficiently simulate multiple physical processes in a small and large region with no associated cost, this study uses the publicly available SWAT–MODFLOW tool. Mainly this tool is selected due to its ability to predict the effect of natural (geogenic) influences on the watershed, which relates to the aim of this research work.

The methodology of this study has the components of data collection, data processing, running models, calibration, validation and model interpretation. The basic activities accomplished to meet the objectives of this research are extensive fieldwork, primary and secondary data collection from concerned offices and open sources. The study started by reviewing different kinds of literature related to the research work.

Table 2. The input data, source and type.

Input data	Type	Source
Topography	Digital elevation model (DEM),30m resolution	Ethiopian Geospatial Information Institute
Land use/Landcover	Ethiopia_Sentinel2_LULC2016	<a href="http://opencommons.org/ethiopia_sentinel2_LULC2016">http://opencommons.org/ethiopia_sentinel2_LULC2016</a>
Soil	Soil raster map	FAO
Weather/climate	Max/min Temperature, Precipitation, Wind, Relative humidity and Solar	CFSR( <a href="https://globalweather.tamu.edu/">https://globalweather.tamu.edu/</a> )
Borehole	Groundwater level, quality data, details for observation wells, subsurface thickness, hydraulic head, pumping scenario, conductivity, specific yield and storage properties.	Circum production and monitoring wells were drilled by RMES in the year 2016, Dallol test wells (DTW) drilled by Beles Engineering in the year 2013 and WWDSE in the year 2013, the fan monitoring wells (FMW) and pumping wells (FPW) drilled during the Yara study since 2015.
Hydrogeological data	Hydrogeological, geological maps and reports	Geological Survey of Ethiopia.

The research study incorporated different activities that were performed during pre-field, field and post-field time. The process flow diagram shows those activities (see figure-26).

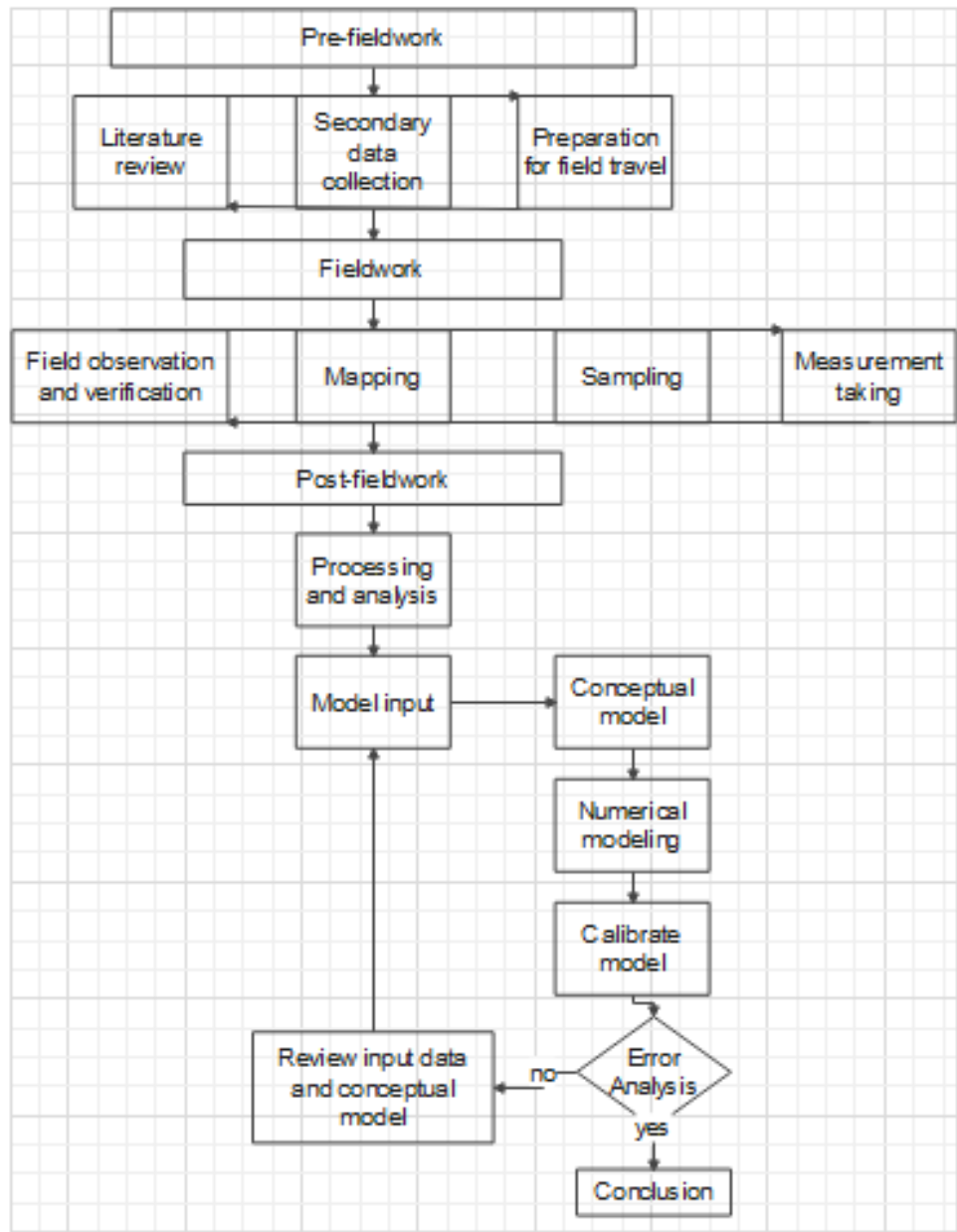


Figure-26. Process flow diagram of the research study.

Table 3. The major software used for this study.

Softwares used	Interface(program)	Purpose
ArcGIS 10.3	-	mapping, geo-referencing and digitizing
QGIS 3.20.2	QSWATMOD2	Coupling SWAT-MODFLOW
SWAT 2012	ArcSWAT2012, pcpSTAT,dew.02, Mapwindow(MWSWAT)	SWAT simulation
ModelMuse 4.3.0.0	MODFLOW-NWT,MT3DMS	MODFLOW simulation
SWAT-MODFLOW-V3	-	Coupling SWAT-MODFLOW
DRASTIC	ArcGIS	Vulnerability mapping
Erdas Imagine	-	Satellite image processing
Global mapper	-	For cross-section
AutoCAD	-	For cross-section

#### 4.2.1 SWAT Model Development

To optimize the utilization of ground water and surface water, there is a need to estimate the ground water recharge for sustainable water management. To know the annual, decadal changes in the ground water recharge several techniques were implemented to access the ground water recharge on smaller scales (Guzman *et.al.*, 2015). In this paper, ground water recharge is estimated by integrating SWAT with the MODFLOW model. The HRUs are disaggregated i.e., converting from multipart to single part polygons. There is a need to spatially locate the HRUs which are generated from the SWAT model (Bailey *et.al.*, 2016).

The surface water hydrology and contaminant transport of the research region were built using the SWAT model with the ArcSWAT 2012 interface. The digital elevation model (DEM), soil, land use land cover, and weather data) that are acquired from various sources are the main input data for SWAT model simulation utilizing the ArcSWAT interface in ArcGIS (see table-3 above).

A digital elevation model (DEM) was then imported and used to delineate the watershed into 6 sub-basins with an area of 1471.492 Km<sup>2</sup> and to replicate the water network of the study area. The model calculates the direction and accumulation of surface water flow based on low elevation points and represents in each sub-basin, a tributary stream that eventually joins into the Regale River. Upon defining the main outlets of the watershed, the boundaries and hydrologic parameters of the entire watershed are then delineated. The Alluvial fans are located on the eastern part of the watershed on the transition zone to the salt plain, which is divided from the upper sub-basin by the escarpment.

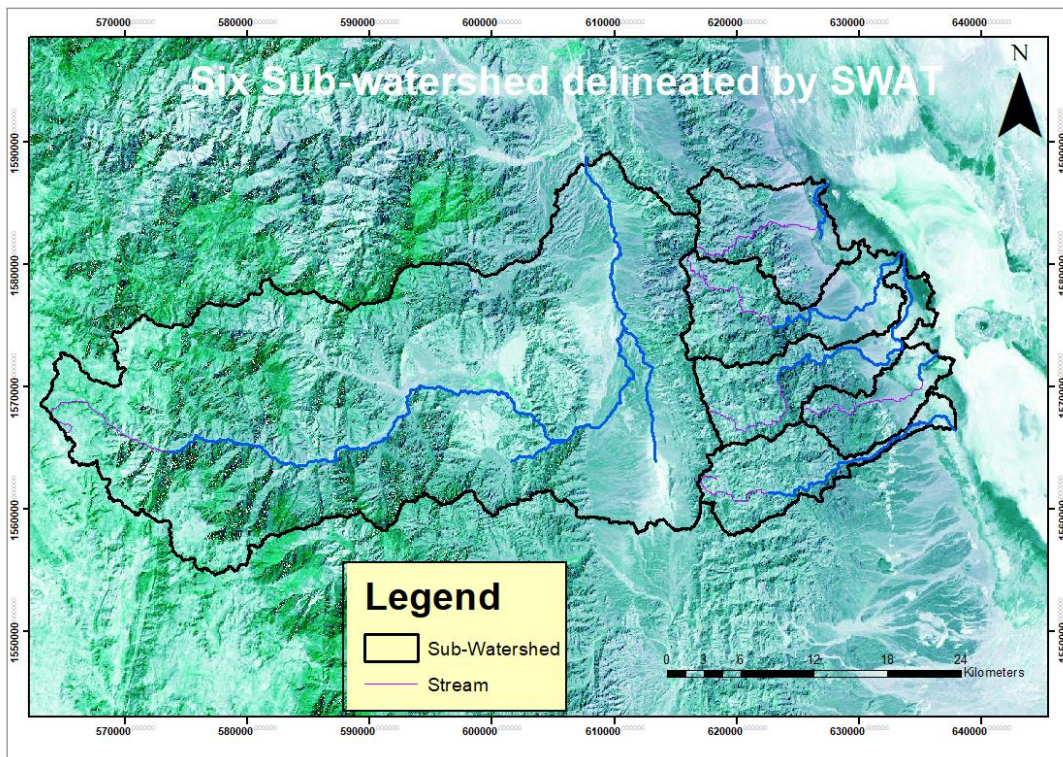


Figure-27. Sub-watershed that contain alluvial aquifer of the transition zone.

Hydrological response units (HRUs) analysis step of SWAT model development was performed followed watershed delineation step. To perform HRUs analysis in the SWAT model the land use and the soil data in a projected shapefile format were loaded into the ArcSWAT interface to determine the area and hydrologic parameters of each land soil category simulated within each sub-watershed. The land cover classes were defined using the look-up table.

Based on existing soil and land use maps, 4 types of soil and 9 land-use types were defined in the study area of Danakil. The major soil type in the study sub-watershed is Clay loam, sandy clay loam, loam and salt (See figure-28).

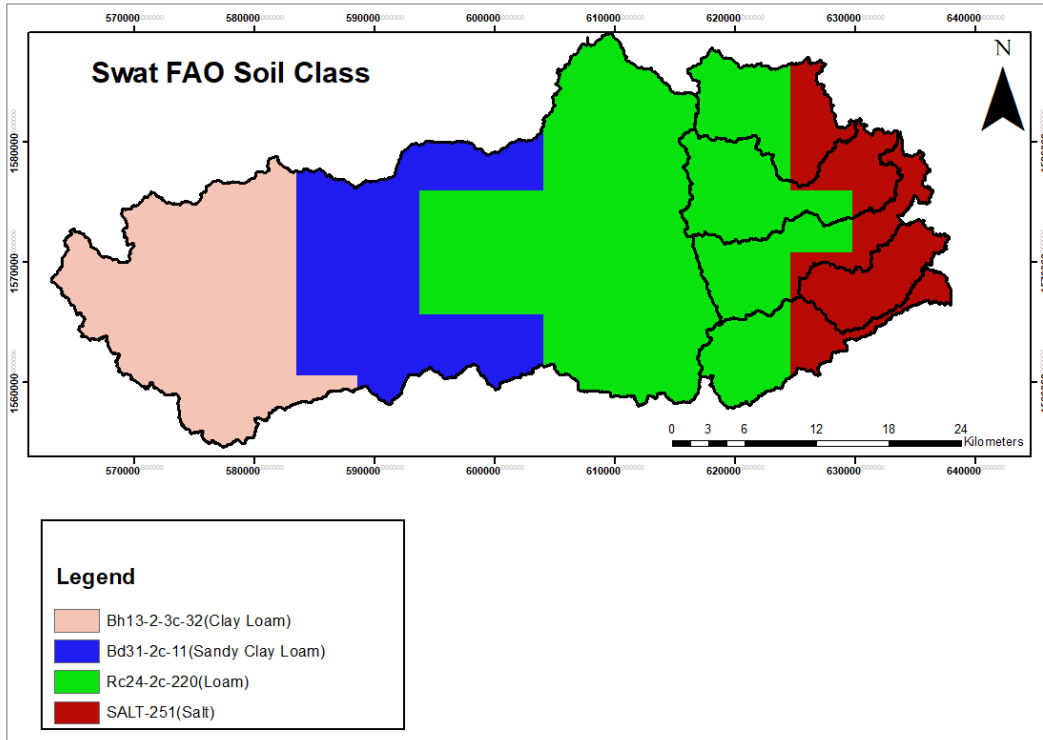


Figure-28. Soil classes in the study area.

There major land use land covers classes in the study area are: trees cover areas, shrubs cover areas, grassland, cropland, vegetation aquatic or regularly flooded, lichen mosses / sparse vegetation, bare areas, built-up areas and open water (See figure-29).

The DEM data used during the catchment delineation was also used for slope classification of the study area. The slope class in the study area ranges from 0% to >121% (see figure-37).

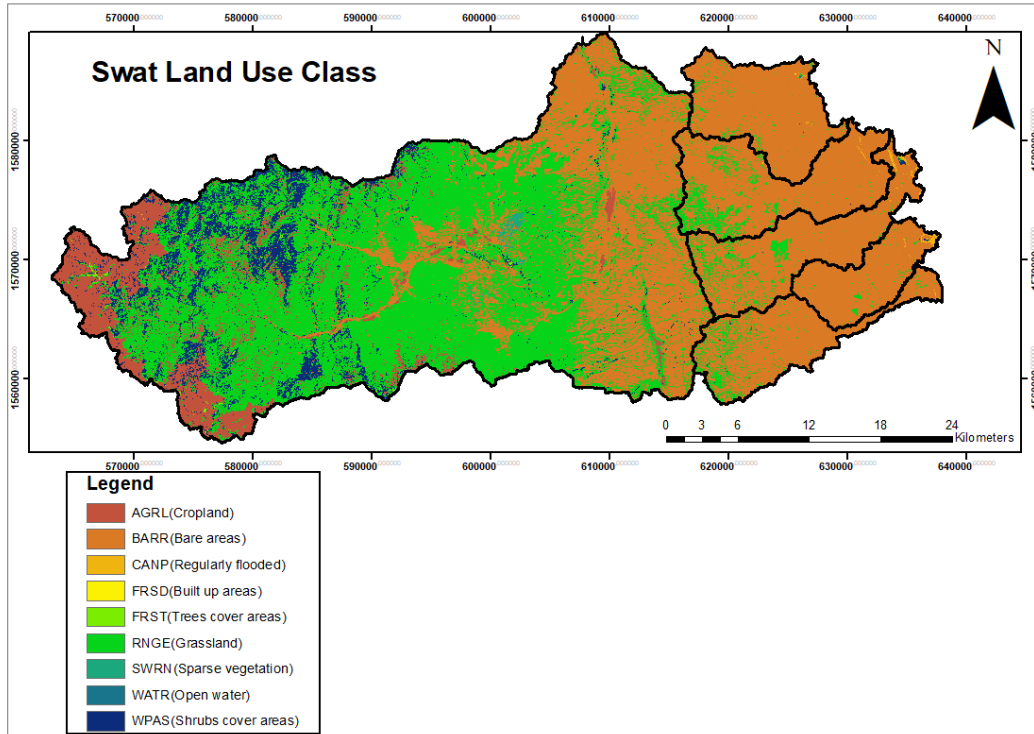


Figure-29. Land use classes in the study area (Source [http://opencommons.org/ethiopia\\_sentinel2\\_LULC2016](http://opencommons.org/ethiopia_sentinel2_LULC2016)).

Hydrological response units (HRUs) were constructed using full physiographic data in this work, resulting in a large number of HRUs, which is crucial for linking the SWAT-MODFLOW model. For this study, the hydrological response units (HRUs) analysis yielded 127 HRUs for six sub-basins (See figure-30).

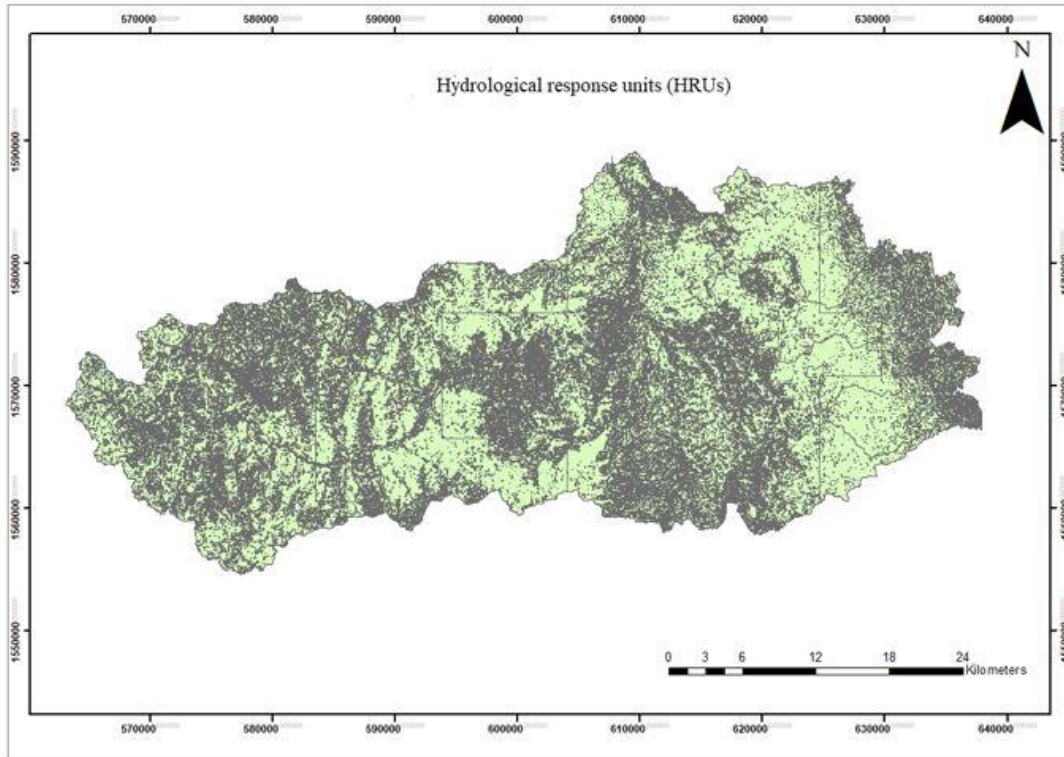


Figure-30. Defined hydrological response units (HRUs) in the study area.

The write input table step of ArcSWAT interface weather data was used. Historical weather data, including precipitation, temperature, relative humidity, wind speed, and solar radiation, were collected from open-source climate forecast system reanalysis (CFSR) and were incorporated into the model for the period 1998 to 2014 (17 total years). From a total of 17 years of weather data, 2 years of the data were used as a warm-up period for SWAT model simulation which makes the total run period 15 years. A weather generator was prepared for all stations of CFSR within the study area and copied into the ArcSWAT reference database.

#### 4.2.1.1 Checking Weather Data Quality

##### 4.2.1.1.1 Daily Rainfall Data Used in Modeling

Daily climate forecast system reanalysis (CFSR) data from 1979 to 2014 were obtained from open-source (<https://globalweather.tamu.edu/>). The CFSR was initially chosen as the preferred option to infill missing rainfall data due to it being commonly used in SWAT applications, and having been previously applied by Worqlul, *et al.*, (2015) and thereby presumably suited for use in this study.

There are six CFSR stations in and around the study area. The resolution of the CFSR dataset is also finer than most similar datasets (grid spacing of 0.25 degrees) capturing rainfall variability more effectively while the record length is sufficiently long at over 30 years, enabling a normalized rainfall record (including average, dry and wet periods).

Table 4. Monthly averages of the CFSR dataset for the study area for the period 1998-2014.

Month	CFSR Stations					
	Station-01	Station-02	Station-03	Station-04	Station-05	Station-06
January	6	8	28	28	7	9
February	10	12	41	34	11	10
March	34	34	96	65	19	10
April	53	50	129	80	16	10
May	49	44	57	35	5	3
June	100	65	40	21	3	2
July	529	378	244	130	20	12
August	587	438	323	182	37	27
September	78	49	40	22	2	2
October	24	24	30	22	3	2
November	6	7	26	25	4	3
December	4	6	16	18	2	3
Total	1480	1107	1054	644	127	90

#### 4.2.1.1.2 Available Meteorological Stations around the Study Area

In the absence of observed streamflow, the development of a hydrological model was necessary to better understand the rainfall-runoff response, as well as the seasonal (monthly) variability of streamflow. It is also necessary to quantify the long-term rainfall-runoff response of an area where observed records are limited (WWDSE, 2013).

The Danakil basin (including the study area) has relatively poor availability of long-term hydrological observations. The collected data from meteorological stations located around the study area were not properly recorded and it is only for a short length of 2-8 years with a limited meteorological data type.

Table 5. List of Meteorological Stations around the study area.

No.	Name of Stations	Location			Data Length
		Elevation	Northing	Easting	
1	Adigrat	2449.8	549638	1577303	1997-2018
2	Wukro	1991.2	564854	1523197	2005-2018
3	Berhale	667	610220	1532659	2007-2019
4	Kuneba	1202.3	593603	1545016	2009-2010

Table 6. Mean monthly rainfall (mm) with two months missing data around the study area.

Station	Jan	Feb	March	April	May	June	July	Aug	Sep	Oct	Nov	Dec	Total
Adigrat	5.2	31.5	53.1	24.4	45.3		152.2	135.9		63.5	35.2	11.7	557.9
Berhale	1.6	3.4	13.0	20.0	15.9	16.6	105.0	120.9	16.9	2.9	2.9	0.5	319.5
Wukro	1.0	3.5	14.8	28.1	24.2	38.3	207.5	209.7	37.7	4.1	3.3	1.9	574.1

#### 4.2.1.1.3 Potential Evapotranspiration Estimation

Potential because it is the generator of atmospheric evaporative demand, evapotranspiration (PET) is another significant climate variable in hydrological modeling. The FAO Cropwat program was used to produce monthly evapotranspiration (PET) values for the Adigrat meteorological station, as shown in table-8. The FAO-56 Penman-Monteith method was used to estimate reference evapotranspiration ( $ET_0$ ), which has been suggested as the standard method.

Table 7. Mean monthly evapotranspiration over the study area.

Month	Min Temp (°C)	Max Temp (°C)	Humidity (%)	Wind (km/day)	Sun (hours)	Mean Monthly Eto(mm)
January	19.2	32.8	54	346	9	196.5
February	21	34.3	57	346	9	186.8
March	22	36.3	55	346	8.5	227.2
April	23.7	38.2	53	346	9.1	240.9
May	26.5	41.1	44	259	9.3	254.5
June	28.3	41.9	44	259	7.9	241.5
July	28	41.3	37	259	6.9	253.0
August	26.6	40.6	44	259	7.7	244.9
September	26.1	40.3	40	259	6.8	234.0
October	23.9	38	40	259	8.4	233.1
November	21.5	36.3	49	346	9.5	223.2
December	20.3	33.7	56	346	8.9	195.6
Average	23.9	37.9	48	302	8.4	2731.2

Zhansheng *et al.* (2018) stated that the Hargreaves method, proposed by Hargreaves is also named Hargreaves-Samani (HS) equation method. The HS method is the most commonly used temperature-based method and is recommended by FAO as an alternative method for PET estimation when observed weather data are unavailable.

$$ET_{HS} = K_{RS} \cdot Ra \cdot (T_{max} - T_{min})^{HE} \left( \frac{T_{max} + T_{min}}{2} + HT \right) \quad (1)$$

Where  $ET_{HS}$  is daily PET in mm/day;  $Ra$  is extraterrestrial radiation in mm/day;  $T_{max}$  and  $T_{min}$  are daily maxima and minimum air temperature in °C respectively;  $k_{RS}$  is the empirical radiation adjustment coefficient;  $HE$  is the empirical Hargreaves exponent, and  $HT$  is empirical temperature.

The CFSR stations within the project area were used to estimate evaporation. In the development of a hydrological model for the study area, PET estimates were derived from climatic variables the CFSR stations provide (i.e. max/min temperature, solar radiation, wind speed, relative humidity). These variables enable the estimation PET using the Hargreaves method.

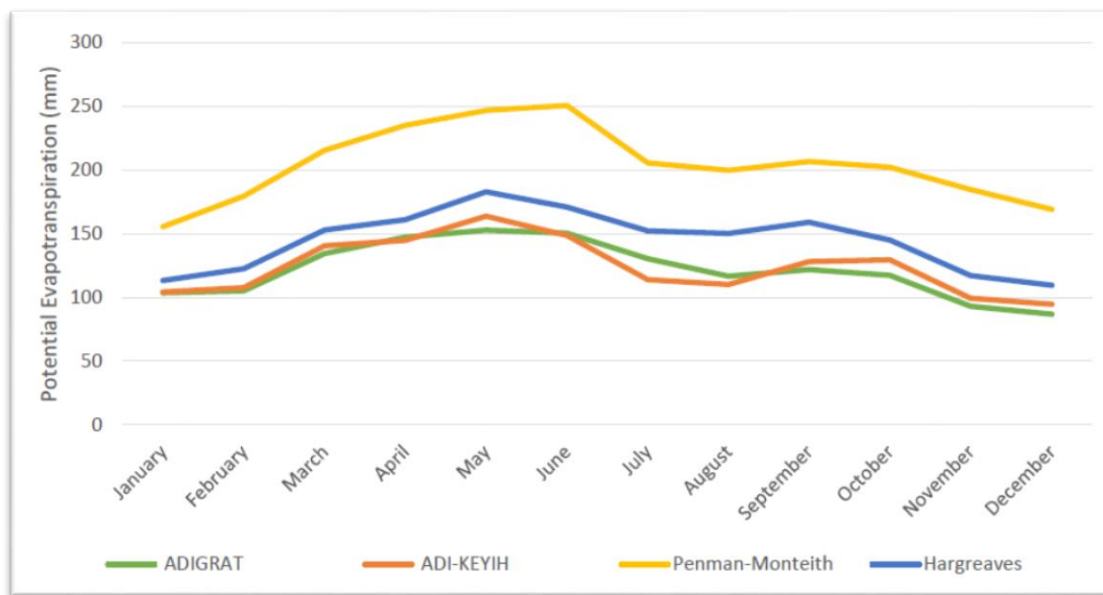


Figure-31. Potential evapotranspiration comparison, showing Penman-Monteith overestimation.

As illustrated by Figure-34 the PET estimates using the Hargreaves method of PET estimation, being closer to the estimates of Adigrat and Adi-Keyih were consequently selected for checking the weather data quality for the SWAT model. A considerable rainfall to PET is consequently present when selecting either the Hargreaves or Penman-Monteith methods.

#### 4.2.2 MODFLOW Model Development

In this study, the groundwater model is developed with software that uses a numerical code to solve the equation that mathematically describes the flow of groundwater and the information contained in the conceptual model is translated into its numerical equivalent which is solved by the numerical code to generate model results.

The MODFLOW package of ModelMuse 4.3.0.0 was used to create the groundwater flow model that encompasses the six sub-basins. MODFLOW is a finite-difference model that solves three-dimensional groundwater flow through porous earth. This study used MODFLOW-NWT version 1.2.0 03/01/2020 (Niswonger *et al.*, 2011), which is a Newton–Raphson formulation for MODFLOW-2005 version 1.12.0 02/03/2017. The modular three-dimensional multi-species-transport model MT3DMS version 5.30 was used to simulate dissolved constituent advection, dispersion, and chemical reactions in groundwater systems.

ModelMuse version 4.3.0.0 was employed as the pre and post-processor to input layer elevations, construct the model boundary conditions and hydraulic parameters, generate input files, run MODFLOW-NWT, and analyze model results before coupling. The main components of the data set that was built using ModelMuse4.3.0.0 are model grid, model layer, hydraulic parameters, storage and porosity, evapotranspiration, recharge/infiltration, basic transport, advection, dispersion and chemical reaction packages.

MODFLOW-NWT uses the upstream weighting (UPW) package to smooth storage variations during cell wetting/drying and transitions between confined and unconfined conditions because the study region is located in the arid zone of the Danakil basin. MODFLOW-NWT provides several benefits over MODFLOW-2005, including the ability to simulate groundwater flow in an unconfined aquifer without switching dry cells to inactive cells and the ability to calculate hydraulic head for dry cells throughout the simulation (Niswonger *et al.*, 2011). The UPW program calculates the groundwater head from the inflow to the dry cells by setting the flow out of the dry cells to zero.

The stream network generated using the SWAT model was imported to MODFLOW to create the stream cells; using the river package in ModelMuse (see Figure-35). Initial hydraulic head, riverbed conductance, and hydraulic conductivity were processed and incorporated into the

model to simulate steady-state groundwater flow. The recharge was summarized from SWAT output in the sub-basin-scale and imported to MODFLOW.

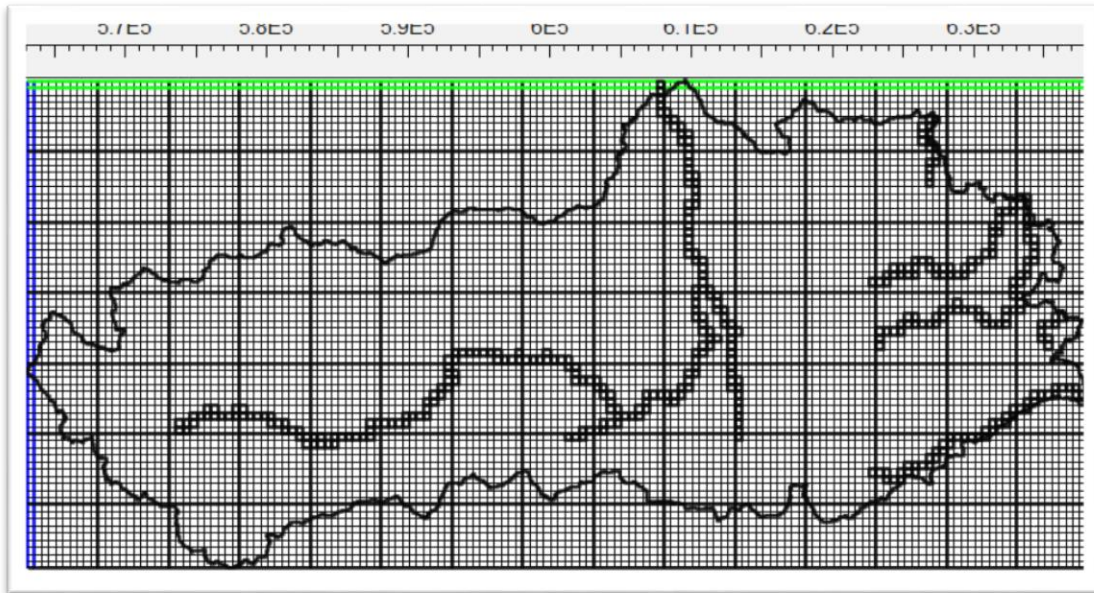


Figure-32. Stream cells in ModelMuse.

The discretized model area was 1471.492 km<sup>2</sup> of active cells, with a length of 75 km in the x-direction and 35 km in the y-direction. The model area was discretized into a 100 m x100 m horizontal resolution, with each grid cell having dimensions of 0.5x0.5 km.

The top elevation of the model was extracted from 30m resolution DEM. The bottom boundary was interpolated from the existing monitoring and production boreholes in the study area. The bottom elevation for the alluvial aquifer layer ranges 100–150m below the surface.

The initial head and hydraulic conductivity were interpolated from the field recorded head and pump test data (8 pumping test wells) of the previous study. In the region, there are 10 monitoring wells and 8 production wells (see figure-36).

Three model layers simulate the hydrogeologic units and the refinements obtained from the 2014 drilling and testing detailed well construction and testing report Yara (MWH, November 2014). Each of the MODFLOW layers corresponds to a geological unit or sub-unit with the formation elevation data (in meters).

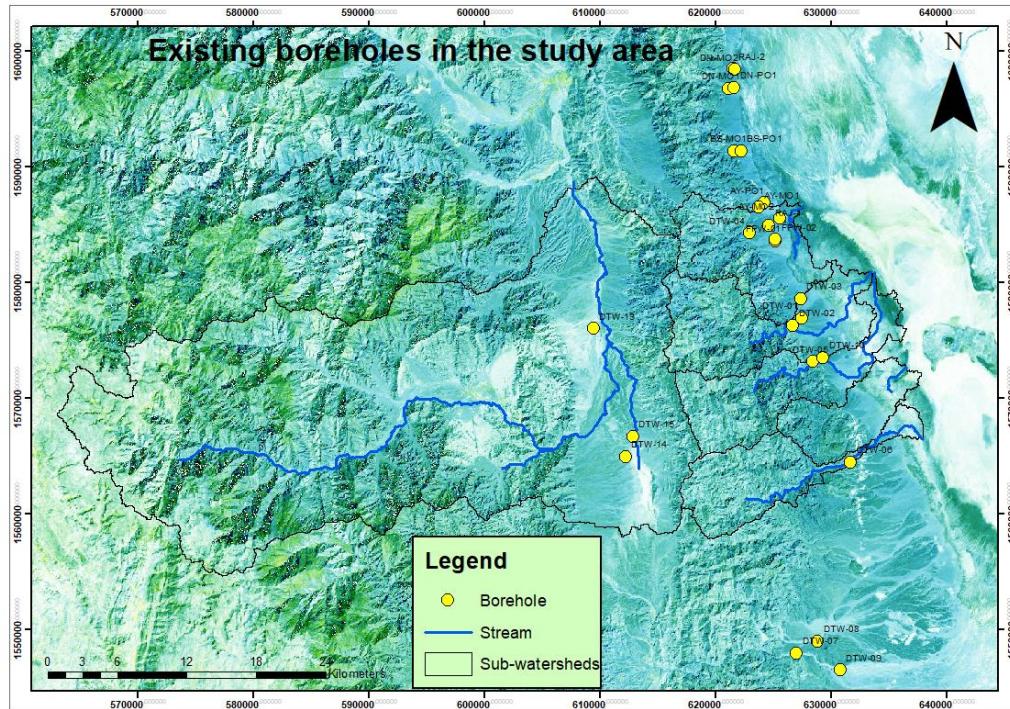


Figure-32. Existing boreholes in the area.

The MODFLOW input data are digital elevation model (DEM), aquifer thickness, hydraulic conductivity, specific storage, specific yield and initial hydraulic head. The MODFLOW is simulated with three-layer units and the hydraulic conductivity ranges for each unit are based on values determined for the study area and estimates based on known lithology using the study area geological map and a measured value of a previous study.

Salinity has more or less a straight line relationship with electrical conductivity (EC). The latter is easily measured and was thus used as a proxy for salinity within the model domain. The location and geometry of the brine interface at the western edge of the salt flats were determined from the Conceptual Model. Elsewhere the EC zones were determined from available EC measurements in wells and water features. The number of EC zones was limited due to the relatively sparse EC data available. Each layer in the model has different conductivity values, which are supported by published and unpublished values regarding the hydrostratigraphy of formations in the study region (WWDSE, 2013).

Assigned vertical hydraulic conductivity values follow the accepted convention of assuming a value of 10 % of the horizontal hydraulic conductivity values unless stated otherwise. Specific

storage was derived from measured storativity values by dividing the storativity by the aquifer unit thickness at the location of the tested well. Porosity was assigned for each model layer based on literature values for similar sediment and rock types (Freeze and Cherry, 1979 as cited in WWDSE, 2013).

To mimic several of the aspects described in the conceptual model, model boundary constraints were assigned. The MODFLOW model was subjected to three types of boundary conditions: rivers (RIV), recharge (RCH), and evapotranspiration packages (EVT). The RIV and RCH data were acquired directly from the respective SWAT model to ensure that the values stayed consistent once the two models were coupled, however, the evapotranspiration package's value was interpolated from the form of the sub-basins.

No-flow boundary conditions are used to simulate the inactive portion of the model domain and to simulate groundwater divides and the model does not calculate flow in these cells. The boundary conditions were also applicable in the water quality of the non-variable density transport model.

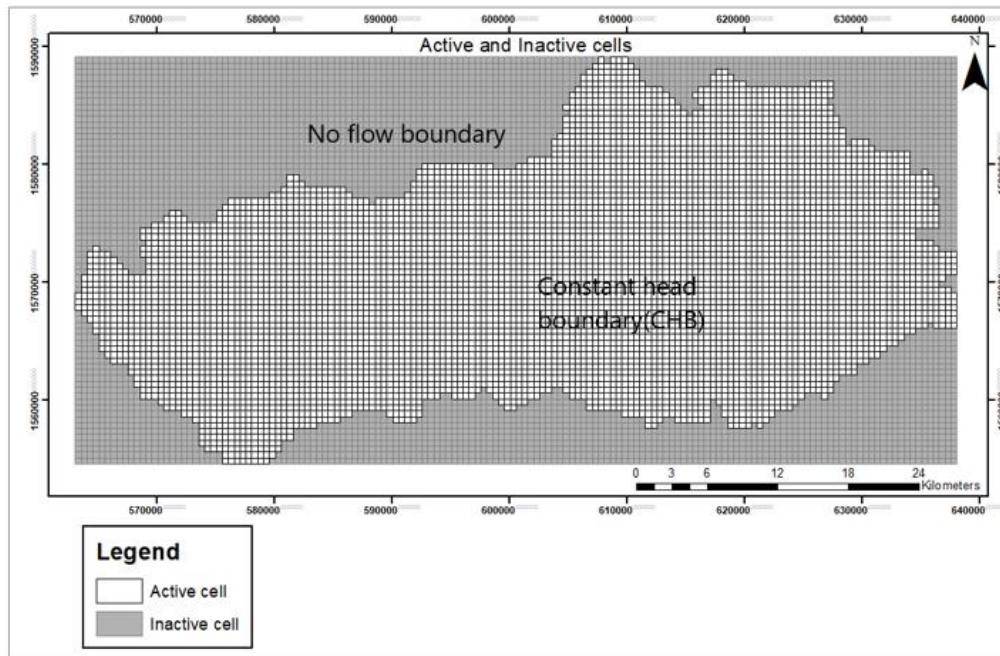


Figure-34. Boundary condition in the study area.

Water quality and density boundary conditions are also applicable in the variable density transport model. Constant head cells are locations of inflow into the model and thus require a specified constant EC concentration value to be assigned.

In model evaluation, a variety of error indices are routinely utilized. One of these is the root mean square error (RMSE). The difference between measured and simulated values is known as residual variance, and it is commonly calculated using the residual mean square or root mean square error (Boyle *et al.*, 2000).

$$REMS = \sqrt{\frac{\sum_{i=1}^n (X_{obs,i} - X_{model,i})^2}{n}} \quad (2)$$

#### 4.2.3 Integrated SWAT-MODFLOW

SWAT-MODFLOW combines SWAT2012 and MODFLOW-NWT, and the linking code allows the two models to share computations daily without having to rewrite and import model inputs. Most crucially, the MODFLOW code in the integrated model replaces the SWAT's groundwater function. The coupling is based on HRUs (disaggregated HRU (DHRU)) that are geographically distributed and a MODFLOW grid shapefile (Bailey *et al.*, 2019).

SWAT HRUs must be disaggregated before being renamed DHRUs to integrate SWAT with MODFLOW. This divides a given HRU into polygons, allowing it to be geo-located and easing the SWAT-MODFLOW connection. On a daily time step, DHRUs send location and surface water flow data to MODFLOW grid cells, which are then returned to SWAT as hydraulic heads and groundwater-surface water interaction flow rates (Bailey *et al.*, 2019).

Hydrological response units (HRUs) analysis for this study created a total of 127 HRUs and 10164 DHRUs. After the disaggregation of the HRUs, linking files were created that tell the SWAT-MODFLOW code how many HRUs, DHRUs and MODFLOW grid cells exist in the sub-basins. Only then can the DHRUs be linked to their corresponding MODFLOW grid cells for data to be transferred.

For this work Python-based graphical interface QGIS interface QSWATMOD (Park, 2016) and versions of executable code SWAT-MODFLOW3 (Bailey *et al.*, 2019) were used. These interfaces can import an existing MODFLOW model and integrate it with the SWAT model. QSWATMOD with SWAT-MODFLOW3 was employed for its flexibility in giving geographical context with maps and post-processing of outputs.

To perform the coupling in QSWATMOD, all the required inputs, namely subbasin, HRUs, and river network shapefiles and ‘textinout’ from the SWAT model and grid shapefile and MODFLOW model native text (‘nam’ file) from MODFLOW-NWT simulation imported.

Accordingly, moderately calibrated models and shapefiles are imported and proceed to the coupling step. The stream network was used from the SWAT model. Then, the HRUs were disaggregated to DHRUs and coupled with the MODFLOW grid cells. Once the models were integrated, all the required linking files were created as a text files.

The MODFLOW-MT3DMS model mapping of pollutant transport cells was completed during the model setup procedure, and the simulation was run from 1998 to 2014, including the first two years of the warmup period. To optimize the primarily particular storage and specific yield, a manual calibration procedure was applied.

During the simulation, the computation exchange was daily. Deep percolation was computed at the HRU-scale transferred to DHRUs and then mapped to MODFLOW grid cells to build the stress values in the recharge package. The aquifer–stream water flux was computed using the river package of the MODFLOW model made for each subbasin.

For this study, MT3DMS were used to simulate a modular 2-D multispecies transport model for advection, dispersion, and chemical reactions of contaminants for salt intrusion in the groundwater systems of the study area. The governing equations for flow and transport can be seen in equation 3 and equation 4 (<http://www.mt3d.org> as cited in Harry, 2018).

Flow equation in MODFLOW

$$S_s \frac{\partial h}{\partial t} = \frac{\partial}{\partial t} \left( k \frac{\partial h}{\partial x} \right) + q_s \quad (3)$$

Transport equation (in MT3DMS) when porosity is constant

$$R \frac{\partial C}{\partial t} = \frac{\partial}{\partial x} \left( D \frac{\partial C}{\partial x} \right) - \frac{\partial}{\partial x} (VC) + q_s C_s + \sum_{R=1}^N R_R \quad (4)$$

#### 4.2.4 Vulnerability Assessment using DRASTIC Method

Many techniques exist for computing groundwater vulnerability, however, the most simple and widely used technique is the DRASTIC index that measures intrinsic vulnerability developed by Aller *et. al*, 1998. Intrinsic vulnerability is independent of the nature of the contaminant and the condition of the area where it is released but it takes into account the hydrological, geological and hydro-geological characteristics of the area under study (Zwahlen, 2004 as cited in Neha, 2014).

Neha (2014) Stated that the DRASTIC index method is very easy to apply in the data insufficient area, where monitoring has been scarce, and also allows a systematic evaluation of the parameters under study. This method accounts for the aquifer parameters like depth to water, net recharge, aquifer media, soil media, the impact of vadose zone and hydraulic conductivity. This type of vulnerability assessment gives fair preliminary results for identifying the vulnerable area and later on focus on management plans, policy planning and decision making.

In the present study an attempt has been made to account for the vulnerability of the alluvial aquifer using an overlay index method, DRASTIC, which is used to prepare a vulnerability map using GIS, of the study area, the Danakil basin. The main data used and their sources have been defined in the table given below.

Table 8 Data used for the Hydro-Geological Parameters for DRASTIC Model

No.	Data Type	Sources	Output Layer
1	Water level Map	Previous data and direct monitoring.	Depth of Water (D)
2	Average annual recharge	SWAT model	Recharge (R)
3	Geology Map	Geological Survey of Ethiopia.	Aquifer (A)
4	Soil Map	MoWIR (FAO).	Soil (S)
5	Topographical Sheet	Ethiopian Geospatial Information Institute	Topography (T)
6	Geological Profile	Geological Survey of Ethiopia.	Impact of Vadose Zone (I)
7	Hydraulic Conductivity	Yara groundwater study by MWH, 2015.	Hydraulic Conductivity (C)

For overlay analysis the weights and ratings are given to each of the seven parameters, each is classified on a scale of 1-10, in which 1 denotes the least vulnerable while 10 is for the most vulnerable areas. This rating is further scaled into weights based on the importance of the parameter in determining aquifer characteristics, these are scaled on 1-5 where 1 is least significant and 5 is most significant. The weights and ratings for this study have been defined in the table given below.

The DRASTIC vulnerability index (DVI) is calculated by linear addition of the weights and rating, the formula is given below (Aller *et al.*, 1987):

$$DVI = DrDw + RrRw + ArAw + SrSw + TrTw + IrIw + CrCw \quad (5)$$

Where,  $Dr$  = Rating for the depth to the water table,  $Dw$  = Weight assigned to the depth to the water table,  $Rr$  = Rating for aquifer recharge,  $Rw$  = Weight for aquifer recharge,  $Ar$  = Rating assigned to aquifer media,  $Aw$  = Weight assigned to aquifer media,  $Sr$  = Rating for the soil media,  $Sw$  = Weight for the soil media,  $Tr$  = Rating for topography (slope),  $Tw$  = Weight assigned to topography,  $Ir$  = Rating assigned to impact of the vadose zone,  $Iw$  = Weight assigned to impact of the vadose zone,  $Cr$  = Rating for rates of hydraulic conductivity and  $Cw$  = Weight given to hydraulic conductivity.

The rating ranges were determined depending on the study area. In this study, all the maps are prepared using GIS techniques. The maps are digitized and are converted into layers through geo-referencing using ArcGIS. The rates and weighting were assigned to the layers and final DVI index was calculated and a vulnerability map of the area was prepared.

Table 9. Drastic Rating and Weighting Values for the Various Hydrogeological Parameter Settings (Aller et al., 1987).

<b>DRASTIC Parameters</b>	<b>Range</b>	<b>Rating</b>	<b>DRASTIC Weight</b>
Depth to Water Table	0-46	10	5
	46-64	7	
	64-76	5	
	76-94	3	
	94-144	1	
Net Recharge	0.01-10.6	1	4
	10.6-21.3	3	
	21.3-32	5	
	32-42.6	7	
	42.6-53.3	9	
	>53.3	10	
Aquifer Media	Sandstone, Limestone, Silt and Phyllites.	7	3
	Limestone, Silt and Phyllites.	9	
	Alluvium, silt sand and gravel.	10	
	Salt, Silt and Gravel.	3	
Soil Media	Absent	10	2
	Loam	9	
	Clay Loam	7	
	Sandy Clay Loam	8	
	Salt	3	
Topography	0- <22	10	1
	22-<46	9	
	46-<76	5	
	76-121	3	
	>121	1	
Impact of Vadose zone	Sandstone-Limestone	10	5
	Alluvium, silt, sand and gravel.	8	
	Phyllites and Slate	5	
	Salt and gypsum	3	
	Clay	1	
Hydraulic Conductivity	0-1	1	3
	1-2.5	5	
	2.5-5	7	
	5-20	10	

#### 4.2.4.1 Depth to Water Table (D)

It is very important from the point of view of the groundwater aquifer as this factor determines the depth to which a contaminant would have to travel before it reaches the water table, i.e. saturated zone of the aquifer (Al-Zabet, 2002 as cited in Neha, 2014). For this data provided had 24 point data, static piezometric heads for those 24 locations had been taken as the average of six years of measurements (2011-2016), water table depth map had been developed, digitized and converted to raster format. The depth of the water table ranges from 0- 145.27 meters below ground level (mbgl). The depth to water table map is given in Figure 35.

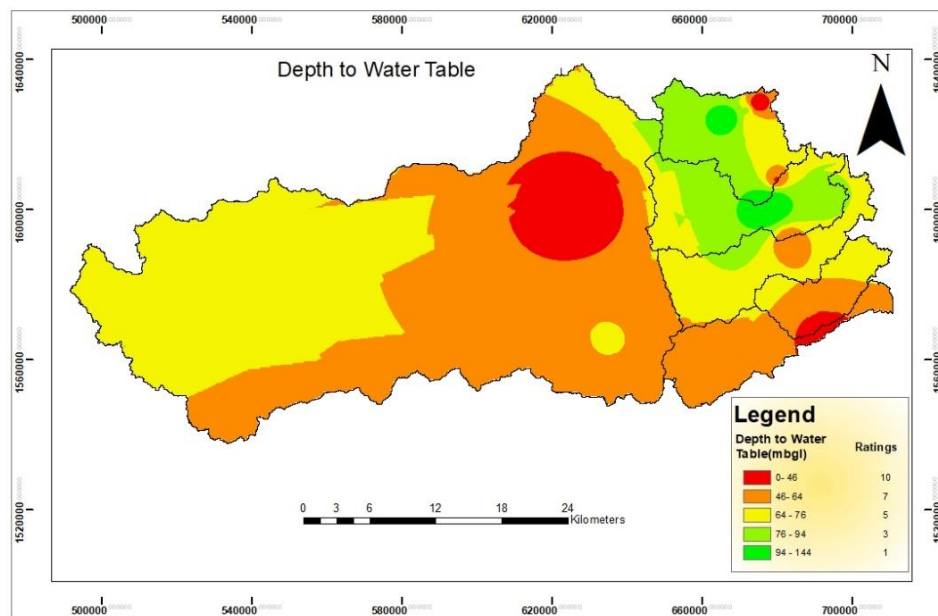


Figure 35. Depth to the water table.

#### 4.2.4.2 Net Recharge

Net recharge for groundwater vulnerability, as the contaminant moves with the rainfall water as infiltration and goes down deep into the aquifer saturated layer. The net recharge for the study area was obtained from the SWAT model. The recharge value ranges from 0.01-53 mm and the rating value lies in the range of 10 to 1.

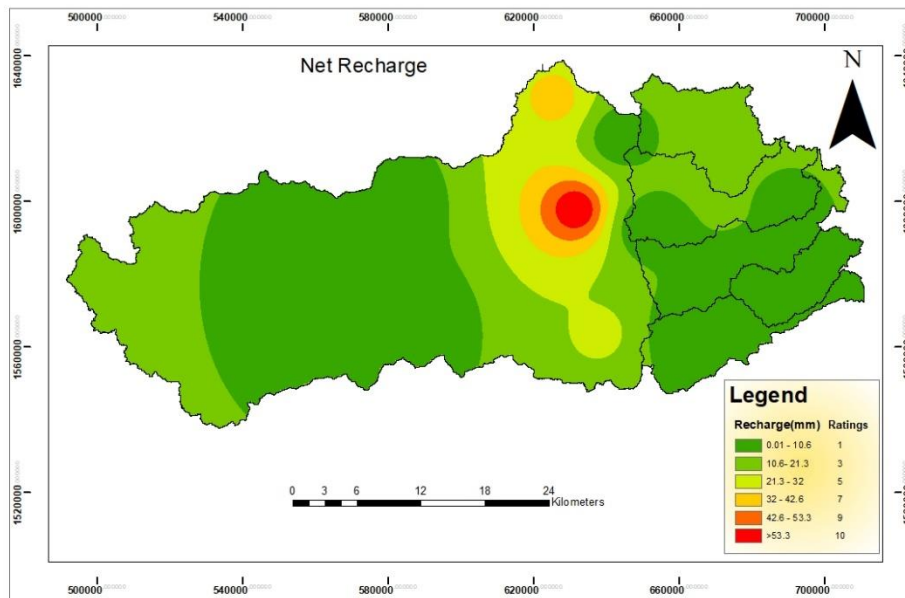


Figure 36. Net recharge.

#### 4.2.4.3 Aquifer Media

This parameter represents the geological formation of the aquifer in the upper layer, the map was prepared from the hydrogeological map (See figure 23 page number 41) and the lithology of the area and the DRASTIC ratings were assigned. It governs the time, and the route followed by the contaminant to reach the water table, various formations have different degrees of permeability and a rating is assigned to each of them based on their permeability. The alluvial aquifers are the most vulnerable to contamination and hence it was assigned the rating of 10 as the permeability is very high. The salt, silt and gravel are the least vulnerable due to their relatively impermeable nature and the rating is 3.

#### 4.2.4.4 Soil Media

It represents the top soil layer extending not more than a few meters from the surface, it is the weathered zone. It has a significant impact on the movement of the amount of recharge water that infiltrates deeper into the aquifer, hence it also affects the downward movement of the contaminants into the vadose zone (Lee, 2003 as cited in Neha, 2014). The study soil raster map was imported and extracted from FAO. The rating was assigned from 10 (absent) to 3 (Salt).

#### 4.2.4.5 Topography

It refers to the slope aspect of an area. Slope plays a major role in the flow rate of the water that falls on the surface. Hilly terrain has a high slope and hence high runoff, therefore the time of contact of water is less and so is the time of infiltration (less vulnerable), however areas with a lower slope withstand water for a longer period and hence allow more water to infiltrate and that makes more vulnerable (Neha, 2014). For this study Digital elevation model (DEM), 30m resolution from the Ethiopian geospatial information institute was used and changed to a slope map using Arc GIS, and the ratings as specified in the table were used to make the vulnerability map. The topography map (slope-aspect) of the study area is given in Figure 37.

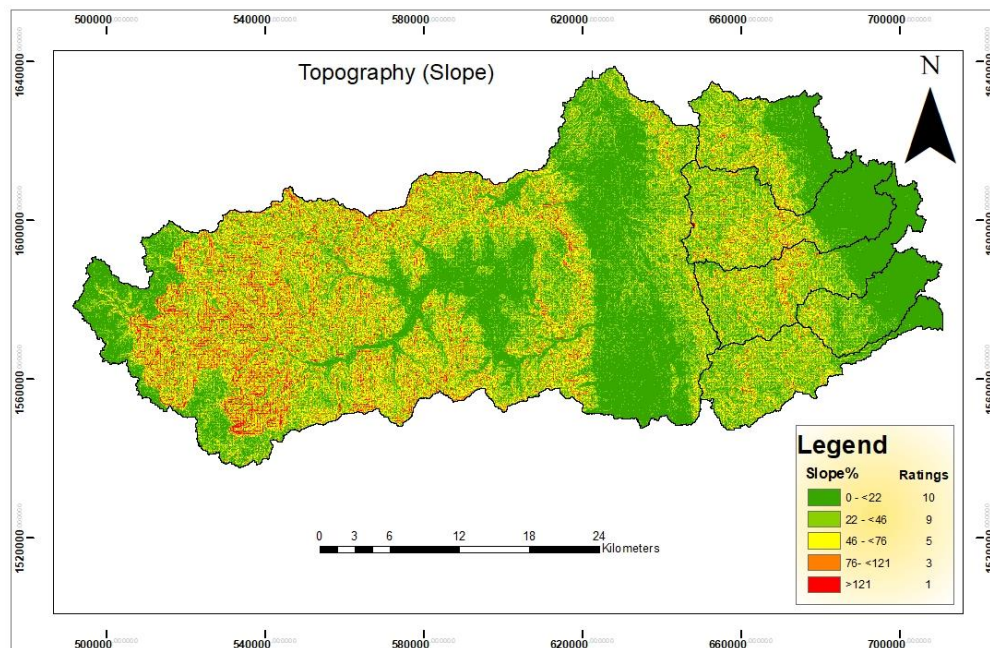


Figure 37. Topography (slope aspect).

#### 4.2.4.6 Impact of vadose Zone

It is the area that lies above the saturated zone; it is made of unsaturated and saturated zones and it varies at depths. Like the soil media, it also plays an important role in the percolation of the recharge water to the aquifer and therefore the contaminants as well (Neha, 2014). The Vadose Zone in the given study area consists of alluvium, gravel, sandy gravel, sandstone, limestone, and clay. The units having clay and loam are less vulnerable as they do not contain much of the water in the vadose zone however; gravel, sandy-gravel, sandstone and limestone areas contain

groundwater and hence are vulnerable. They have been assigned a rating from 10 to 1 according to their properties.

#### **4.2.4.7 Hydraulic Conductivity**

Hydraulic conductivity is an important aquifer parameter that is characteristic of geological properties. It governs the rate at which the water flows in the aquifer's saturated zone. Hence, contaminant transportation is checked by the hydraulic conductivity of the aquifer system. Hydraulic conductivity of the alluvial aquifers varies between  $8.72 \times 10^{-6}$  and  $2.242 \times 10^{-4}$  m/s (Seyman 2005 as cited in Neha, 2014). The hydraulic conductivity values for the given study area were taken from the Yara groundwater study by MWH, 2015.

#### **4.2.4.8 Single Parameter Sensitivity Analysis (SPSA)**

Single-parameter sensitivity analysis is a widely used method to assess the impact of selected parameters on groundwater vulnerability assessment (Napolitano and Fabbri 1996 as cited in Alamne *et al.*, 2022) and helps to understand the effect of subjectivity and weights allocated to each parameter (Babiker *et al.*, 2005; Gogu *et al.*, 2003 as cited Alamne *et al.*, 2022). The single parameter sensitivity analysis was used and adopted in this study to evaluate the effect of each factor on the vulnerability index (Huan *et al.*, 2012a as cited in Alamne *et al.*, 2022). The single parameter sensitivity analysis (SPSA) is introduced by Napolitano and Fabbri (Napolitano and Fabbri 1996 as cited in Alamne *et al.*, 2022).

## CHAPTER 5: RESULTS AND DISCUSSIONS

### 5.1 SWAT Model

The regionalization approach, the information transfer technique from one watershed to another Blöschl *et al.*,1995 as cited in Bisrat *et al.*,2020) was used to estimate the parameters for the ungauged watershed(subbasins). The arithmetic mean, spatial proximity, physical similarity, regression, and watershed-runoff response similarity approaches can be employed to transfer optimized parameters from gauged watersheds to ungauged watersheds(Tegegne *et al.*,2018 as cited in Bisrat *et al.*,2020). In this study since gauging stations for streamflow were not significant, the physical similarity approach was employed. The physical similarity technique uses watersheds' properties commonly LULC, soil classes, and topography as descriptors. The soil, LULC, and slope features of subbasins compared with the SWAT's HRU report table were used as an indicator of similarity.

SUFI2 is one of the stochastic calibration programs in SWAT-CUP that was used in this study. The model parameters from calibrated catchment were transferred to the ungauged catchment (study area), based on the regionalization with physical similarity approach. After the transfer of calibrated parameter values, the model was run, and the major components of the catchment water balance (particularly long-term annual runoff volume) were compared with previous studies of the area for simple inspection of model results.

After the SWAT Model run using the ArcSWAT interface was conducted the SWAT output was checked using a SWAT CHECK. As a first check, it is important to understand something about the quality of the data. This involves running a script to calculate potential ET/rough actual ET using a crop factor. This can help to get an understanding of the data quality (Zhansheng *et al.*, 2018).

For this study calculating annual PET estimates as averaged over the upper sub-basin of the study area helped to select the proper PET calculation method for the SWAT model in the Edit SWAT input section. Therefore Penman-Monteith method was overestimated and was replaced by the Hargreaves method.

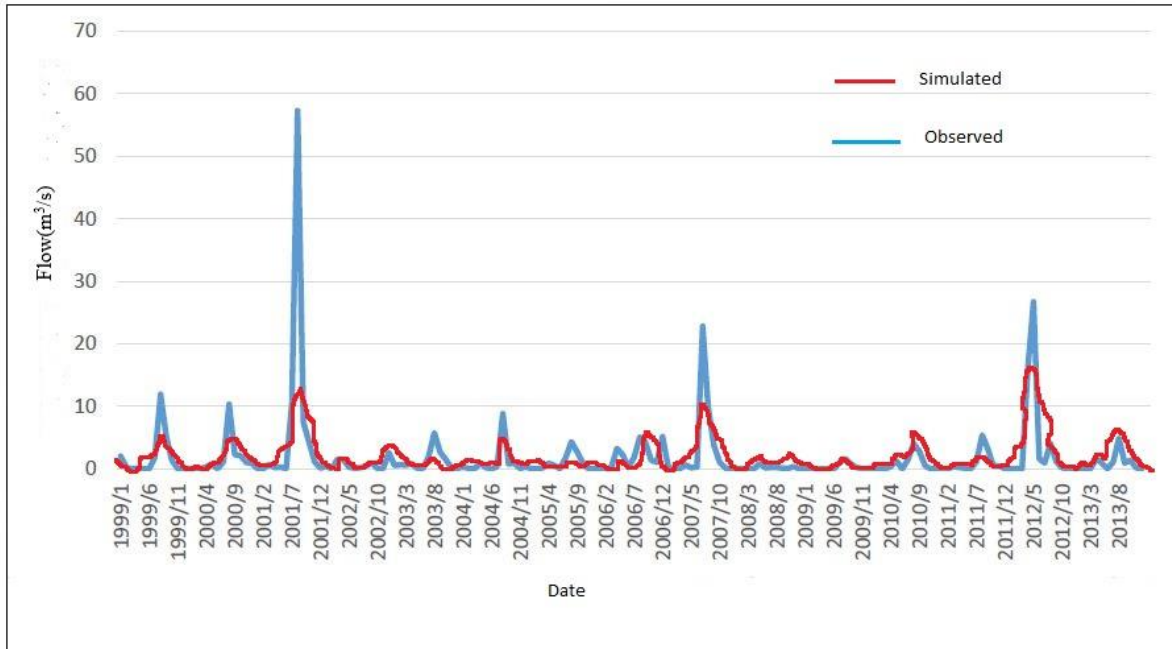


Figure 38. Comparison of measured and predicted monthly stream flow during the calibration period (1999–2013).

Estimating the recharge using the SWAT model of the total catchment area is important to link the SWAT output with MODFLOW and to use as recharge output for DRASTIC methods of vulnerability assessment.

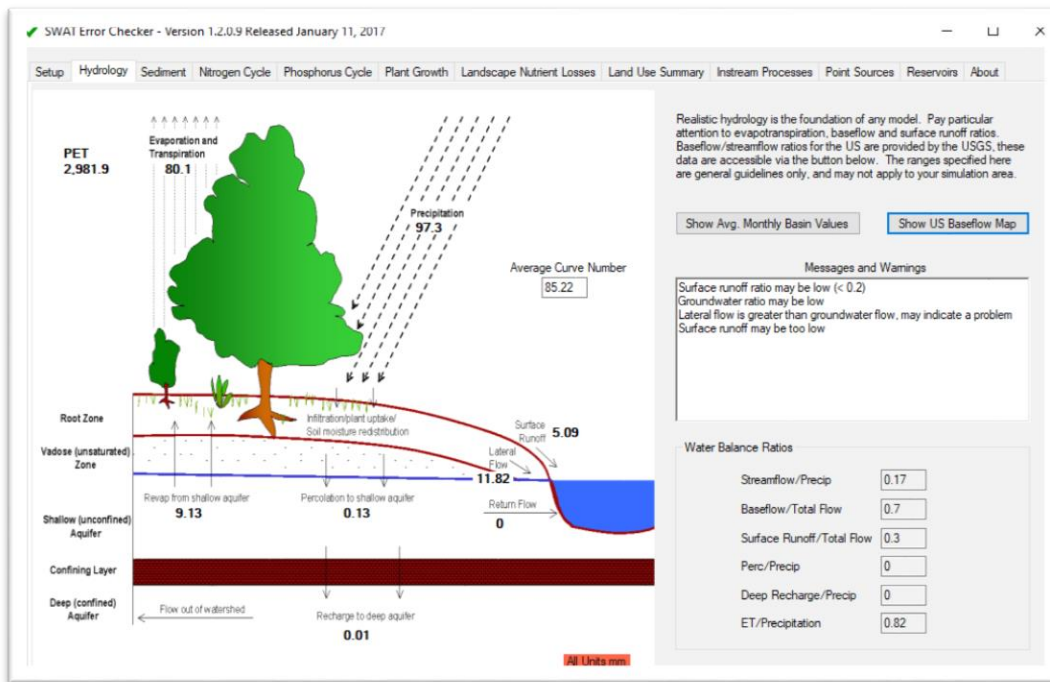


Figure 39. The hydrologic cycle.

## **5.2 MODFLOW Model**

### **5.2.1 Steady-State Calibration**

During steady-state calibration, hydraulic conductivity and boundary conditions are adjusted to match calibration water level targets. Steady-state calibration does not take into account time-dependent variables (e.g. seasonal water level fluctuations) that are dependent on aquifer storage. The purpose of this calibration is to develop a reasonable hydraulic conductivity distribution across the model domain that produces simulated heads that match average hydrologic conditions. The steady-state water level calibration thus provides the basis for the subsequent and more refined transient calibration.

The selection of steady-state water level calibration targets for the model was selected based on data availability and reliability. Previous studies of well construction records were assessed to identify well screen intervals to determine if the well water level data were consistent with the model layering and therefore whether the well and spring water levels could be used for baseline calibration characterization.

For this study, the steady-state MODFLOW model was calibrated using measured groundwater level data from 21 wells available from the Circum production and monitoring wells drilled by RMES in the year 2016, Dallol test wells (DTW) drilled by Beles Engineering in the year 2013 and WWDSE in the year 2013, the fan monitoring wells (FMW) and pumping wells (FPW) drilled during the MWH study since 2019.

The study setup and initial runs were carried out under steady-state conditions, to establish an initial condition for subsequent runs. This was done so that the initial heads file could be used to run transient simulations. After this initial run, recharge data were added to the model, with the corresponding SWAT model as its source. These recharge data were subdivided by SWAT sub-basin and were added to the top layer of the MODFLOW model in the corresponding locations.

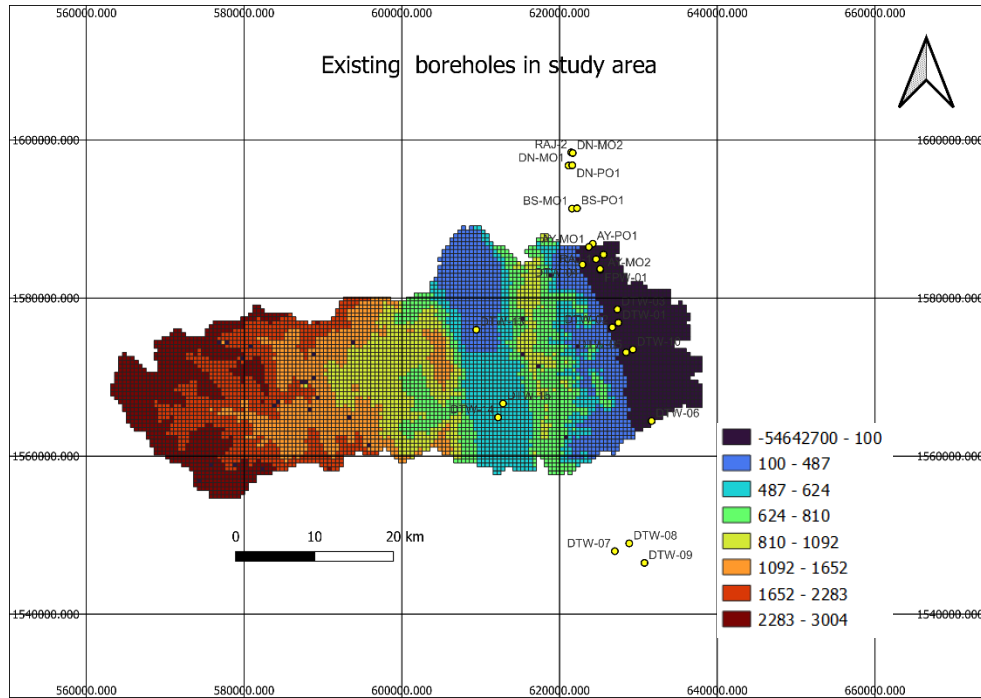


Figure 40. MODFLOW Head with existing boreholes before calibration in ModelMuse.

Each calibration well's water levels were converted to hydraulic head data by subtracting them from the corresponding ground elevations from a 30m DEM, with screen elevations assumed to be at the bottom of each well. Within the MODFLOW modeled area, a total of 21 water wells were accessible, with several falling beyond the research area watershed to help depict regional groundwater conditions from the western highlands to the alluvial fans. Calibration was limited to available borehole measurements recorded in the last six years of the simulation period due to a large number of data points. During the field study, the most recent groundwater level measurement was taken.



Figure 41. Groundwater level measurement on AY-MO1 (monitoring well).

Calibration criteria for hydraulic heads follow the United States Department of the Interior Bureau of Land Management (BLM) guidelines which establish that the difference between simulated and actual field measurements should be less than 10 percent of the variability in the field data across the model domain. Residuals are defined as the difference between simulated values and the measured water levels (BLM, 2008).

The narrow, pinching-out spots in the model presented problems for vertical flow at the start of MODFLOW calibration. Because the simulated water couldn't efficiently flow down through the cells, locations, where hydraulic heads built up, were higher than what could be seen (or is expected to be realistic). The addition of Constant Head Boundary Conditions (CHB) around the MODFLOW model area reduced the simulated hydraulic heads to a more realistic range. The ground elevation and the MODFLOW hydraulic head map in ModelMuse were used to create these CHBs. Aside from imposing CHBs around the research area, modifying the hydraulic conductivity of a body of water.

Table-11: presents the water level data from the 21 wells used in the steady-state calibration. The table shows the hydrogeological unit in which the well is completed as well as the last date for which water level data are available. Generally, the most recent water level measurements available in the vicinity of the wells were used.

Table 10. Water level data from the 21 wells, was used in the steady-state calibration.

Well ID	Location		Measured	Aquifer
	Easting	Northing	Water Level	
	(m)	(m)	(m aSL)	
DTW-01	627462	1576873	-112.55	Alluvial Fan
DTW-02	626691	1576283	-113.07	Limestone
DTW-03	627337	1578555	-122.92	Alluvial Fan
DTW-04	622916	1584222	-28.87	Basement
DTW-05	628438	1573114	-52.1	Danakil
DTW-06	631676	1564435	-21.01	Danakil
DTW-07	627010	1547959	92.58	Danakil
DTW-08	628837	1548947	67.18	Danakil
DTW-09	630771	1546472	25.61	Danakil
RAJ-1	624631	1584916	-106.7	Alluvial Fan
RAJ-2	621479	1598423	-115	Alluvial Fan
DN-MO2	621678	1598343	-117.7	Alluvial Fan
DN-MO1	621132	1596748	-123	Alluvial Fan
DN-PO1	621615	1596788	-120	Alluvial Fan
BS-MO1	621579	1591304	-117.7	Alluvial Fan
BS-PO1	622220	1591347	-117	Alluvial Fan
AY-PO1	624215	1586860	-112	Alluvial Fan
AY-MO1	623712	1586459	-104.2	Alluvial Fan
AY-MO2	625581	1585494	-111.6	Alluvial Fan
FPW-01	625167	1583569	-106.1	Alluvial Fan
FPW-02	625150	1583666	-105	Alluvial Fan

The outcomes of the model steady-state calibration for all model layers are plotted in Figure-42. This type of plot compares the measured versus simulated water levels for all the calibration wells. The closer the data points are to a 45-degree line the better the calibration results. The calibration RMS error for all water levels is 11.4 m which is approximately 5.9% of the 223.7-meter range in measured water levels. This calibration error is well below the established statistical guidelines and indicates an acceptable match between observed and simulated water levels. One target in layer 2 is outside the 10% RMS model error. The targets in layer 2 with greater than 10% RMS error are in the western part of the model domain, representing the

Regale river. At these locations, the errors are insignificant because it has no material impact on the model results in the potential future alluvial fan wellfield areas.

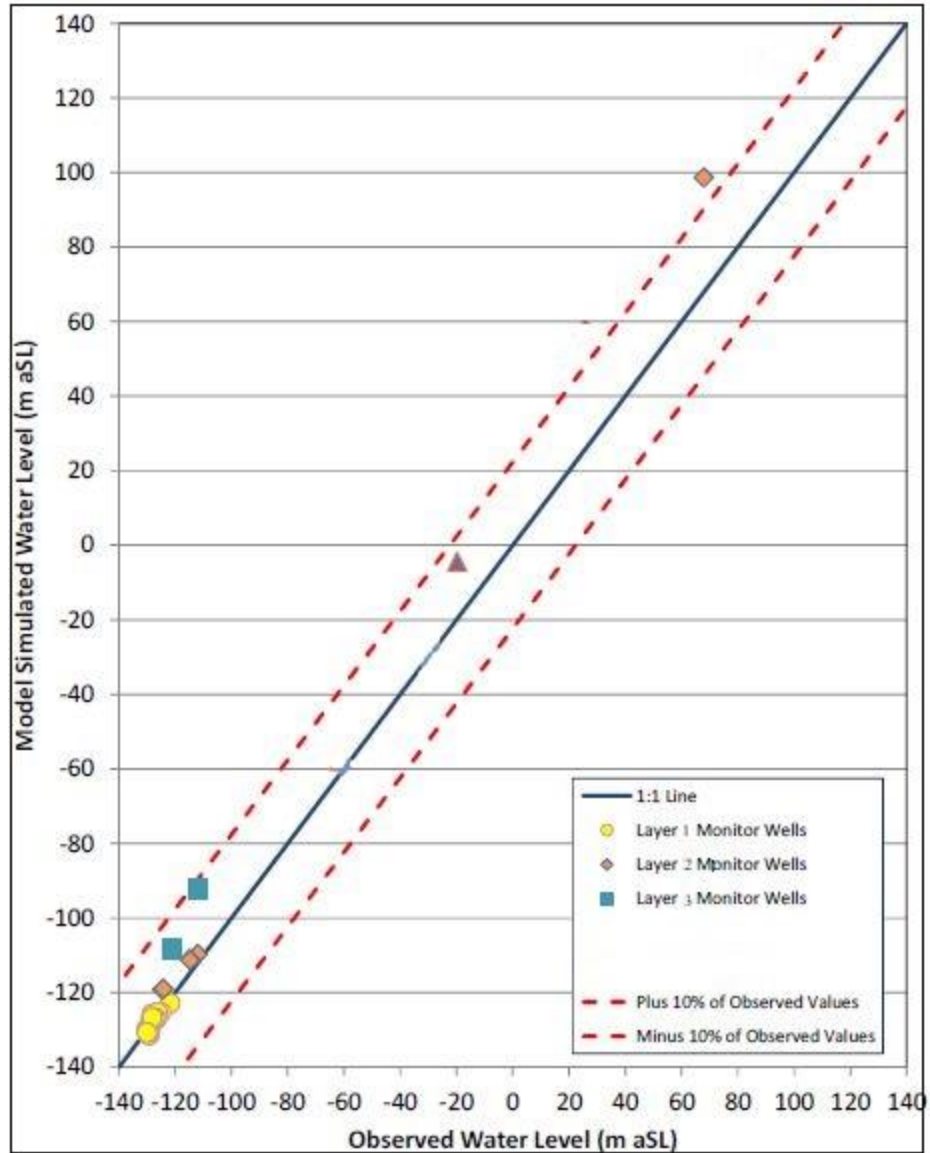


Figure 42. Steady-state calibration water level results.

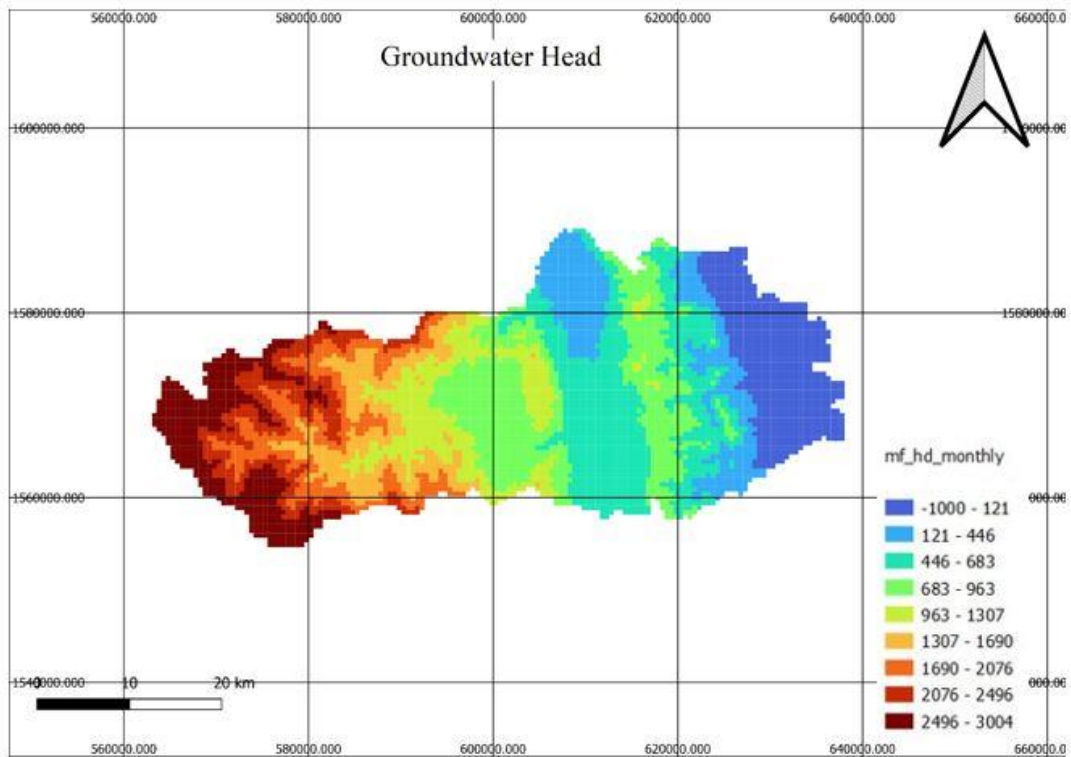


Figure 43. Groundwater head.

### 5.2.2 Density Dependent Transient Water Level Calibration

The model was calibrated to density-dependent transient water level conditions following the completion of the steady-state calibration. The initial heads for the transient model simulation used the water level head values generated from the calibrated steady-state water level model. The transient model was calibrated with 6 stress periods that correspond to the pumping and recovery periods of DTW-01, DTW-10 and FPW-01 recorded. All three pumping wells are screened in (pump water from) the model layer of the Quaternary Alluvial Sand & Gravels (source: well construction and testing report Yara by MWH, November 2014).

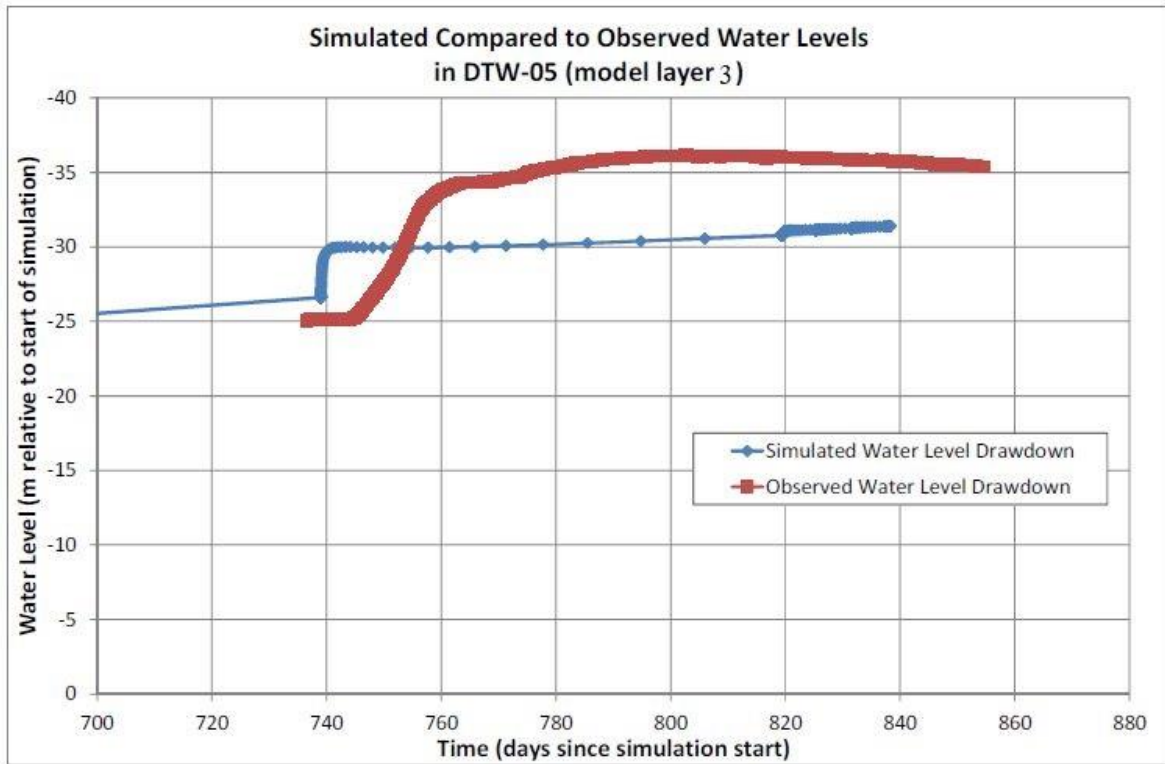


Figure 44. Transient Calibration in DTW-05 water level drawdown.

The model uses EC values to calculate water levels based on the corresponding density in addition to the calibration of solute transport. Higher EC values have higher densities, which depress water levels and influence water flow. Initial EC concentrations were input into the model domain based on recent measurements from monitoring wells. Specific yield and specific storage values were assigned to each of the model layers consistent with the aquifer units. Porosity values were also assigned as this parameter constrains the velocity of the solute transport which then impacts the density adjustment of water levels.

EC has a more or less straight line relationship with water density and was used as a proxy for the fluid density within the model domain. Higher EC concentrations have higher densities, which reduces water levels compared to fresh water. In exclusively fresh water systems groundwater flows from areas of high groundwater levels to areas of low groundwater levels. However, in variable-density systems groundwater can flow from locations of low groundwater levels to high groundwater levels due to density differences. Consequently, computation of the density can be important. For instance, the lower groundwater level in DTW-02 compared to

DTW-01 in the Gehertu Fan must be due to density effects, or else the groundwater would have to flow back up the geometrically nonsensical fan.

MODFLOW-MT3DMS computes water levels based on variable-density flow and transport in the model, so water levels change through time based on the movement of EC (salinity) within the model domain, in addition to transient changes in well pumping.

There is a lack of knowledge regarding precise EC values in groundwater in the fans and transferred into the fans via faults, which is reflected in the model by the use of simplistic initial EC zones. The only time-variant EC field data available for the model calibration period was from wells DTW-10 and FPW-01.

Model calibration to EC, as the initial observed values compared to simulated results values may differ. Nevertheless, the model results are still useful. For instance, a deteriorating change in fan EC values occurs in response to steady-state and transient flow conditions, this is indicative of the presence of a significant thickness of fresh water flowing through the Precambrian bedrock. Secondly, the difference in EC values between brackish and fresh water within the model is small and not enough to significantly impact water levels based on the corresponding density. Consequently, the EC limitations of the current model do not affect the groundwater head and flow calibration.

As a consequence the fan and playa salt flat EC simulated in the model was calibrated against a single steady-state measured value obtained from the pumped discharge during each fan well-pumping test and the well development discharge from each monitoring piezometer. Similarly, the bedrock was assigned a brackish EC value consistent with the values obtained from DTW-02 and DTW-04.

### **5.3 SWAT-MODFLOW**

The study area applies the coupled SWAT MODFLOW model, to estimate groundwater recharge and to use it as a parameter for DRASTIC methods of vulnerability assessment. The parameters considered to estimate ground water recharge are precipitation, temperature and aquifer parameters like hydraulic conductivity, specific storage, specific yield, and aquifer thickness. The ground water recharge is simulated from 1999 to 2013. The estimated annual ground water recharge from rain fall on the water shade areas draining as sub-surface flow to the fan aquifer is

10 Mm<sup>3</sup>, Infiltration of Run-Off coming from uplands is 36 Mm<sup>3</sup> and Infiltration of direct rain fall on the fan sediments is 1.15 Mm<sup>3</sup>.

The simulated groundwater-surface water exchange data show that overall exchange trends remain fairly constant throughout the simulation period, while the western (upstream) portion of the river showed the most pronounced fluctuation between the wet and dry months. The simulated water balance shows the overall exchange trends (see figure-45).

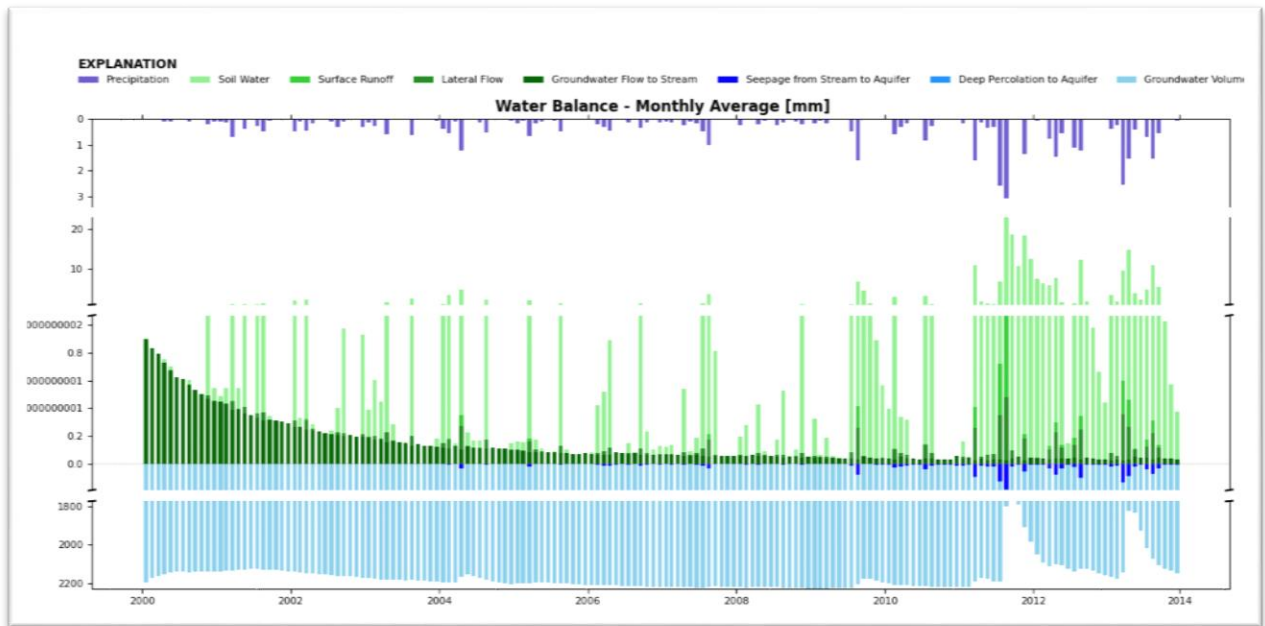


Figure 45. Water balance monthly average (mm) in the study area.

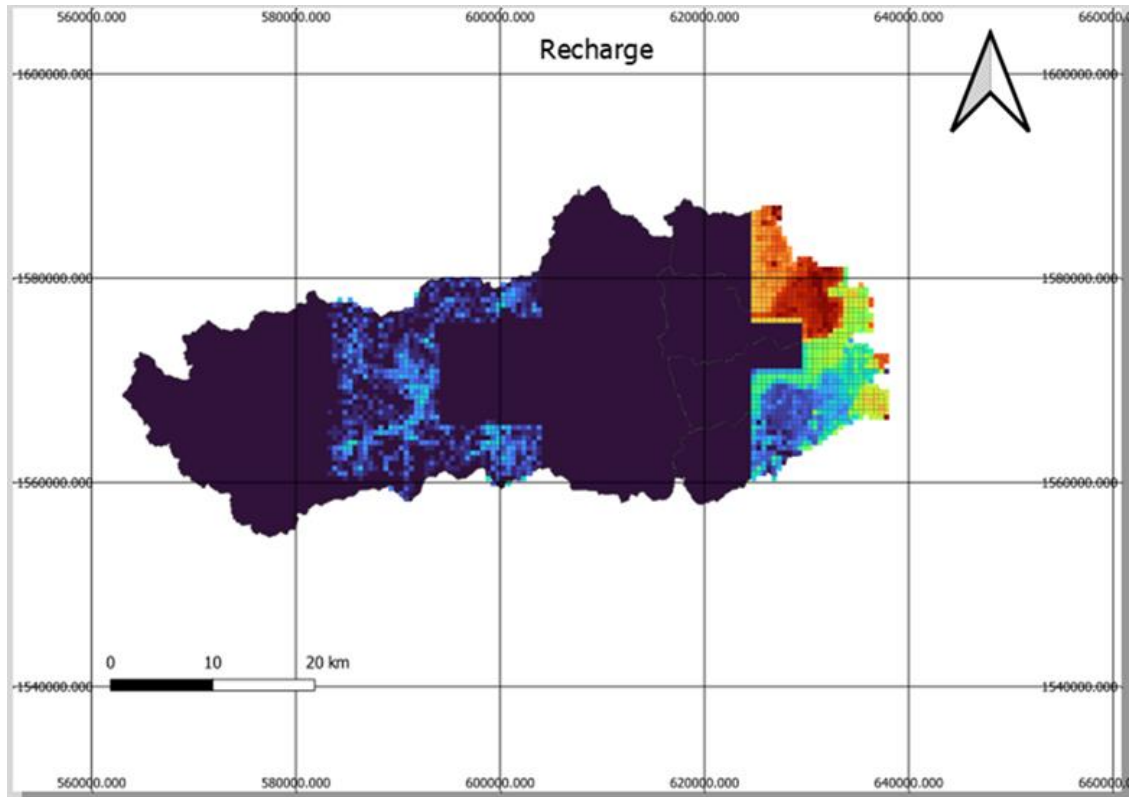


Figure 46. Visualizing the exported recharge on the QGIS canvas, the recharge of the year 2011. This study also employed the integrated MODFLOW-MT3DMS, from a vulnerability perspective, which can help to better understand the effects of geogenic influence on salt intrusion within a watershed. For example, the Sulfate concentration in the model result ranges from 0-850 mg/l.

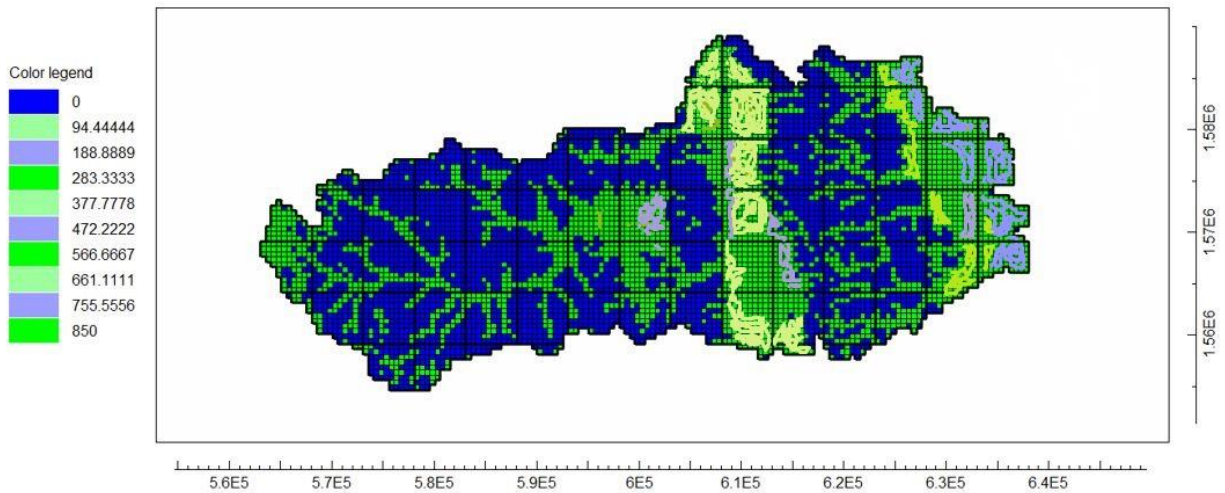


Figure 47. Sulfate concentration in MODFLOW-MT3DMS.

The drawdown in the alluvial fans of the study area is relatively small in magnitude and expands north and south. It does not penetrate significantly to the east due to the hydraulic barrier effect of the low permeability of the silts and clays and is potentially protected by the clay layers in the alluvial fans providing the wells and clay units are properly sealed between the protecting clay layers.

Consequently, the impact of pumping is not expected to cause saltwater intrusion providing the freshwater safe yield is not exceeded. However if the pumping rate exceeds the freshwater safe yield, the deficit will be met by brackish water flow from the bedrock or saltwater inflow from the rift. This will progressively cause saltwater intrusion and salinization of the freshwater reserve. The rate of salinization will be a function of the deficit rate although the very high freshwater storage volumes in the fans will slow this rate significantly. The wider exploration of the fans may reveal a different setting and greater risks.

The drawdown map shows that in the contaminant risk zone there is low groundwater drawdown over the alluvial aquifer, which implies the three will not be uplifted of groundwater contamination to some extent following over-abstraction (see figure-48).

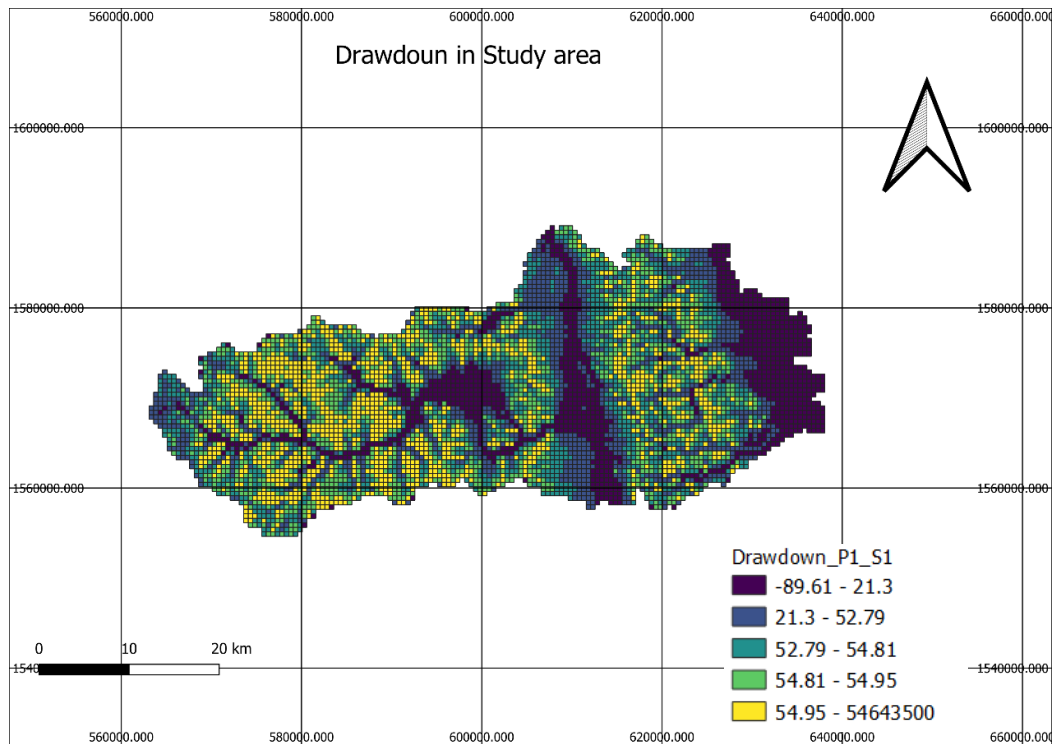


Figure 48. Drawdown map of the study area.

#### 5.4 DRASTIC Method

The DRASTIC Method used produced the map given below shows the area of low, medium and high vulnerability. The district's geological and hydrogeological setup determines the aquifer characteristics and in the present study area, the alluvial aquifers in the graben area are less protected by the soil, aquifer media, vadose zone, and also topography. Around 50% of the study area shows moderate vulnerability and around 20% shows low vulnerability while the other 30 % of the area is highly vulnerability. The alluvial aquifer in the east of the escarpment is low to moderately vulnerable, while the alluvial aquifer in the graben area (west of the escarpment) is highly vulnerable to groundwater contamination.

Table 11. Vulnerability group.

Vulnerability group	Index ranges
Low	50-73.92
Medium	73.92-104.90
High	104.90-149.60

Aquifer vulnerability methods require validation to reduce subjectivity in the selection of rating ranges and to increase reliability (Leal and Castillo 2003 as cited Alamne *et al.*, 2022). Statistical analysis was performed to analyze and display the results of each DRASTIC parameter.

Based on the results, net recharge had the highest effect in single-parameter sensitivity analysis it had the highest mean modified weight (5.4) among all other parameters whilst topography showed the least sensitivity (0.8). In addition, aquifer media, soil media, and impact of vadose less exceeded the original weight and had the mean modified weight of 3.2, 2.3, and 5.1, respectively. The rest of the parameters showed lower weight compared to the original weight. Figure 49 below shows the vulnerability map after the modification.

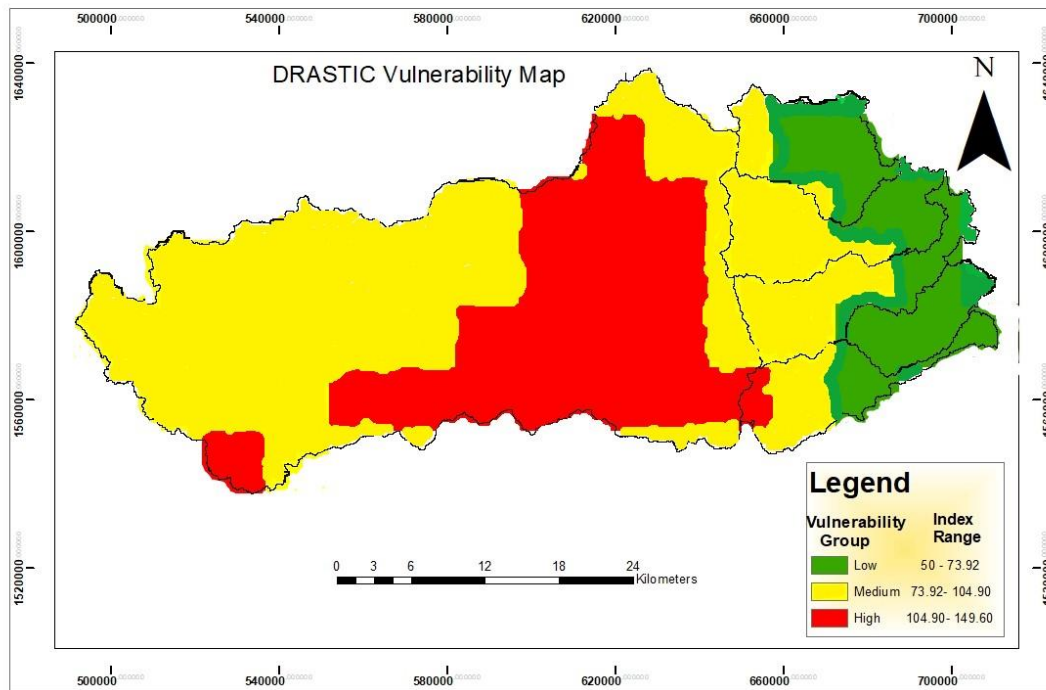


Figure 49. DRASTIC vulnerability map.

## CHAPTER 6: CONCLUSIONS AND RECOMMENDATIONS

### 6.1 Conclusions

Based on the assessed rainfall datasets, the average monthly rainfall distribution indicates the majority of rainfall occurs during July and August. The recharge to the alluvial aquifers is from high rainfall along the escarpment and direct infiltration since the aquifer in the study area comprises an unconfined aquifer.

An effective conceptual groundwater model has been determined for the model area that provides a reasonable explanation of the groundwater occurrence (flows, levels and water quality) observed throughout the groundwater model area. However, there are significant data gaps especially within the bedrock system to the west of the alluvial fans.

The results showed that there is a need to manage groundwater resources sustainably; to avoid over exploitation and contamination of ground water. Also, allowing sufficient recharge to prevent draft exceeding the recharge. This study highlighted areas of high vulnerability and medium vulnerability; where specific measures can be taken to improve the condition of the groundwater resources.

From the conceptual and numerical model, it is also concluded that the recharge components play a major role in the groundwater quantity and quality fluctuation of the study area and over-abstraction during pumping can be a cause of salt water intrusion. The numerical model was suitable as a tool to improve our understanding of the groundwater flow system in response to recharge and abstractions and to estimate the aquifer properties of the study area.

The vulnerability of alluvial aquifers to contamination in the study areas varies with different factors. The depth, the lithology of the fan sediment and thickness of the fan are the major controlling factors for the variation of groundwater quality at depth and laterally. The groundwater chemistry of the watershed is generally characterized as moderately fresh water. Fresh groundwater for domestic use is only limited in shallow boreholes on the major fan areas of Musley, Gehertu and adjacent fan areas.

The model results imply that there are not many salt intrusions on the upper watershed(west of the escarpment). The excessive Chloride, Sulfate and Sodium of the boreholes in the alluvial

aquifers implies that the major source of contamination in the alluvial aquifer (east of the escarpment) is the geogenic origins of salt intrusion.

Test boreholes where the bottom depth of drilling crossed the fresh and saltwater interface have yielded highly saline groundwater in the fan area. The alluvial fans transmit fresh, and also brackish, water from the bedrock to the salt flats. Alluvial fans display a clear trend of improving water quality from the north to the south. This is possibly the result of fresher water recharge from the Antalo Group limestones and Adigrat Formation sandstones to the west and the boreholes being situated further away from the fault zone. Fault structures extend into the escarpment which increases the likelihood of them being significant conduits of groundwater flow from the plateau to the alluvial fans. The water quality also improves from the fan toe seeps to the wadis at the head of the fans (from east to west).

The challenges in supplying groundwater to the community of acceptable or usable quality and targeting the fresh groundwater lenses in areas where it can be accessed at the shallowest depths. As needed in terms of sustainable volume, and as possible in terms of water quality requirements, the abstraction should be limited.

## **6.2 Recommendations**

This study used the DRASTIC method of vulnerability assessment however, a different approach can also be used to assess the groundwater vulnerability. For example, land use land cover data can be used to assess the area where this resource is under stress. Furthermore, the collection of new data would help in carrying out the study further; other methods can also be used to assess the same. Many other parameters like the social perception of the people and government policies can be included and studied in detail.

With additional data, further refinement of the groundwater modeling for salt intrusion is required. Further extensive field-based observations combined with more water sampling and quality assessment are required.

Therefore based on the findings of the study, it is recommended that a few additional weather stations be considered for upper and lower watershed areas so that a better understanding of the spatial variability of rainfall can be gained.

Meteorological data and Hydrological data are not properly registered for a few existing stations and data quality was the main challenge for this study, therefore proper data registration and good database development in the sectors are recommended. Build flow gauges are also needed in the study area.

As drilling, testing and sampling data become available, the models should be upgraded. Better refine the depth of the wadi sands and gravels and the understanding of how this unit transfers groundwater from the bedrock into the top of the alluvial fans.

A more local scale model of the fan may be useful in elucidating some of the uncertainties which remain in the model. Understanding how regional tectonics will be crucial for understanding groundwater flow systems in detail.

## References

- Alamne, Tewodros, T., Assefa, Sisay, A., Samuel, B., Belay, Misbah, A., and Hussein. (2022). Mapping groundwater nitrate contaminant risk using the modified DRASTIC model: a case study in Ethiopia. *Environmental Systems Research*, 11:8,1-16.
- Alemayehu, T. (2006). *Groundwater Occurrence in Ethiopia*. UNESCO.
- Aller, L., Bennett, T., Lehr, H., and Petty, J. (1985). *DRASTIC: A Standardized system for evaluating groundwater pollution potential using hydrogeologic settings*. US EPA, Robert S. Kerr Environmental Research Laboratory, 163.
- Anderson, P., and Woessner, W. (1992) .*Applied Groundwater Modeling*. Acad. Press, San Diego, USA.
- Anteneh, Z., Assefa, M., Yewendwesen, M., and Birlew, A. (2016). *Groundwater Vulnerability Analysis of the Tana Sub-basin: An Application of DRASTIC Index Method*. Springer International Publishing Switzerland, DOI 10.1007/978-3-319-18787-7\_21,435-461.
- Ayeneu, T., Demlie, D., and Wohlich, S. (2008). Hydrogeological framework and occurrence of groundwater in the Ethiopian aquifers. *Journal of African Earth Sciences*, 52, 97-113.
- Bailey, R., Wible, T., Arabi, M., Records, R., and Ditty, J. (2016). Assessing regional-scale spatiotemporal patterns of groundwater-surface water interactions using a coupled SWAT MODFLOW model. *Journal of Hydrology*, 30, 4420–4433.
- Bailey, R., and Park, S. (2017). *SWAT-MODFLOW Tutorial Version 2. Documentation for preparing model simulations*. Department of Civil and Environmental Engineering, Colorado State University.
- Bailey, R., and Park, S. (2019). *SWAT-MODFLOW Tutorial Version 3. Documentation for preparing and running SWAT-MODFLOW Simulations*. Department of Civil and Environmental Engineering, Colorado State University.
- Barbulescu, A. (2020). Assessing Groundwater Vulnerability: DRASTIC and DRASTIC-Like Methods: A Review. *Water*, 12, 1356.

- Beyene, A., and Abdulselam, M. (2005). Tectonics of Afar depression. The University of Texas at Dallas, Richardson, TX75083-0688, USA.
- Bisrat, A., Il-Moon, C., Min-Gyu, K., and Sun-Woo, C. (2020). Assessment of Groundwater Recharge in Agro-Urban Watersheds Using Integrated SWAT-MODFLOW Model, Department of Land, Water and Environment Research, Korea. Sustainability, 12, 6593.
- Blake, D., Hartnady, M., Hay, E., and Botha, F. (2017). Groundwater resources of the Danakil Depression (northeastern Ethiopia). Umvoto Africa (Pty) Ltd, South Africa.
- Boyle, D., Gupta, V., and Sorooshian, S. (2000). Toward improved calibration of hydrologic models: Combining the strengths of manual and automatic methods. Water Resources Res. 36(12): 3663-3674.
- CFSR, (2016).The Climate Forecast System Reanalysis. Online Available at: <https://globalweather.tamu.edu/>.
- Darrah, T., Tedesco, D., Tassi, F., Vaselli, O., Cuoco, E., and Pored, R. (2012). Gas chemistry of the Dallol region of the Danakil Depression in the Afar region of the northernmost East African Rift. Chemical Geology.
- David, C., Monireh, F., Brian, S., and Daniel, S. (2019). Application of an Integrated SWAT MODFLOW Model to Evaluate Potential Impacts of Climate Change and Water Withdrawals on Groundwater–Surface Water Interactions in West-Central Alberta, Canada. Water, 11, 110.
- Eagles, G., Gloaguen, R., and Ebinger, C. (2002). Kinematics of the Danakil microplate. Earth and Planetary Science Letters, 203(2), 607-620.
- ERCOSPLAN, (2015). Technical Report: In support of disclosure of Preliminary Economic Assessment of SOP Production, Allana Potash Corp., Danakil Project, Afar State, Ethiopia.
- Fusco, F., Allocca, V., Coda, S., Cusano, D., Tufano, R., and De-Vita, P. (2020). Quantitative Assessment of Specific Vulnerability to Nitrate Pollution of Shallow Alluvial Aquifers by Process-Based and Empirical Approaches. Water, 12,269.

- Gebresilassie, S., Tsegab, H., Kabeto, K., Gebreyohannes, T., Sewale, A., Amare, K., Mebrahtu, A., Zerabruk, S., Mebrahtu, G., Gebrehiwot, K., and Haile, M. (2011). Preliminary study on geology, mineral potential and characteristics of hot springs from Dallol area, Afar rift, northeastern Ethiopia: implications for natural resource exploration. *Mekelle University*, 3 (2):17-30.
- Gassman, P., Reyes, M., Green, C., and Arnold, J. (2007). *The Soil Water Assessment Tool: Historical Development, Applications and Future Research Directions*. 50(4).
- GSE, (2009). *Geology of Ethiopia*. 1:2 000 000 scales, Geological Survey of Ethiopia, Addis Ababa, Ethiopia.
- GSE, (2014). *Hydrogeological map of Axum-Adigrat with scale 1:250000*, Geological Survey of Ethiopia, Addis Ababa, Ethiopia.
- Harry, L. (2018). *MODFLOW-MT3DMS with Floppy project topics & contaminant transport simulation*.
- Holwerda, J. and Hutchinson, R. (1968). Potash-bearing evaporites in the Danakil area, Ethiopia. *Economic Geology*, 63: 124-150.
- Kebede, S. (2013). *Groundwater in Ethiopia*. Verlag Berlin Heidelberg: Springer.
- Ketema, A., Lemecha, G., Schucknecht, A., and Kayitakire, F. (2016). Hydrogeological study in drought-affected areas of Afar, Somali, Oromia and SNNP regions in Ethiopia. European Union and United Nations Children's Fund (UNICEF).
- Kim, W., Chung, M., Won. S., and Arnold, G. (2008). Development and application of the integrated SWAT–MODFLOW model. *Journal of Hydrology*, 356, 1– 16.
- Mesfin, A., and Yohannes, E. (2014). The Geology of Northern Danakil Depression and its Geothermal Significance. *Proceedings 5th African Rift Geothermal Conference, Tanzania*.
- Michael, J., Thomas, E., Michael, G., and Dennis, R. (2013). *Assessing Groundwater Vulnerability to Contamination: Providing Scientifically Defensible Information for Decision Makers*. USGS.

- MWH, (2015). Water Supply Feasibility Study: Yara Dallol BV.
- Neha, G.(2014). Groundwater Vulnerability Assessment using DRASTIC Method in Jabalpur District of Madhya Pradesh. International Journal of Recent Technology and Engineering,3,36-43.
- Niswonger, G., Panday, S., Motomu, I., and MODFLOW-NWT. (2011). A Newton Formulation for MODFLOW-2005: Techniques and Methods 6–A37, U.S. Geological Survey: Reston, WV, USA.
- Nugraha, U., Ridwansyah, I., Marganingrum, D., Hartanto, P., Lubis, F., and Bakti, H. (2021). Transport Modelling in Jakarta Groundwater Basin using QSWATMOD. Earth and Environmental Science, 789, 012045.
- Park, S., Nielsen, A., Bailey, R.T., Trolle, D., and Bieger, K. (2019). A QGIS-based graphical user interfaces for application and evaluation of SWAT-MODFLOW models. Environmental modeling & software, 111,493-497.
- Pelletier, J., Blainey, B., and Jon, D. (2008). Infiltration on alluvial fans in an arid environment: Influence of fan morphology. Journal of geophysical research, 113, 1-4.
- Qaisar, H., and Roberto, S. (2014). Application of SWAT Model for Hydrologic and Water Quality Modeling in Thachin River Basin, Thailand. Arabian Journal of Science Engineering 39(3):1671–1684.
- Terence, B., and John, M. (1994). Alluvial fans and their natural distinction from rivers are based on morphology, hydraulic processes, sedimentary processes and facial assemblages. Journal of sedimentary research, A64, 450-455.
- Todd, K. (2005). Groundwater hydrology. Wiley, Hoboken.
- Towers, L. (2017). Water resource evaluation in the Danakil basin, Ethiopia: Groundwater supply for potash solution mining. Cape Town: University of the Free State.
- Umvoto Africa, (2017). Water Resource Assessment for Potash Mining: Volume 1. Physiography and Geology. Danakil Potash Project, Danakil Depression, Northern Ethiopia.

- UNICEF, (2019). Situation Analysis of Children and Women: Afar Region.
- Warren, K. (2016). Evaporites a Geological Compendium, Cham Heidelberg New York Dordrecht London: Springer.
- Winchell, M., Srinivasan, R., Diluzio, M., and Arnold, J. (2013). ArcSWAT interface for SWAT2012, User guide. A&M University, Texas.
- Worqlul, A., Collick, A., Tilahun, S., Langan, S., Rientjes, T.H.M., and Steenhis, T. (2015). Comparing TRMM 3B42, CFSR and ground-based rainfall estimates as input for hydrological models, in data-scarce regions: the Upper Blue Nile Basin, Ethiopia. Hydrol. Earth Syst. Sci. Discuss., 12, 2081-2112.
- WWDSE, (2013). Groundwater Potential Assessment and Evaluation of Danakil basin. Ministry of Water, Irrigation and Energy, Ethiopia.
- WWDSE, (2015). Danakil basin Groundwater Potential Assessment Project: The Upper Catchments of the Danakil basin (Ayshet Graben) Groundwater Potential Evaluation. Annex-2: Well Completion Report.
- Zhansheng, L., Yuan, Y., Guangyuan, K., and Yang, H. (2018). Study on the Applicability of the Hargreaves Potential Evapotranspiration Estimation Method in CREST Distributed Hydrological Model (Version 3.0) Applications. Water 10, 1882.
- Zheng, C., Hill, M.C., Cao, G., and Ma, R. (2012). MT3DMS: Model Use, Calibration and Validation. Transactions of the ASABE, 55(4), 1549-1559.